Multiuser Transmissions and Multihop Communications in Cellular Network

A thesis submitted in partial fulfillment of
the requirements for the degree of

Doctor of Philosophy

by

Kannan. G
(Roll No. 04407604)

Under the guidance of
Prof. S. N. Merchant

DEPARTMENT OF ELECTRICAL ENGINEERING
INDIAN INSTITUTE OF TECHNOLOGY–BOMBAY
2008

Thesis Approval

The thesis entitled

Multiuser Transmissions and Multihop Communications in Cellular Network

by

Kannan. G
(Roll No. 04407604)

is approved for the degree of

Doctor of Philosophy

_____	_____
Examiner	Examiner
_____	_____
Guide	Chairman

Date: _____

Place: _____

INDIAN INSTITUTE OF TECHNOLOGY BOMBAY, INDIA

CERTIFICATE OF COURSE WORK

This is to certify that **Kannan. G** (Roll No. 04407604) was admitted to the candidacy of Ph.D. degree Dec 2004, after successfully completing all the courses required for the Ph.D. programme. The details of the course work done are given below.

S.No	Course Code	Course Name	Credits
1	EE 608	Adaptive Signal Processing	6
2	EE 636	Matrix Computations	6
3	EE 678	Wavelets	6
4	EES 801	Seminar	4
5	EE 603	Digital Signal Processing and Its Applications	6
6	EE 703	Digital Message Transmissions	6
7	IT 601	Mobile Computing	6
8	IT 605	Computer Networks	6
9	EE 708	Information Theory and Coding	6
10	EE 764	Wireless and Mobile Communications	6
		Total Credits	**58**

IIT Bombay

Date: Dy. Registrar (Academic)

Abstract

In this thesis we devise multiuser transmission strategies as well as multihop relaying communications for DS-CDMA based cellular network.

The performance of DS-CDMA communication systems is limited by the interference caused by other users known as Multiple Access Interference (MAI) and by the channel caused Inter Symbol Interference (ISI). Receiver based multiuser detection techniques that utilize the knowledge of the downlink channel by the mobile terminals (MT) have been extensively studied in the literature, in order to deal with MAI and ISI. However, these techniques result in high MT receiver complexity. Recently, work has been done on algorithms that transfer the complexity from the MT to the base station by exploiting the fact that in Time Division Duplex (TDD) mode the downlink channel can be known to the transmitter.

Algorithms based on the Minimum Mean Squared Error (MMSE) criterion are optimal for 'ideal' AWGN channels. However, in the case of multiple access wireless multi-path channels, wherein MAI and ISI are inherent, MMSE based algorithms do not offer the optimal framework. Minimum Probability of Error (MPOE) based algorithms have been shown to perform significantly better than MMSE based approaches in these scenarios. In order to reduce the complexity of the MT, we develop two precoding algorithms at the base station to minimize the probability of error at the MTs receiver. In one algorithm we use a joint prefilter for all users and hence, jointly minimize the probability of error and in the another algorithm an individual prefilters are employed for each users. Complete channel knowledge has been assumed in designing the prefiltering coefficients. Also we employ maximal ratio transmitter (MRT) beamformer at the transmitter using the available channel knowledge. We further relax the assumption of complete channel knowledge and design the prefilters and maximal ratio beamformers by using only first and second order statistics of the channel.

In a cellular network it is desired to let the MTs stay connected as long as possible. But, this is quite a challenge because of the limited power MTs produce and also the interference

in the network that must be reduced. A possible way to achieve large coverage areas and less interference is to use multihop relaying. Therefore, we introduce multihop relaying in cellular domain and resolve some of the problems that arise. Relaying systems use several shorter communication links instead of the conventional point-to-point transmission. This can allow for a lower power requirement and also frequency re-use may be more efficiently exploited.

The routing of data packets in MCN must be performed to minimize interference at the MT simultaneously ensuring proper Quality of Service (QoS) constraints. Furthermore, end-to-end delay and end-to-end throughput are important QoS metric in voice and data communications. We propose a unified cross layer routing by taking all the essential metrics into consideration. We also propose an incentive scheme to stimulate the cooperation for relaying. In case of dynamic call dropping we propose a route resilience scheme to keep the communication intact.

The simultaneous allocation of CDMA code to the mutually audible users affects system performance through co-channel interference. To attempt to minimize this, a novel scheduling scheme is developed based on the probability of error criterion. The proposed scheduling scheme is heuristic in nature and has linear complexity with respect to number of users. Simulation results show that the proposed scheduling scheme achieves greater spatial reuse and end-to-end throughput.

In addition, we also determine a lower bound on the transmission range of nodes as a function of number of nodes in the network in order to keep the network fully connected. With thus obtained lower bound, we derive an optimal transmission range to increase the spatial reuse as well to enhance the effective connectivity in the multihop cellular network.

To further increase the throughput performance in multihop relay networks we design a OFDM-CDMA based access mechanism. The source to destination route path is grouped and a single CDMA code is assigned to that group. Inside the group the intermediate links are distinguished using OFDM orthogonal carriers. Hence, the proposed scheme has two level of demodulation, therefore greater end-to-end performance.

The advantages and the performance of the proposed techniques, along with a variety of characteristics are demonstrated by means of Monte Carlo simulations.

Contents

List of Tables

List of Figures

Chapter 1

Introduction

Wireless communications were attempted as early as in the 1860's by Mahlon Loomis in the United States. However, a clear understanding of the basic principles of radio only emerged after the theoretical work of the Scottish physicist James Clerk Maxwell in the 1860's and the experimental work of the German physicist Heinrich Hertz in the 1880's. More than decade later, Guglielmo Marconi understood Hertz's work and formed the Wireless Telegraph and Signal province in 1897 to manufacture and sell radio equipments. The first long range wireless transmission was established in the early part of twentieth century. Marconi and his colleagues transmitted the three dots of the letter "S" from Cornwall, England in the early afternoon of December 12, 1901 and the signal was heard several times fading in and out of the background interference at the receiver station set up by them at Cape Cod, Massachusetts, U.S.A. Thus the first transatlantic wireless telegraph had been proven possible. But Marconi's wireless telegraph transmitted only signals. Voice over the air came into existence only in 1921. Marconi went on to introduce short wave transmissions in 1922. Since then, due to the continuous efforts of notable scientists and organizations, wireless communication has become an essential part of our daily lives today.

In the present age, wireless communication capture the attention of wide variety of researchers around the globe. It is almost impossible to keep track of the technical journals, magazines, symposiums and articles concerning this subject. It is clear, therefore, that wireless communication is by any measure, one of the most rapidly growing segments of the telecommunications market. A wireless communication system, where at least one terminal moves is classified as a mobile communication system. Mobile systems may have a terrestrial component

and/or satellite component. Our focus in this thesis is on the terrestrial component.

The mobile communication revolution that has happened till now, can be broadly classified as first generation, second generation (2G) and third generation (3G) mobile systems.

The first mobile radio systems were introduced by the military and were limited only to voice communication systems. The handsets provided very poor voice quality, low talk time and were rather bulky in size. The first public cellular phone system known as Advanced Mobile Phone System (AMPS) was introduced in 1979 in the United States. This was followed shortly by the introduction of the Nordic Mobile Telephone (NMT) systems in Denmark, Finland, Norway, Sweden and the Total Access Communication System (TACS) and Nippon Mobile Telephone System (NAMTS) in the UK and Japan respectively. These systems were widely considered as first generation mobile phone systems and they were based on analog Frequency Division Multiple Access (FDMA) technique.

By 1987, there were 5 incompatible first generation analog systems operating across Europe. However, it is obvious that any version of a global mobile communication system needs international roaming and therefore a common mobile standard. Hence, the network operators, equipment manufacturers, research establishments and policy makers came together and jointly launched a Global Standard for Mobile communications otherwise known as GSM. GSM was designed based on TDMA/FDMA scheme with an operating frequency band of 900 MHz. However, the 900 MHz frequency band allotted for GSM in Europe was not available in the US and also there was strong pressure on US researchers and manufacturers to develop a competitive standard for the US market which could work irrespective of the frequency band. The result was the development of a narrowband Code Division Multiple Access (CDMA) standard otherwise known as IS-95 (Interim Standard-95). GSM and IS-95 are classified as 2G systems. These systems are now commercially successful and deployed in more than 110 countries with the subscriber numbers reaching in excess of 3 billion. The maximum data rate promised by GSM is 9.6 kbps [1].

By the late 1990s, the very success of GSM and IS-95 again raised questions about the future demand for high date rates, enhanced multimedia services, seamless mobility and flexible

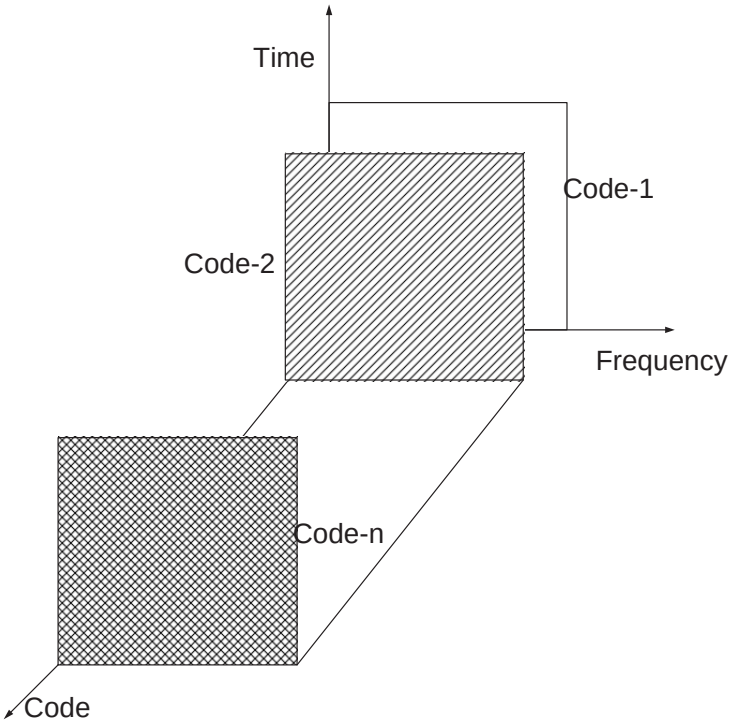

Figure 1.1: CDMA Illustration

QoS. Though the GSM community has proposed standards like HSCSD (High-Speed Circuit-Switched Data), GPRS (General Packet Radio Service) and EDGE (Enhanced Data rates for GSM Evolution), the highest data rate offered was 128 kbps, which was far below than the demand. So multinational collaboration was again initiated to identify and agree to a suitable technology that could be used with new spectrum to provide more capacity, high bandwidths and offer international roaming. Hence, the wireless research community has started working on global technological and interoperable air interface standard for 3G wireless services in late 1990s and started 3rd Generation Partnership Project (3GPP) and 3GPP2. In Europe 3G has become UMTS (Universal Mobile Telecommunication System) and in Japan and US the 3G system often carries the name IMT-2000 (International Mobile Telephony 2000) [2, 3].

The 3G mobile communication systems aim to provide enhanced voice, text and data services to the user at a minimum transmission rates of 144 kbps in mobile (outdoor) and 2 Mbps in fixed (indoor) environments. Based on these requirements, in 1999 the ITU (International Telecommunication Union) approved five radio interface modes for IMT-2000 standards (Recommendation 1457). Three of the five approved standards (CDMA2000, TD-SCDMA, WCDMA) are based on CDMA. Many CDMA techniques have been proposed in literature

(DS-CDMA, FH-CDMA, TH-CDMA, MC-CDMA, etc.,). Each of them differs in the way the user signature waveforms are designed. DS-CDMA has been the most popular amongst the CDMA techniques and is adopted for 3GPP WCDMA standard. Hence, we use DS-CDMA as the default access technique in the rest of the thesis unless otherwise stated.

To summarize, mobile communication systems are widely classified as three different generations i.e first generation analog FDMA based AMPS mobile phone systems, second generation TDMA based GSM systems and third generation CDMA based 3GPP, 3GPP2 and UMTS systems.

1.1 CDMA Multiple Access Communication and Multiuser Transmissions

DS-CDMA is a widely used technique for multiple access communication in wireless systems. It differs from the classical Time Division Multiple Access (TDMA) and Frequency Division Multiple Access (FDMA) in the context that all users transmit across the entire frequency band and many users can transmit simultaneously as shown in Fig 1.1.

DS-CDMA uses linear modulation with wideband pseudonoise (PN) sequences to generate signals. These sequences, also known as spreading codes, spread the spectrum of the modulating signal over a large bandwidth, simultaneously reducing the spectral density of the signal. Various CDMA signals occupy the same bandwidth and appear as interference to each other. Each user data is assigned with an individual code at the time of call initiation. This code is used both for spreading the signal at the time of transmission and despreading it at the time of reception. The principle of DS-CDMA is that the codes are orthogonal between each other to allow for decoupling at the receiver. On downlink the base station transmits to all users synchronously and this preserves the orthogonality of various codes assigned to different users. The orthogonality, however, is not preserved between different components arriving from different paths in multipath propagation. Hence, although the spreading codes are designed to be orthogonal with each other, there are scenarios under which the orthogonality cannot be controlled. This results in interference from user to user. This type of interference is called multiple access interference (MAI) and imposes a limitation to CDMA systems.

The detection is done on the basis of a filter matched to the PN sequence of the user. We refer to this detector as the conventional matched filter detector. Since the conventional matched filter is designed for orthogonal signature waveforms, it suffers from MAI and Inter Symbol Interference (ISI) due to complex multi path time-varying propagation channels and simultaneous usage of bandwidth by many users. MAI and ISI are often added to the background thermal noise modeled as Additive White Gaussian Noise (AWGN). Thus, the system performance is limited by the amount of total interference instead of the background noise exclusively as in other cases. In other words, the Signal to Interference plus Noise Ratio (SINR) is the limiting factor for a mobile communication system instead of the Signal to Noise Ratio (SNR). Therefore, in systems employing CDMA, the two problems of equalization and signal separation have to be solved simultaneously to increase the SINR and achieve a good performance. In the state of the art CDMA systems, MAI and ISI are addressed using multiuser signal processing techniques which offer better performance than the conventional matched filter detector.

1.1.1 Multiuser signal processing

Multiuser signal processing techniques can be broadly classified into two categories:

1. Multi-User Detection (MUD): MUD has been studied extensively and a number of solutions have been proposed. These techniques are all receiver based, they usually require channel estimation, knowledge of all the active users' signature waveforms and have considerable computational cost. While this is feasible for the base station (for the uplink scheme), it contrasts with the desire to keep portable units (for the downlink scheme), like simple and power efficient mobile phones.

2. Multiuser Transmission: An alternative to multiuser detection is to precode the transmitted signal such that the ISI and MAI effects are minimized before transmission in the downlink [4]. The extra computational cost is transferred to the base station where power and computational resources are more readily available. These schemes involve some pre-processing at the transmitter with the aim of keeping the receiver at the mobile handset simple. The low computational burden at the receiver makes them better alternative for deployment in the downlink.

1.1.2 Precoding optimization criterion

The main issue in designing the precoding filter is to develop a suitable optimization criterion. The fast growth in popularity and customer base of wireless systems has led to a lot of techniques from the wired world being deployed directly to the wireless scenarios without a thorough study on the optimality of the algorithms. Minimum Mean Squared Error (MMSE) based demodulation schemes are one such example being used extensively at the physical layer in wireless systems. The optimality of MMSE based algorithms is well-known for Additive White Gaussian Noise (AWGN) channels. Wired channels being very close to ideal AWGN channels, most conventional detectors used the MMSE criterion for demodulation and detection of digital symbols. The advent of wireless technologies saw these being directly adapted to the wireless scenarios where they are being used till date. Wireless channels are incomparably more hostile and different from wired channels and hence, the performance of MMSE based approaches is severely degraded and stands much below optimal for these systems. Thus there is a necessity to develop optimal algorithms for demodulation in multi-path, ISI inducing wireless channels. Minimum Probability of Error (MPOE) turns out to be a natural choice for the optimality criterion for digital communication systems.

In this thesis, we present two multiuser transmission schemes based on novel MPOE criterion. We also propose a Maximal Ratio Transmission (MRT) beamforming to further enhance the prefiltering performance.

1.2 Multihop Relaying

The radio frequency bandwidth used for mobile communications has become a scarce and expensive medium as the number of mobile users increased to a greater extent of late and there is a huge demand of high data rate applications. Given the limitation on the spectrum, many researchers have attempted to increase the amount of data we can send with complex receiver structures, modulation schemes, error correction and so on. Probably the greatest single advance in bandwidth utilization is the cellular concept. This means that bandwidth can be reused. CDMA systems promise a frequency re-use-factor of 1. However, its potential is limited by co-channel interference as CDMA is a interference limited multiple access system. Because all users transmit on the same frequency, internal interference generated by the system is the most significant factor in determining system capacity and call quality. The transmit power

for each user must be reduced to limit interference, however, the power should be enough to maintain the required SNR at the desired receiver for satisfactory call quality. Moreover, mobile users rely on a small battery to power the terminal. It is desirable to try and achieve the lowest transmitted power possible by breaking the transmission from a direct link into a series of smaller hops using other users, or strategically placed relays.

In addition to the above, cellular networks still have some areas where coverage is yet to be provided. These areas are often referred as dead spots. Dead spots include subway train platforms, indoor environments and underground areas. Moreover, in dense areas known as hot spots, such as downtown areas and amusement parks, subscribers tend to experience higher call blocking.

Multihop relaying has been proven to be effective in increasing the coverage, reducing the call blocking probability and decreasing the per node transmission power. With relaying, the only requirement is that users can achieve the required signal strength at the next relay, meaning that coverage and high data rates should be available to more users and to the users even at the edge of the cell. Furthermore, with a conventional system if the user has a poor channel established directly to the base station, they may have no choice but to change location to achieve communication. However, in multihop relaying, mobiles with no good path to any base station may instead relay their calls through other mobiles with better propagation conditions.

Relaying of wireless communication signals is not a new idea. The principle behind relaying traces its roots back to 500 B.C. Darius I, the king of Persia, devised an innovative communication system that was used to send messages and news from his capital to the remote provinces of his empire by means of a line of shouting men positioned on tall structures. This system was more than 25 times faster than normal messengers available at that time. In 1970, Norman Abramson and his fellow researchers at the University of Hawaii invented the ALOHA protocol for multiple access systems. The success and novelty of ALOHA triggered widespread interest in different directions of communications including wireless relay communication systems. Relaying has also been used in satellite communications, to boost the signal in fixed microwave links and in Defense Advanced Research Projects Agency (DARPA) using one of the first implementations of packet based communications [5]. In fact multihop relaying is the

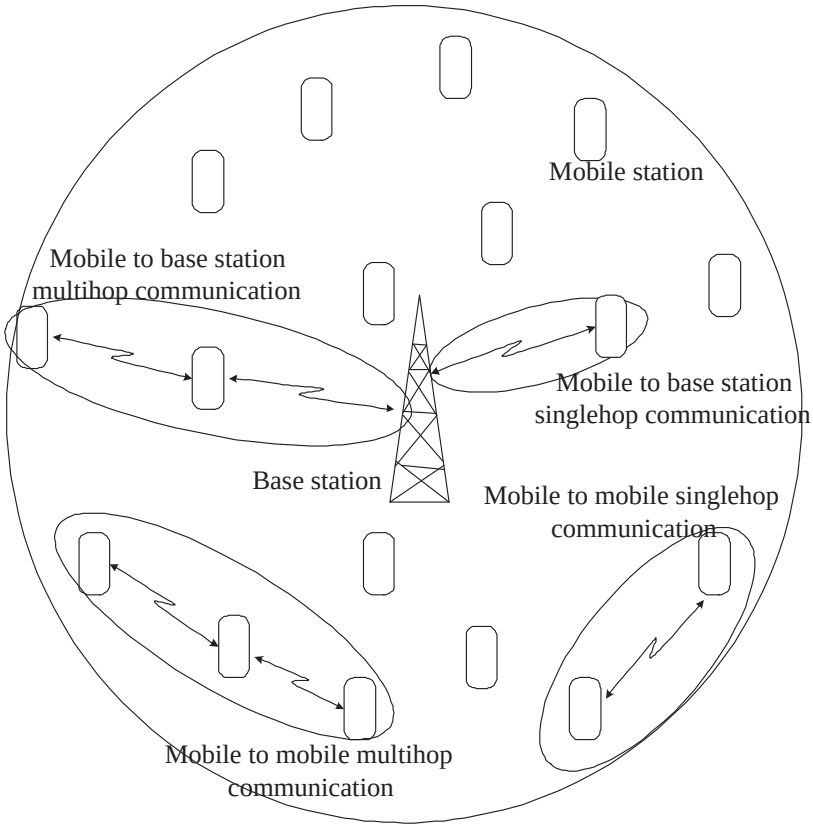

Figure 1.2: Multihop relaying in cellular network illustration

principal strategy followed in Mobile Adhoc Network (MANET), since in MANET due to the lack of infrastructure and the limited transmission range of each node, data needs to be routed to the destination by the nodes in a multihop fashion.

Encouraged by the above facts there have been interests in incorporating multihop relay communications into cellular networks as shown in Fig 1.2. Such a network is often referred as Multihop Cellular Network (MCN) which merges the benefits of both ad-hoc networks and centralized cellular networks and at the same time overcomes the drawbacks of both. This is the concept behind Opportunity Driven Multiple Access (ODMA) proposed in 3GPP [6]. To Provide a relaying capability service in next-generation ad-hoc GSM (AGSM) is also under study [7]. For data networks also, multihop cellular networks have been proposed in [8]. Being an effective solution, MCN heavily depends on the mutual interference between nodes for the capacity, coverage and power requirements of a network. Thus, it is necessary to understand the properties of the topology which minimizes the total transmit power in the presence of interference. Finding a suitable routing strategy is still an open problem in MCN. This problem

is computationally intractable and heuristic algorithms are mainly used. Furthermore, suitable medium access mechanism, link scheduling and optimal selection of transmission power are some of the issues which need immediate attention. In this thesis we address some of these important issues in a comprehensive fashion.

1.3 Thesis Contributions and Organization

- In Chapter 2, two prefiltering techniques have been devised using MPOE optimization assuming complete knowledge (complete channel state information) of the forward channel at the base station transmitter. In the first prefiltering model, a common filter is optimized to minimize the probability of error in the simple handset having matched filter receiver matched with the CDMA PN code of the user. In the second prefiltering model, an individual prefilter is employed for each and every user. Performances of the proposed prefiltering models are compared against the corresponding MMSE based prefiltering systems.

  Since complete channel knowledge is assumed at the transmitter we further utilize this information by employing the MRT technique at the base station where the MRT weights are optimized based on the available knowledge of the channel.

- We further relax the assumption of complete channel knowledge and design the MMSE/MPOE joint as well as individual precoding filter based only on the first and second order statistics of the channel (partial channel state information) in Chapter 3. A novel MRT scheme is proposed to optimize the MRT weights based only on the partial channel state information.

- In Chapter 4, a cross layer routing strategy is introduced to find an optimal path from a given source to destination using multiple path as well as node constraints. In case of dynamic call dropping, a time effective route resilience scheme is presented to find an alternate path without breaking the ongoing communication. The performance of the proposed routing and route resilience schemes have been compared against existing algorithms.

- Chapter 5 introduces a heuristic cross layer scheduling to reuse the CDMA codes such that the probability of error in all links in the network is optimized. The proposed algorithm is

based on both graph theoretic as well as physical interference. It has minimal complexity and superior performance compared to standard algorithms.

- In Chapter 6, an analytical relationship has been derived between coverage and transmission range, so that the transmission power of the mobile nodes can be controlled effectively while ensuring connectivity of the nodes. With the proposed solution, communication can be established in a more power effective manner between any two nodes in the cell.

- A group based CDMA-OFDM access mechanism for the effective use of CDMA codes and OFDM carriers in MCN is proposed in Chapter 7. The proposed scheme has high potential to increase the user capacity and to ensure higher end-to-end throughput.

- Summary of the work and conclusion of the thesis are given in Chapter 8. Furthermore, future areas of research and extensions are also presented.

Chapter 2

MPOE Prefiltering and MRT Beamforming for DS-CDMA Systems

To reduce the complexity of the mobile receiver, two prefilter models using a linear FIR prefilter for minimizing the probability of error is proposed in this chapter. A multiuser downlink transmission scenario is considered. The first system model, consists of a single common prefilter for all users at the base station and the second system model has individual prefilter for each and every user. Complete knowledge of the channel at the base station is assumed. In order to fully utilize the knowledge available at the transmitter, the filter weights are computed, conditioned on the transmitted bit vector sequence. This also makes the computation of the prefilter coefficients linear in the number of users as opposed to the exponential complexity otherwise. Coefficients of FIR prefilter are computed by minimizing the conditional probability of error and the mean square error. To further improve the performance of the proposed models, Maximum Ratio Transmission (MRT) beamforming is considered at the base station for both the models. Simulation results illustrate the performance of the proposed system models.

2.1 Introduction

Multiple Access Interference (MAI) and Inter Symbol Interference (ISI) mitigations have been a challenging research topic since the very beginning studies on DS-CDMA systems. The frequently considered approach of performing multiuser detection at the receiver is quite unattractive for the downlink because it entails an increase of complexity and power consumption at the mobile terminals. The solution lies in transferring the work load to the base station trans-

mitter in the form of prefiltering. This chapter explores a prefiltering scheme at the transmitter which can allow for considerably simplified receiver structures. It is evident that prefiltering will only be useful if the channel variation timescales are relatively slower than the time taken for the channel to be estimated at the transmitter [9]. The downlink channel can be estimated at the transmitter by using some feedback from the receiver [10–13]. Alternately, for TDD based systems, estimates of the uplink channel can be used as the channel parameters for the downlink channel as well, if the time interval between switching from uplink to downlink is small enough [14–17]. In this chapter complete knowledge of the channel is assumed at the base station.

Two approaches for prefiltering is considered: the first one considers a common prefilter for all users as shown in Fig 2.1. Such an approach is termed as joint prefiltering. Since the precoding (prefiltering) is done jointly for all users, the performance of joint prefiltering will not be up to the mark. To improve the performance significantly further, the second case considers a system which has individual prefilter for each user at the base station transmitter as shown in Fig 2.2. Such a model is termed as individual prefiltering.

Minimum Mean Squared Error (MMSE) has traditionally been used as the optimization criterion in the design of most of the prefiltering systems. However, since the symbols are of significance for a digital communication systems, the optimum prefilter should be the one which minimizes the probability of symbol error at the receiver [18–22]. Such a system is referred as the Minimum Probability of Error (MPOE) based system [18–22]. Usually MPOE optimization tends to be computationally expensive but since ample computational resources are considered at the base station, using MPOE instead of MMSE as the optimization criterion for prefiltering can be justified. Moreover, by conditioning the filter weights on the transmitted bits, one can design a MPOE prefilter with linear complexity [18–25].

The second part of the chapter, considers a MRT beamforming by taking advantage of the available channel knowledge for improving the Bit Error Rate (BER) performance of the proposed prefilter models. The strategy to adapt weights in MRT essentially depends on the knowledge about the propagation channel that is available for prefiltering at the base station. A standard single user receiver (conventional matched filter detector) is used for all the proposed system models [9, 16, 26–28].

The contributions of this chapter are follows:

- The concept of MPOE based joint and individual prefilters are developed.

- The use of MRT beamforming to further improve the performance of proposed prefilters is also explored.

The rest of the chapter is organized as follows: Section 2.2 describes the related work in the area of prefiltering, MPOE optimization and MRT beamforming. The system model is introduced in Section 2.3. MPOE and MMSE based joint prefiltering is derived in Section 2.4. The individual prefiltering with MPOE and MMSE optimization is discussed in Section 2.5. Sections 2.6 and 2.7 explain the MRT beamforming for joint and individual prefiltering respectively. Prefiltering system model with rake receiver is considered in Section 2.8. Simulation results and analysis of the results are provided in Section 2.9. Finally some concluding remarks are given in Section 2.10.

2.2 Related Work

Significant amount of research work have been carried out in the area of prefiltering over the last few years. But almost all the research work have been directed towards the design of MMSE based prefiltering wherein the optimization criterion is to minimize the mean squared error between the transmitted and received waveforms [9], [14–16, 29], [26–28, 30–34]. Vojcic and Jang in [9], Hons *et al* in [30], Reynolds *et al* in [31], Luna-Rivera *et al* in [26] considered a synchronous multiuser CDMA system and designed the prefilter using MMSE criterion. In all these work the analyzes were carried out by assuming zero ISI. In [16], a prefilter approach is proposed where the receiver is matched with both the channel and prefilter coefficients. But this method requires the receiver to know the precoder coefficients and perfect channel knowledge which will increase the receiver complexity. Linear/nonlinear precoder is designed by assuming only the long term channel estimate with MMSE criterion in [32]. Decorrelating prefilter and jointly optimized sequences algorithm have been proposed in [33], but the optimization criterion is MMSE. Minimum Bit Error Rate (MBER) optimization for linear combiner decision feedback equalizer receiver was proposed in [35] and adaptive MBER linear multiuser detector was proposed in [23–25]. Dua and Desai in [18] proposed the MPOE optimization method for general DS-CDMA system. Later Dua *et al* in [19], Sood *et al* in [20], Mohit *et al* in [21] and Wang *et al* in [22] extended it to different scenarios. In [18–22] it was established that MPOE

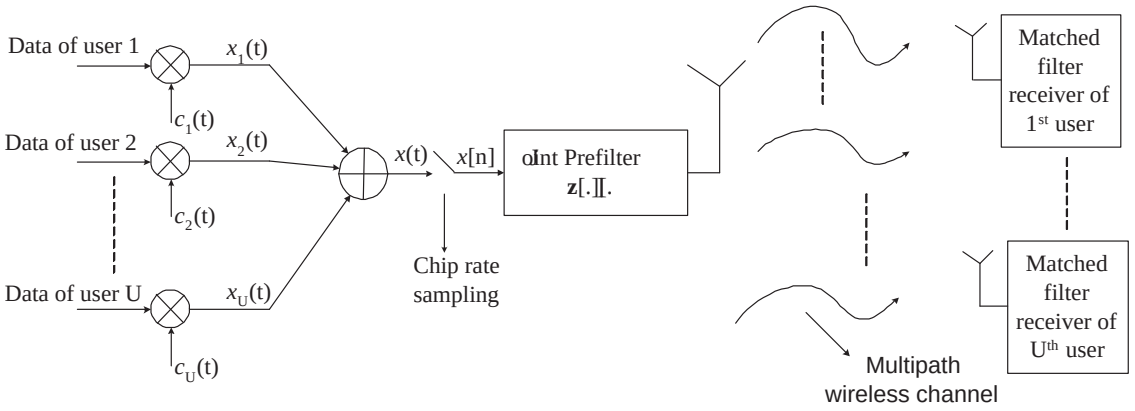

Figure 2.1: DS-CDMA system model for a multipath channel with joint transmitter prefiltering

optimization has better performance than MMSE optimization. Moreover, in [20–22] a linear computational complexity MPOE filters (with respect to the number of users) were proposed. In [36] Ding *et al* proposed a precoder and in [37] Palomar *et al* derived a transceiver based on minimum BER method for Zero-Forcing (ZF) equalizer at the receiver. These receivers need training or both the channel and precoding filter knowledge at the receiver hence, a relatively complex receiver is required which may not be desirable. Furthermore, the Maximal Ratio Combiner (MRC) rake receiver used in 3rd generation WCDMA also requires the receiver to estimate the channel which impairs the purpose of prefiltering [38]. The primary objective of prefiltering is to simplify the receiver structure hence, we work with a conventional single-user detector at the receiver. Georgoulis *et al* in [14–16] and Reynolds *et al* in [28, 31] have used a simple matched filter receiver by considering a general channel model with ISI while optimizing the filter on the basis of the MMSE criterion. MRT beamforming was first proposed in [39] and further analyzed in [40–43]. Prefiltering with ZF criterion and transmit antenna array is considered in [43], but it does not take advantage of available channel information. To the best of our knowledge there is no treatment on MPOE based prefiltering. In this chapter, MPOE based prefiltering with ISI and MAI is proposed in the first part. Also the performance of the MPOE based prefiltering system is substantially improved using MRT beamforming in the second part.

2.3 System Model

Consider a DS-CDMA system with U users as shown in Fig 2.1. Assume Binary Phase Shift Keying (BPSK) constellation for generating the input bits. The uth user transmits BPSK bit

$b_u(i)$ with amplitude A_u in ith bit interval and the length of signaling interval for each user is T_{bit} [44–46]. Let us assume user u is assigned with a spreading waveform $c_u(.)$ whose support is [0, T_{bit}] and $\mathbf{s}_u = [s_{u0}, s_{u1}, \ldots, s_{uN-1}]$ denotes the corresponding spreading sequence. Then,

$$c_u(t) = \sum_{k=0}^{N-1} s_{uk} rect[t - (k-1)T_c], \qquad u = 1, 2, \ldots, U \tag{2.1}$$

where, $rect(t)$ is a rectangular waveform with unit amplitude in [0, T_c], T_c is the chip period and N is the processing gain of the system. The baseband signal of the uth user in the ith bit interval can now be expressed as

$$x_u(t) = A_u b_u(i) c_u(t - iT_{bit}), \qquad iT_{bit} \leq t < (i+1)T_{bit} \tag{2.2}$$

By adding up all the users' signals at ith bit interval we get,

$$x(t) = \sum_{u=1}^{U} x_u(t) = \sum_{u=1}^{U} A_u b_u(i) c_u(t - iT_{bit}), \qquad iT_{bit} \leq t < (i+1)T_{bit} \tag{2.3}$$

Assume that $x(t)$ is sampled at T_c (chip rate sampling), then the resulting sequence $x[n]$ is

$$\begin{aligned} x[n] &= \sum_{u=1}^{U} A_u b_u(i_N) c_u(nT_c - iT_{bit}) \\ &= \sum_{u=1}^{U} A_u b_u(i_N) \sum_{k=0}^{N-1} s_{uk} rect(nT_c - iT_{bit} - (k-1)T_c) \\ &= \sum_{u=1}^{U} A_u b_u(i_N) \tilde{\mathbf{s}}_u[n] \end{aligned} \tag{2.4}$$

where $i_N = \lfloor \frac{i}{N} \rfloor$ because of chip rate sampling (note that $NT_c = T_{bit}$) and the sequence $\tilde{\mathbf{s}}_u[n] = s_{un},\ s_{un+1}, \ldots,\ s_{uN},\ s_{u0}, \ldots, s_{un-1}$ where n is the sampling instant. Note that $\lfloor a \rfloor$ denotes the floor operation which rounds the value of a to the nearest integer towards $-\infty$. For a fixed i, $\tilde{\mathbf{s}}_u[n]$ will be of length N, but when the input data is infinitely long, then $\tilde{\mathbf{s}}_u[n]$ will cyclicly repeat as [$\ldots,\ s_{uN-1},\ s_{u0},\ s_{u1},\ s_{u2}, \ldots,\ s_{uN-1},\ s_{u0},\ s_{u1}, \ldots$]. The prefilter for a particular bit period i is assumed to be a Finite Impulse Response (FIR) filter ($\mathbf{z}[.][i]$) of length L_z and it will be calculated adaptively at every bit interval. The idea is to compute these filter coefficients using MPOE and MMSE criteria. The prefiltered signal which will be sent through the wireless channel is

$$x[n] \otimes \mathbf{z}[.][n] \tag{2.5}$$

where $\otimes$ denotes the convolution operation and $\mathbf{z}[.][n]$ is the prefilter at time instant n. A general multipath frequency selective channel is assumed in our system. The multipath wireless channel

is modeled as a FIR filter and the channel coefficients are assumed to be constant over one bit period. The channel for the uth user at the ith bit interval is denoted as $\mathbf{h}_u[.][i]$ which is of length L_h^u for all i.

The elements of the channel FIR filter ($h_u[l][n]$) are assumed to be complex Gaussian with both real and imaginary parts following the *i.i.d* (identical independent distribution) Gaussian distribution [47]. The noise ($\eta_u[n]$) is assumed to be $i.i.d$ zero mean Additive White Gaussian (AWGN). The signal received at user u is

$$r_u[n] = \mathbf{h}_u[.][n] \otimes x[n] \otimes \mathbf{z}[.][n] + \eta_u[n] \tag{2.6}$$

where $\mathbf{h}_u[.][n]$ is the channel FIR filter at time instant n. Converting $r_u[n]$ into a parallel stream of N samples (number of chips per bit period), we obtain

$$\mathbf{r}_u[n] = [r_u[iN], \ldots, r_u[iN + N - 1]]^T \tag{2.7}$$

where superscript T denotes transpose. A simple matched filter receiver is assumed. The received signal at the uth user after matched filtering is

$$y_u[i] = \mathbf{s}_u^T \mathbf{r}_u[i] = \sum_{k=0}^{N-1} s_{uk} r_u[iN + k] \tag{2.8}$$

From (2.6) and (2.8)

$$y_u[i] = \sum_{k=0}^{N-1} s_{uk} \sum_{m=0}^{L_h^u - 1} h_u[m][j_1] \Bigg(\sum_{l=0}^{L_z - 1} z[l][j_2] \sum_{v=1}^{U} A_v b_v[j_2] \tilde{\mathbf{s}}_v[iN + k - m - l] \Bigg) + \sum_{k=0}^{N-1} s_{uk} \eta_u[iN + k] \tag{2.9}$$

where

$$j_1 = \left\lfloor \frac{iN + k - m}{N} \right\rfloor, \quad j_2 = \left\lfloor \frac{iN + k - m - l}{N} \right\rfloor \tag{2.10}$$

are index parameters in the convolution. In (2.9) $\sum_m$ gives the ISI term due to the multipath channel while $\sum_u$ is the MAI component due to multiple user transmission. Since BPSK constellations are used for input data, the decision statistics is given by $\Re(y_u[i]) = y_u^R[i]$, where $\Re(y_u[i])$ denotes real part of $y_u[i]$. In the following section the MPOE and MMSE algorithms for the demodulation at the uth user with the above decision statistic $(y_u^R[i])$ is derived.

2.3.1 Signal model for MPOE prefiltering

This section compute the conditional probability of error ($P_{E|\mathbf{B}[i]}$) conditioned on transmitted bit vector sequence $\mathbf{B}[i] = \mathbf{b}[i], \mathbf{b}[i-1], \ldots$, where $\mathbf{b}[i] = b_1[i], b_2[i], \ldots, b_U[i]$ is the vector of bits transmitted at time instant i for all the users. The conditional mean ($\mu_{y_u^R|\mathbf{B}[i]}$) of the decision statistics of the received signal is

$$\mu_{y_u^R|\mathbf{B}[i]}[i] = E(y_u^R|\mathbf{B}[i]) = E\Bigg(\Re\Bigg[\sum_{k=0}^{N-1} s_{uk} \sum_{m=0}^{L_h^u-1} h_u[m][j_1]\Bigg(\sum_{l=0}^{L_z-1} z[l][j_2]. \cdot \sum_{v=1}^{U} A_v b_v[j_2]\tilde{\mathbf{s}}_v[iN+k-m-l]\Bigg)\Bigg]\Bigg) + E\Bigg(\Re\Bigg[\sum_{k=0}^{N-1} s_{uk}\eta_u[iN+k]\Bigg]\Bigg) \tag{2.11}$$

where j_1, j_2 are given in (2.10). By using the fact that $E[\Re(a)] = \Re(E[a])$ for any a, $E(\eta_u[iN+k]) = 0$ and except $\eta_u[iN+k]$ all other quantities are deterministic, the above equation can be written as

$$\mu_{y_u^R|\mathbf{B}[i]}[i] = E(y_u^R|\mathbf{B}[i]) = \Re\Bigg[\sum_{k=0}^{N-1} s_{uk} \sum_{m=0}^{L_h^u-1} h_u[m][j_1]\Bigg(\sum_{l=0}^{L_z-1} z[l][j_2]. \cdot \sum_{v=1}^{U} A_v b_v[j_2]\tilde{\mathbf{s}}_v[iN+k-m-l]\Bigg)\Bigg] \tag{2.12}$$

The conditional variance ($\sigma^2_{y_u^R|\mathbf{B}[i]}$) of the decision statistics is

$$\begin{aligned}
\sigma^2_{y_u^R|\mathbf{B}[i]}[i] &= var\Bigg(\Re\Bigg[\sum_{k=0}^{N-1} s_{uk} \sum_{m=0}^{L_h^u-1} h_u[m][j_1]\Bigg(\sum_{l=0}^{L_z-1} z[l][j_2] \sum_{v=1}^{U} A_v b_v[j_2]\tilde{\mathbf{s}}_v[iN+k-m-l]\Bigg)\Bigg] \\
&\qquad + \sum_{k=0}^{N-1} s_{uk}\eta_u[iN+k]\Bigg) \\
&= var\big(\Re \sum_{k=0}^{N-1} s_{uk}\eta_u[iN+k]\big) \\
&= N\frac{\sigma^2}{2}
\end{aligned} \tag{2.13}$$

For simplicity the variance of the channel noise is assumed to be constant for all users in (2.13). Now the conditional probability of error is

$$P_{E|\mathbf{B}[i]}[i] = Q\left(\frac{b_u[i]\mu_{y_u^R|\mathbf{B}[i]}[i]}{\sigma\sqrt{N/2}}\right) \tag{2.14}$$

where

$$Q(a) = \frac{1}{\sqrt{2\pi}} \int_a^\infty e^{\frac{-x^2}{2}} dx \tag{2.15}$$

The probability of correct detection is

$$Q\left(-\frac{b_u[i]\mu_{y_u^R|\mathbf{B}[i]}[i]}{\sigma\sqrt{N/2}}\right) \tag{2.16}$$

where we have used the fact that $1 - Q(x) = Q(-x)$.

2.4 Proposed Joint Prefiltering Algorithm

2.4.1 MPOE based prefilter

In joint prefiltering, we have one common prefilter and we would like to minimize the joint conditional probability of error for all users, namely,

$$P_{EJ}[i] = 1 - P[y_1^R \in \alpha_1, y_2^R \in \alpha_2, \ldots, y_U^R \in \alpha_U] \tag{2.17}$$

here $P[y_u^R \in \alpha_u]$ is the probability of correct demodulation for the uth user, α_u is decision region for symbol detection for uth user and J denotes joint probability of error. The conditioning markers and index i in right hand side of the above equation are dropped for notational ease. Since the noise vectors for all users are independent of each other, the joint conditional probability of error becomes

$$P_{EJ}[i] = 1 - P[y_1^R \in \alpha_1]P[y_2^R \in \alpha_2] \ldots P[y_U^R \in \alpha_U] \tag{2.18}$$

The decision region for BPSK constellation α_u, for any user u, is given by $(0,\ \infty)$ when $b_u[i] = +1$ and $(-\infty,\ 0)$ when $b_u[i] = -1$. Using (2.16) and (2.18), P_{Ej} can be written in closed form as

$$P_{EJ}[i] = 1 - \prod_{u=1}^{U} Q\left(-\frac{b_u[i]\mu_{y_u^R|\mathbf{B}[i]}[i]}{\sigma\sqrt{N/2}}\right) \tag{2.19}$$

Thus the MPOE optimization problem now becomes

$$min_{\mathbf{z}[.][i]} P_{EJ}[i] \tag{2.20}$$

i.e., the filter coefficients ($\mathbf{z}[.][i]$) of length L_z for each bit interval i is calculated by minimizing the above formulated probability of error. A stochastic gradient descent approach can now be used to minimize the joint probability of error with respect to the prefilter coefficients. In gradient descent, the prefilter coefficients are updated according to the rule

$$\mathbf{z}[.][i+1] = \mathbf{z}[.][i] - \mu\frac{\partial P_{EJ}}{\partial \mathbf{z}[.][i]} \tag{2.21}$$

where μ is an appropriately chosen step-size parameter. μ could be chosen adaptively based on the received signal energy.

2.4.2 MMSE based prefilter

Let us assume that $\mathbf{y}^R[i] = y_1^R[i],\ y_2^R[i],\ y_3^R[i], \ldots, y_U^R[i]$ is a vector of decision statistics of all users. Therefore, the cost function in case of MMSE based algorithm can be written as

$$\begin{aligned} \xi^2_{J|\mathbf{B}[i]}[i] &= E\left[\|(\mathbf{y}^R[i] - \mathbf{b}[i])\|^2|\mathbf{B}[i]\right] \\ &= \sum_{u=1}^{U} E\left[((y_u^R)^2 + b_u^2 - 2y_u^R b_u)|\mathbf{B}\right] \\ &= \sum_{u=1}^{U}\left[(E(y_u^R)|\mathbf{B})^2 + \sigma^2\frac{N}{2} + 1 - 2b_u(E(y_u^R|\mathbf{B}))\right] \end{aligned} \tag{2.22}$$

where b_u^2 = 1 as a consequence of BPSK modulation and $E(y_u^R|\mathbf{B})$ is given by (2.12). J in the above equation denotes the joint norm for all the users. Index i is dropped for notational simplifications. Now the filter weights are calculated from

$$min_{\mathbf{z}[.][i]}\xi^2_{J|\mathbf{B}[i]}[i] \tag{2.23}$$

An exactly similar optimization framework as of (2.21) is followed to optimize the MMSE prefilter weights.

2.5 Proposed Individual Prefiltering Model

In this model the data for user u after being spread is prefiltered by a FIR filter of length L_z^u with a discrete time impulse response $\mathbf{z}_u[.][n]$ as shown in Fig 2.2. The resulting modified signals are summed to form the final transmitted signal. The prefilters $\mathbf{z}_u[.][n]$, $u = 1, \ldots, U$ are designed such that the probability of error for that particular user is minimum at the receiver. Each user's prefilter is designed individually by taking into account the channel information and the transmit code of that particular user. The signal for user u at base station is

$$x_u(t) = A_u b_u(i) c_u(t - iT_{bit}), \qquad iT_{bit} \leq t < (i+1)T_{bit} \tag{2.24}$$

This signal is sampled at chip rate as given in (2.4) and will be processed through a prefilter $\mathbf{z}_u[.][i]$. The prefiltered signal corresponding to user u at time instant n is given by

$$x_u[n] \otimes \mathbf{z}_u[.][n] \tag{2.25}$$

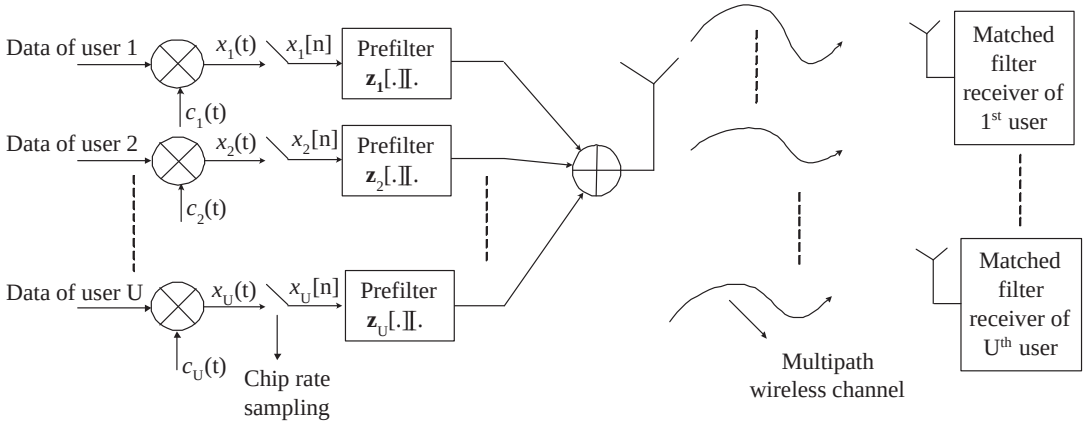

Figure 2.2: DS-CDMA system model for a multipath channel with individual prefiltering

Now the transmitted signal is given by

$$\sum_{u=1}^{U} x_u[n] \otimes \mathbf{z}_u[.][n] \tag{2.26}$$

By analyzing along the similar lines as in (2.6)-(2.9) and using (2.26) in place of $x[n]$, the received signal for user u after matched filtering is

$$y_u[i] = \left[\sum_{k=0}^{N-1} s_{uk} \sum_{m=0}^{L_h^u-1} h_u[m][j_1]\left(\sum_{l=0}^{L_z^u-1}\sum_{v=1}^{U} z_v[l][j_2]A_v b_v[j_2]\tilde{\mathbf{s}}_v[iN+k-m-l]\right)\right] + \sum_{k=0}^{N-1} s_{uk}\eta_u[iN+k] \tag{2.27}$$

where j_1 and j_2 are given by (2.10). The decision statistics is $\Re(y_u[i]) = y_u^R[i]$.

2.5.1 MPOE based prefilter

The probability of error for a user u ($P^u_{E|\mathbf{B}[i]}[i]$) can be formulated in the same way as given in (2.14), except the fact that the prefilter is different for each user.

$$P^u_{E|\mathbf{B}[i]}[i] = Q\left(\frac{b_u[i]\mu_{y_u^R|\mathbf{B}[i]}[i]}{\sigma\sqrt{N/2}}\right) \tag{2.28}$$

where $\mu_{y_u^R|\mathbf{B}[i]}[i]$ is conditional mean of decision statistics, which can be found by following the same procedure of (2.12) and is given by

$$\mu_{y_u^R|\mathbf{B}[i]}[i] = E(y_u^R|\mathbf{B}[i]) = E\left(\Re\left[\sum_{k=0}^{N-1} s_{uk}\sum_{m=0}^{L_h^u-1} h_u[m][j_1]. \cdot\left(\sum_{v=1}^{U}\sum_{l=0}^{L_z^u-1} z_v[l][j_2]A_v b_v[j_2]\tilde{\mathbf{s}}_v[iN+k-m-l]\right)\right]\right) \tag{2.29}$$

Now the filter of length L_z^u at time instant $i+1$ for user u is calculated using stochastic gradient search method as follows

$$\mathbf{z}_u[.][i+1] = \mathbf{z}_u[.][i] - \mu \frac{\partial P_E^u}{\partial \mathbf{z}_u[.][i]}, \qquad u \in \{1, 2, \ldots, U\} \tag{2.30}$$

2.5.2 MMSE based prefilter

The function to be optimized for the case of MMSE individual prefiltering can be written as

$$\begin{aligned} \xi^2_{u|\mathbf{B}[i]}[i] &= E\left[\|(y_u^R[i] - b_u[i])\|^2 | \mathbf{B}[i]\right] \\ &= E\left[((y_u^R)^2 + b_u^2 - 2y_u^R b_u) | \mathbf{B}\right] \\ &= (E(y_u^R)|\mathbf{B})^2 + \sigma^2 \frac{N}{2} + 1 - 2b_u E(y_u^R|\mathbf{B}) \end{aligned} \tag{2.31}$$

where $E(y_u^R[i]|\mathbf{B})$ is given in (2.29). Index i is dropped for notational simplifications. Now the individual MMSE prefilter coefficients are calculated using gradient search by minimizing $\xi^2_{u|\mathbf{B}[i]}[i]$ as follows

$$min_{\mathbf{z}_u[.][i]} \xi^2_{u|\mathbf{B}[i]}[i] \tag{2.32}$$

The similar procedure of (2.30) is followed to optimize the MMSE prefilter.

2.6 MRT Beamforming for Joint Prefilter

In MRT beamforming each user data will be transmitted through M antennas with M different weights as shown in Fig 2.3. Note that in Fig 2.3 prefilter (**z**[.][.]) is common for all users and all antennas. By following the same procedure in (2.4) the signal transmitted from base station for user u after chip rate sampling can be written as

$$x_u[n] = A_u b_u[n_N] \tilde{\mathbf{s}}_u[n] \tag{2.33}$$

The uth user data at mth path will be multiplied by MRT weight w_{um}. The weights w_{um} will be calculated at every bit interval and assumed to be constant over one bit interval because channel is constant over one bit interval. Now the signal transmitted for user u at mth MRT path is

$$x'_{um}[n] = A_u b_u[n_N] \tilde{\mathbf{s}}_u[n] w_{um}[n] \tag{2.34}$$

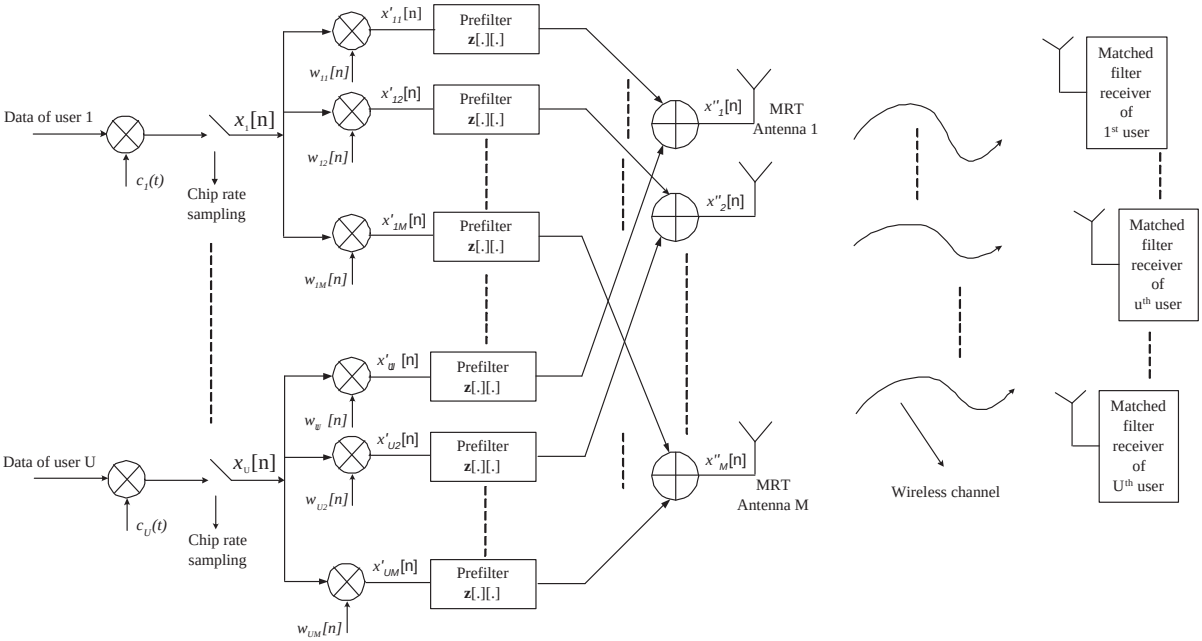

Figure 2.3: DS-CDMA system model with joint transmitter prefiltering and MRT beamforming

The MRT weights for user u is concatenated in vector format as

$$\mathbf{w}_u[i] = \big[w_{u1}[i], w_{u2}[i], \ldots, w_{uM}[i]\big]^T \tag{2.35}$$

Assume that the wireless channel between M MRT transmitter antennas and a mobile receiver antenna for user u is $\mathbf{h}_u[i]$ which can be represented as

$$\mathbf{h}_u[i] = \big[h_{u1}[i], h_{u2}[i], \ldots, h_{uM}[i]\big]^T \tag{2.36}$$

where $h_{um}[i]$, ($u = 1, \ldots, U,\ m = 1, \ldots, M$) is the channel coefficient between mth MRT path of uth user and receiver antenna at ith bit interval. The channel is assumed to be a single coefficient ($L_h^u = 1$) FIR filter with the coefficient being complex Gaussian [38]. Hence the channel is flat fading in MRT model. Note that though channel is flat fading, the prefilter ($L_z > 1$) at the transmitter to mitigate MAI, itself is a source of ISI, hence still ISI is the factor of concern. Flat fading is assumed to simplify the MRT weight calculation. MRT can be applied even when the channel is frequency selective. In case of frequency selective channel we can employ MC-CDMA (or CDMA-OFDM) access mechanism to convert a frequency selective channel to a set of flat fading channels and then use MRT [32]. However, such an analysis is out of scope of this work.

Assume that the transmit beamforming vector is $\mathbf{w}$, where the time index is dropped for notational convenience. The instantaneous SNR at the receiver is given by $\mathbf{w}^H(\mathbf{h}\mathbf{h}^H)\mathbf{w}$, where

the superscript H denotes Hermitian transpose. Now, among all possible unit-norm transmit beamforming vectors $\mathbf{w}$, the one which maximizes the instantaneous received SNR is the dominant eigenvector of $\mathbf{h}\mathbf{h}^H$. Since $\mathbf{h}\mathbf{h}^H$ is a rank 1 matrix the dominant eigen vector computation of $\mathbf{h}\mathbf{h}^H$ would be rather simple (in fact dominant eigen vector would be proportional to $\mathbf{h}$ itself) [32]. Once the weight vector $\mathbf{w}$ is computed, the next step is to determine the prefilter coefficients ($\mathbf{z}[.][i]$). The total signal transmitted for all U users after prefiltering is

$$x'[n] = \left[\sum_{u=1}^{U}\sum_{m=1}^{M} A_u b_u[n_N]\tilde{\mathbf{s}}_u[n]w_{um}[n]\right] \otimes \mathbf{z}[.][n] \tag{2.37}$$

By using the linearity property of convolution the above equation can be written as

$$\begin{aligned} x'[n] &= \sum_{u=1}^{U}\Big(A_u b_u[n_N]\tilde{\mathbf{s}}_u[n]w_{u1}[n] \otimes \mathbf{z}[.][n]\Big) + \sum_{u=1}^{U}\Big(A_u b_u[n_N]\tilde{\mathbf{s}}_u[n]w_{u2}[n] \otimes \mathbf{z}[.][n]\Big) + \ldots \\ &\quad + \sum_{u=1}^{U}\Big(A_u b_u[n_N]\tilde{\mathbf{s}}_u[n]w_{uM}[n] \otimes \mathbf{z}[.][n]\Big) \end{aligned} \tag{2.38}$$

Now the signal transmitted from MRT antenna m is

$$x''_m[n] = \sum_{u=1}^{U}\Big(A_u b_u[n_N]\tilde{\mathbf{s}}_u[n]w_{um}[n] \otimes \mathbf{z}[.][n]\Big) \tag{2.39}$$

The $x[n]$ in (2.6) can be replaced with (2.37) and the similar steps of (2.8) and (2.9) can be followed to find the received signal at the receiver of uth user ($y_u[i]$)

$$\begin{aligned} y_u[i] = \sum_{k=0}^{N-1} s_{uk} \sum_{l=0}^{L_z-1} z[l][j_2] \sum_{v=1}^{U}\sum_{m=1}^{M} A_v b_v[j_2]\tilde{\mathbf{s}}_v[iN+k-l]w_{vm}[j_2]h_{um}[j_1] \\ + \sum_{k=0}^{N-1} s_{uk}\eta_u[iN+k] \end{aligned} \tag{2.40}$$

since $L_h^u = 1$, j_1 and j_2 are given by

$$j_1 = \left\lfloor \frac{iN+k}{N} \right\rfloor, \quad j_2 = \left\lfloor \frac{iN+k-l}{N} \right\rfloor \tag{2.41}$$

Now the decision statistics is $\Re(y_u) = y_u^R$. The MPOE and MMSE based algorithms are derived in the following sections.

2.6.1 MRT beamforming for MPOE joint prefilter

By using same procedure of (2.12) and replacing $y_u[i]$ of (2.12) with (2.40) the conditional mean of the decision statistics is given by

$$\mu_{y_u^R|\mathbf{B}[i]}[i] = E\Bigg[\Re\Bigg(\sum_{k=0}^{N-1} s_{uk} \sum_{l=0}^{L_z-1} z[l][j_2] \sum_{v=1}^{U}\sum_{m=1}^{M} A_v b_v[j_2]\tilde{\mathbf{s}}_v[iN+k-l]. \\ .w_{vm}[j_2]h_{um}[j_1]\Bigg)\Bigg] \tag{2.42}$$

The conditional variance of the decision statistics is given by

$$\begin{aligned}\sigma^2_{y_u^R|\mathbf{B}[i]}[i] &= var\left(\Re\left[\sum_{k=0}^{N-1} s_{uk}\eta_u[iN+k]\right]\right) \\ &= N\frac{\sigma^2}{2}\end{aligned} \tag{2.43}$$

The probability of error at particular instant of time i for user u is

$$P_{E|\mathbf{B}[i]}[i] = Q\left(\frac{b_u[i]\mu_{y_u^R|\mathbf{B}[i]}[i]}{\sigma\sqrt{N/2}}\right) \tag{2.44}$$

The joint probability of error P_{Ej} can be computed using (2.44) in (2.18). P_{Ej} can now be used as cost function in (2.21) to determine the prefilter coefficients as follows:

$$min_{\mathbf{z}[.][i]} P_{EJ}[i] \tag{2.45}$$

2.6.2 MRT beamforming for MMSE joint prefilter

The find the MMSE cost function we can follow the similar procedure of Section 2.4.2 with $y_u[i]$ of (2.40).

$$\begin{aligned}\xi^2_{J|\mathbf{B}[i]}[i] &= \sum_{u=1}^{U} E\Big[((y_u^R)^2 + b_u^2 - 2y_u^R b_u)|\mathbf{B}\Big] \\ &= \sum_{u=1}^{U}\Big[(E(y_u^R)|\mathbf{B})^2 + \sigma^2\frac{N}{2} + 1 - 2b_u E(y_u^R|\mathbf{B})\Big]\end{aligned} \tag{2.46}$$

In the above equation index i is dropped in the right hand side for notational convenience. The above formulated mean square error will be used as the cost function in (2.21) to determine the prefilter weights.

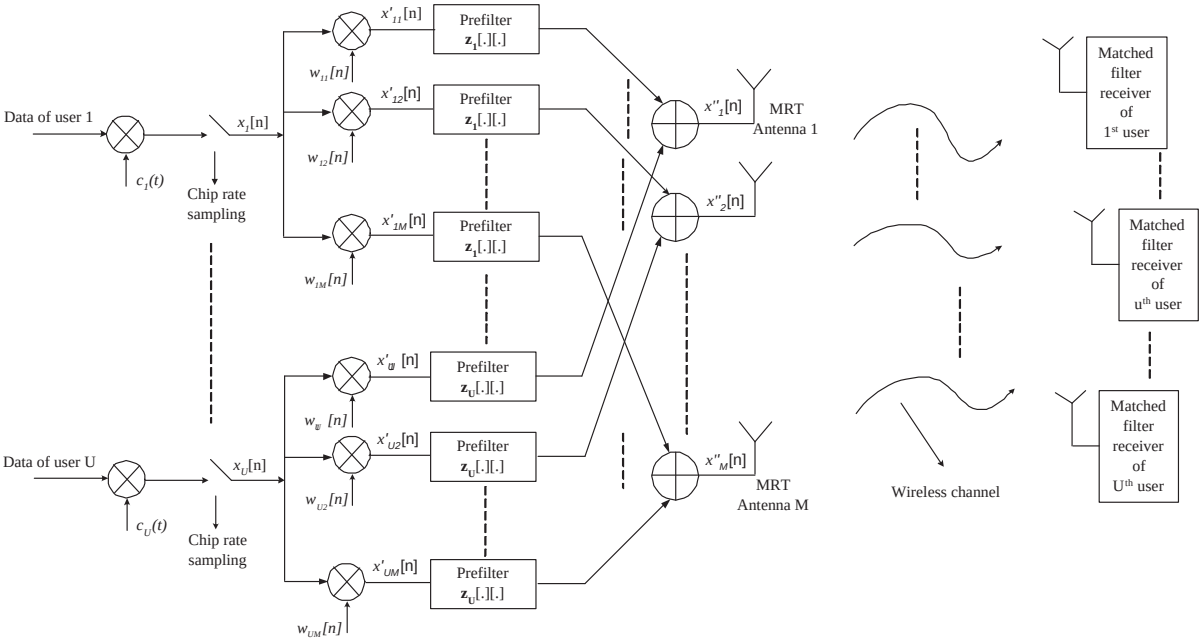

Figure 2.4: DS-CDMA system model with individual prefiltering and MRT beamforming

2.7 MRT Beamforming for Individual Prefilter

Each user is assumed to have M MRT paths with an individual prefilter for each user as shown in Fig 2.4. Note that in Fig 2.4 the prefilter ($\mathbf{z}_u[.][.]$) is common for all M MRT paths of user u but different for different users. The total transmitted signal is

$$x'[n] = \sum_{u=1}^{U} \sum_{m=1}^{M} (A_u b_u(i) \tilde{\mathbf{s}}_u[n] w_{um}[n] \otimes \mathbf{z}_u[.][n]) \tag{2.47}$$

By following the same steps of (2.37)-(2.39), the signal transmitted from MRT antenna m is

$$x''_m[n] = \sum_{u=1}^{U} \Big(A_u b_u[n_N] \tilde{\mathbf{s}}_u[n] w_{um}[n] \otimes \mathbf{z}_u[.][n] \Big) \tag{2.48}$$

By following similar analysis in Sections 2.5 and 2.6, we can derive the individual prefilter weights. The received signal after matched filtering, by following (2.4)-(2.9) and by replacing $x[n]$ in (2.6) with (2.47) is

$$y_u[i] = \sum_{k=0}^{N-1} s_{uk} \sum_{l=0}^{L_z^u-1} \sum_{v=1}^{U} \sum_{m=1}^{M} z_v[l][j_2] A_v b_v[j_2] \tilde{\mathbf{s}}_v[iN+k-l] w_{vm}[j_2] h_{um}[j_1] + \sum_{k=0}^{N-1} s_{uk} \eta_u[iN+k] \tag{2.49}$$

where j_1 and j_2 are same as in (2.41).

2.7.1 MRT beamforming for MPOE individual prefilter

The conditional mean and variance of the decision statistics can be found in same way as that of (2.12) and (2.13) and are given by

$$\mu_{y_u^R|\mathbf{B}[i]}[i] = E(y_u^R|\mathbf{B}[i]) = \Re\Bigg(E\Big[\sum_{k=0}^{N-1} s_{uk}\Big(\sum_{l=0}^{L_z^u-1}\sum_{v=1}^{U}\sum_{q=1}^{M} z_{vq}[l][j_2]A_v b_v[j_2]. \\ .h_{vq}[j_1]\tilde{\mathbf{s}}_{vq}[iN+k-l]w_{vq}[j_2]\Big)\Big]\Bigg) \tag{2.50}$$

$$\sigma^2_{y_u^R|\mathbf{B}[i]}[i] = var\left(\Re\Big[\sum_{k=0}^{N-1} s_{uk}\eta_u[iN+k]\Big]\right) = N\frac{\sigma^2}{2} \tag{2.51}$$

The probability of error at particular instant of time i for uth user's data is

$$P^u_{E|\mathbf{B}[i]}[i] = Q\left(\frac{b_u[i]\mu_{y_u^R|\mathbf{B}[i]}[i]}{\sigma\sqrt{N/2}}\right) \tag{2.52}$$

$P^u_{E|\mathbf{B}[i]}$ can now be used as cost function in stochastic gradient search of (2.30) to find the prefilter coefficient $\mathbf{z}_u[.][i]$.

2.7.2 MRT beamforming for MMSE individual prefilter

An approach similar to that of Section 2.4.2 can be followed to find the MMSE cost function. By replacing $y_u[i]$ in Section 2.4.2 with (2.49) the cost function can be written as

$$\xi^2_{J|\mathbf{B}[i]}[i] = \left[(E(y_u^R)|\mathbf{B})^2 + \sigma^2\frac{N}{2} + 1 - 2b_u E(y_u^R|\mathbf{B})\right] \tag{2.53}$$

where index i is dropped for notational ease. The above formulated cost function $\xi^2_{J|\mathbf{B}[i]}[i]$ can be used in (2.30) to determine the prefilter weights.

The prefilter coefficients are normalized at every instant in both MPOE and MMSE algorithms in all the proposed models to reduce the effect of power boosting. The normalization is carried out by dividing the prefilter coefficient vector by its norm.

2.8 System Model with Rake Receiver

The system model with rake receiver is shown in Fig 2.5. The main objective of the prefiltering system is to avoid the channel estimation at the receiver. On the contrary, MRC demands

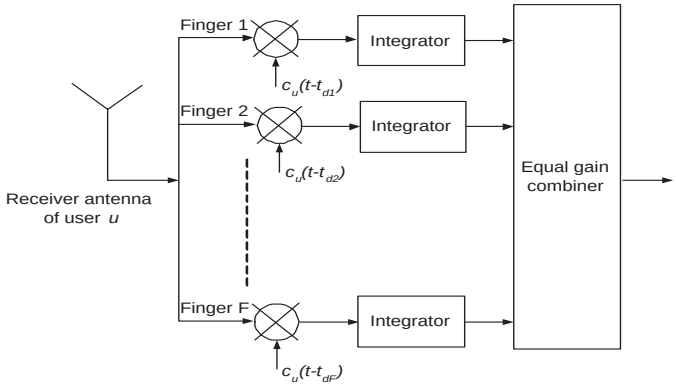

Figure 2.5: DS-CDMA system with rake receiver

channel estimation at the receiver. Therefore, we use simple Equal Gain Combiner (EGC) rake receiver. The rake receiver fingers of the uth user are matched with the delayed version of spreading waveform $c_u(t)$. All fingers are assumed to receive signal from one common receiver antenna as shown in Fig 2.5. The spreading code of uth user is chosen such that

$$\sum_{n=1}^{N} c_u(nT_c - t_{df})c_u(nT_c - t_{dF}) \approx 0 \tag{2.54}$$

where t_{df} and t_{dF} are the estimated excess propagation delay at any two fingers f and F of rake receiver. In general the excess propagation delays are multiples of T_c. Now the received signal for the joint prefiltering system of Fig 2.1 is

$$y_u[i] = \sum_{f=1}^{F}\sum_{k=0}^{N-1} s_{uk}^{(f)} \sum_{m=0}^{L_h^u-1} h_u[m][j_1]\left(\sum_{l=0}^{L_z-1} z[l][j_2] \sum_{v=1}^{U} A_v b_v[j_2]\tilde{\mathbf{s}}_v[iN+k-m-l]\right) + \sum_{f=1}^{F}\sum_{k=0}^{N-1} s_{uk}^{(f)}\eta_u^{(f)}[iN+k] \tag{2.55}$$

where F is the number of fingers and $s_{uk}^{(f)}$ is the sampled version of spreading code corresponding to fth finger and $\eta_u^{(f)}[.]$ is the additive white Gaussian noise at fth finger of uth user.

Received signal corresponding to individual prefiltering system and systems with MRT can also be written similarly. The probability of error and mean square error can be derived by following steps (2.12)-(2.14) and Section 2.4.2. The simulation results are presented in the following section.

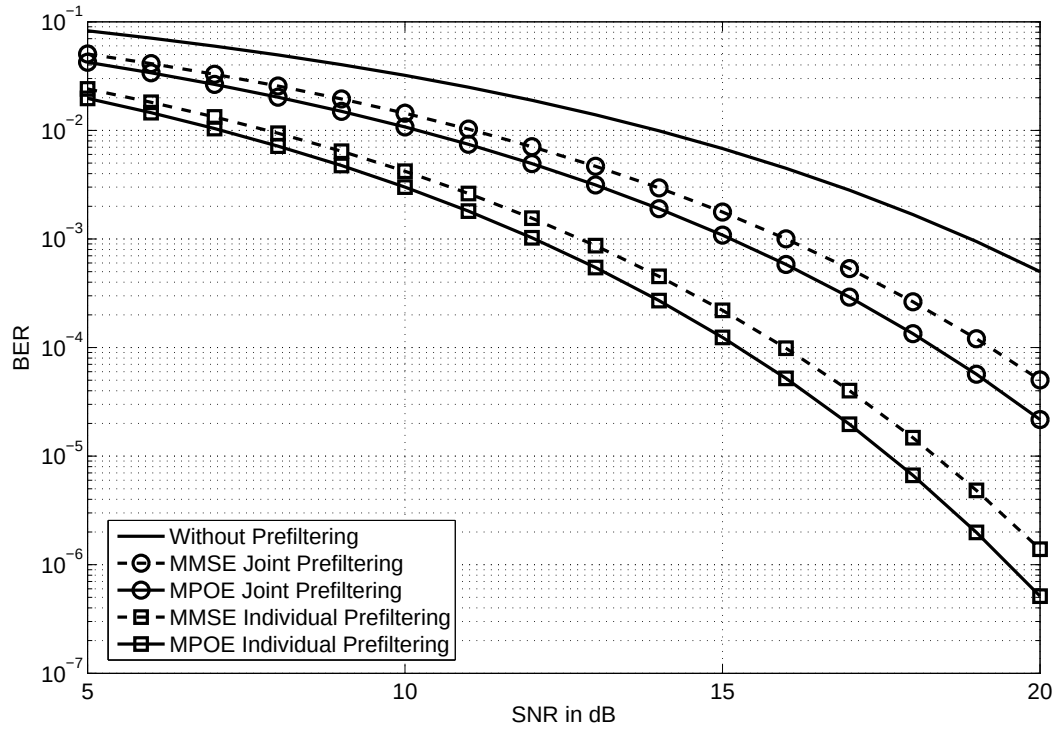

Figure 2.6: Performance of MPOE and MMSE transmitter prefiltering with 16 users

2.9 Simulations and Results

Extensive simulations were carried out to calculate the prefilter coefficients and the corresponding BER for various SNRs for MPOE and MMSE prefilters. BPSK constellation for bits was assumed with equal probability for bits +1 and -1. The processing gain N, was assumed to be 32 and the number of users was taken to be 16. Orthogonal spreading codes were assumed. Channel was assumed to be complex Gaussian with both real and imaginary parts follow $i.i.d$ Gaussian distribution with σ value as 0.1655 and mean as 0.5. Channel length, L_h^u was taken to be 4 for systems without MRT and 1 for systems with MRT. The prefilter length was assumed to be 5 (for both joint and individual prefiltering). Step size parameter μ was calculated based on the received signal energy. We chose μ as $10^{-2} \times received\ signal\ energy$.

2.9.1 BER performance of joint and individual prefiltering

BER performance for various SNRs were plotted for both individual and joint prefiltering. BER was calculated independently for each channels and BERs of 1000 such channels were averaged for each SNR. All the users were assumed to transmit with equal amplitude. The BER perfor-

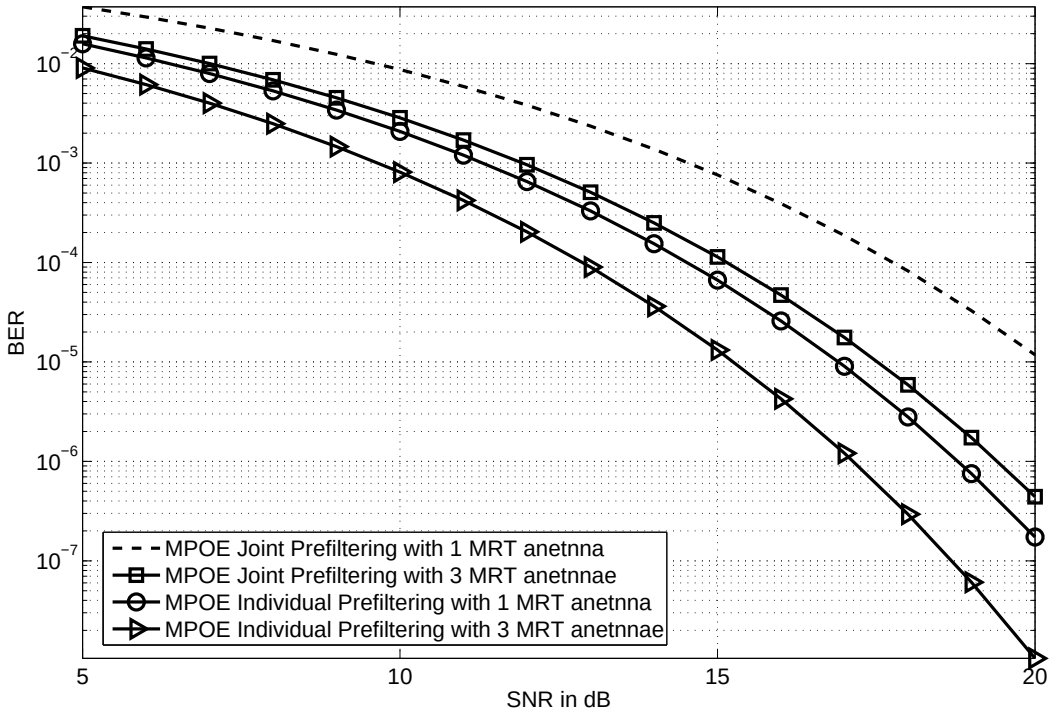

Figure 2.7: BER performance for various SNRs with MRT beamforming

mance is shown in Fig 2.6. From Fig 2.6, we observe that individual prefiltering performs much better than joint prefiltering and MPOE prefiltering always performs better than that of MMSE prefiltering. This is because individual prefilter has U prefilters and the length of the individual prefilter is effectively U times that of corresponding joint prefilter. Therefore, the MAI and ISI are better compensated and also the individual probability of error is minimized in the case of individual prefilter and thus the better performance. On the other hand joint prefilter jointly minimizes all the users' probability of error using just single prefilter. Hence, its performance is inferior compared to individual prefilter model.

2.9.2 MRT results and discussions

The BER performances of MPOE joint and individual prefiltering with MRT beamforming were plotted. Since MPOE performs better than MMSE at all SNRs we have considered only MPOE case for MRT beamforming to better visualize the plots. Results for varying SNRs is shown in Fig 2.7. Single and 3 MRT weights (paths) for each user were assumed at the base station. From Fig 2.6 and Fig 2.7 one can infer that BER of MPOE prefilter with MRT is better than

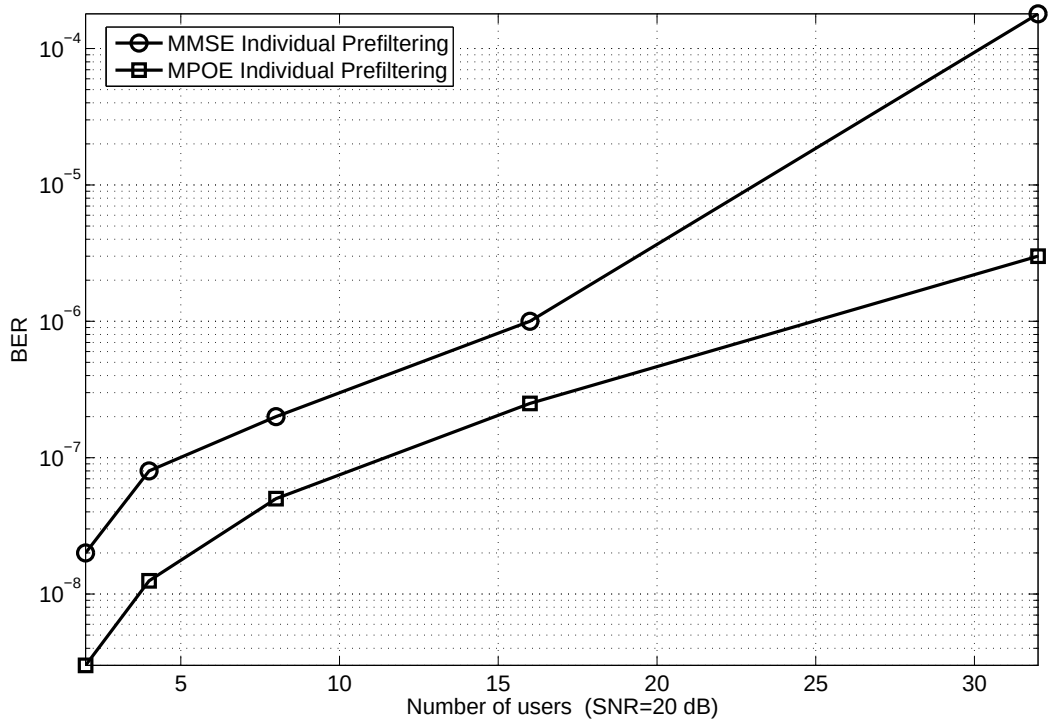

Figure 2.8: BER against number of users for a fixed SNR of $20\ dB$

that of MPOE without MRT. This is because the weights are proportional to the dominant eigen vector of $\mathbf{h}\mathbf{h}^H$. Hence we will transmit the signal proportional to channel coefficient, which will mitigate the channel effect. The performance improvements are quite significant at higher SNRs. Better performance could be obtained by increasing the number of MRT weights per user but at the cost of higher complexity. Though we increase the number of weights at the transmitter for each user, MRT beamforming will not increase the transmission power at base station since the weights are equal to maximum eigenvector which has unit energy.

Since the individual prefiltering offers better performance than joint prefiltering, we will consider the performance of individual prefiltering (without MRT) under a general channel model (MAI+ISI) for various scenarios in the following sub sections.

2.9.3 Varying number of users

The effect of increasing the number of users in the system for a SNR of $20\ dB$ is shown in Fig 2.8. It is evident that more the number of users, more the interference will be seen in the system.

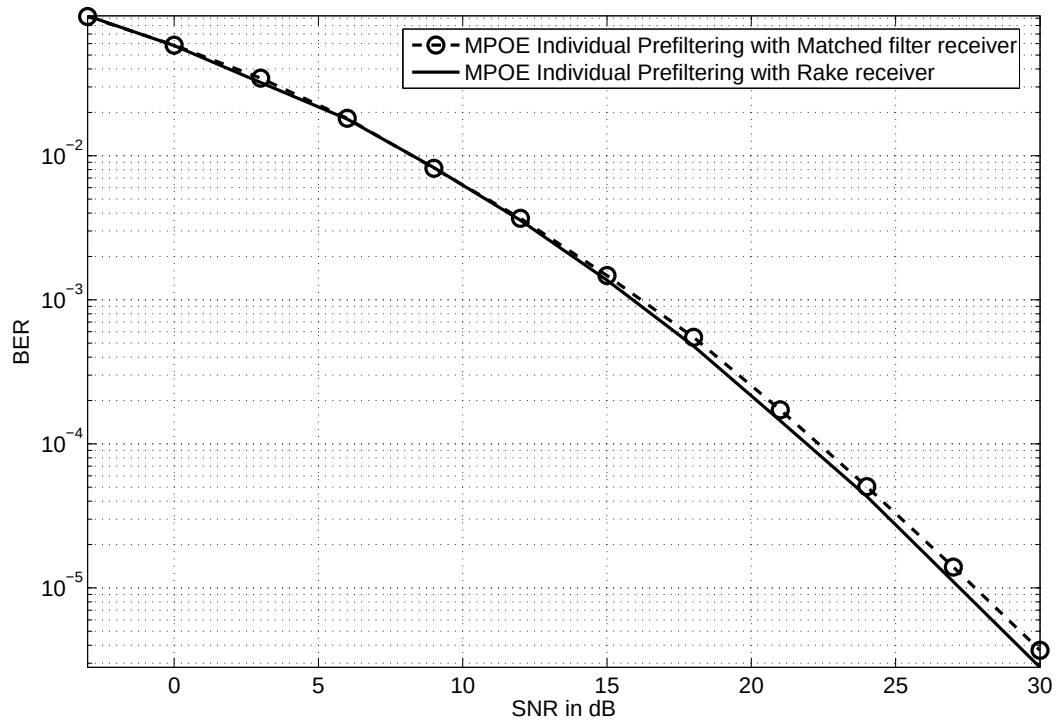

Figure 2.9: BER comparison of MPOE individual prefiltering systems with rake receiver and conventional matched filter

Therefore, as the number of users increases the BER performance reduces. Moreover, as the number of users increases the performance difference between MPOE and MMSE prefilters increases. This is because MPOE prefilter better compensates MAI and ISI in the increasing multiuser interference environment.

2.9.4 Performance comparison with rake receiver

The proposed MPOE individual prefiltering system model is compared with the MPOE individual prefiltering system which uses rake receiver. Rake receiver with 3 fingers is considered. Conventional autocorrelation based path search algorithm is used to estimate the excess propagation delay at each finger. The performances of both the proposed system and the prefiltering system with EGC rake receiver are shown in Fig 2.9. One can infer that while using prefiltering the conventional single user detector performance is very close to the EGC rake receiver's performance. This can be explained as follows:

1. Since we use prefiltering, the multipath effect is precompensated. In other words the precoder and channel combination is effectively a single tap channel. Therefore, the

diversity gain obtained due to multipath effect is less significant.

2. Any additional gain will not be obtained by channel equalization at the receiver and transmitter simultaneously. Equalization at one end would be the optimal solution.

3. Since a multiuser scenario is assumed and the system is interference limited, the performance gain from EGC is rather minimal in the case of interference limited system.

2.10 Conclusion

Two system models have been proposed for MPOE and MMSE based prefiltering technique for DS-CDMA systems under a general channel conditions. Simulation results show that MPOE prefilter outperforms MMSE prefilter in terms of BER and also the individual prefiltering is superior to that of corresponding joint prefiltering. The prefiltering performance is analyzed by varying number of users. And also the proposed system performance is compared with the prefiltering system which employs rake receiver and found that the performance is almost similar in both the system models. The performance of the proposed system is further enhanced by using MRT beamforming so that it can be considered for practical implementation.

Chapter 3

MPOE Prefiltering and MRT Beamforming for Statistical Channel Model

A precoding filter based only on the statistical knowledge of the channel for DS-CDMA systems is proposed in this chapter. The proposed prefilter (precoder) minimizes the probability of error in downlink multiuser transmission. The receiver at mobile terminal is assumed to be a simple matched filter to reduce the computational complexity. By following the similar procedure in the previous chapter, two approaches have been investigated for the proposed algorithm. The first approach has a system model where a common FIR precoding filter is used for all users and the prefilter is optimized to jointly minimize the probability of error of all users. The second approach has separate precoders for each user which are obtained by minimizing the probability of error for the respective user. In order to fully utilize the knowledge available at the transmitter, in both approaches the filter weights are computed conditioned on the transmitted bit vector sequence, this makes the computation of the optimal prefilter coefficients linear in the number of users. In addition to the above, the performance of the proposed statistical channel prefilter models are further enhanced by using MRT beamforming strategy. The results of the proposed approach based on the statistical channel model are compared with the results based on assuming complete knowledge of the channel. Simulation results clearly show that precoders based only on the statistical knowledge of the channel provide acceptable BERs. Also the proposed prefilter achieves better performance compared to existing algorithms.

3.1 Introduction

In this work, we explore a prefiltering scheme at the base station transmitter when only statistical parameters of the channel available at the base station. Prefilter design is less complicated when the transmitter has complete Channel State Information (complete CSI) $i.\ e.$ the transmitter knows channel coefficients at every instant as explained in Chapter 2. The drawback with this assumption is that it requires significant amount of feedback from the receiver to the transmitter [40, 48, 49]. This is especially true in Frequency Division Duplex (FDD) channel where the downlink and uplink channels are uncorrelated. In this chapter, we explore the approach of working only with the first and second order statistics of the channel at the transmitter for optimizing the precoding filter [50–52]. The basic assumption is that the first and second order statistics of the channel change at a much slower rate than the channel coefficient itself. Hence, it is easier to track the statistics of the channel which makes practical implementation feasible.

As explained in the previous chapter, two approaches are considered for prefiltering: The first one considers the common prefilter for all users as shown in Fig 2.1. To further improve the performance significantly, a second approach is considered wherein an individual prefilter is used for each user as shown in Fig 2.2. The standard single user receiver (conventional matched filter detector) is used in our model in order to significantly reduce the receiver complexity [9, 16, 26–28]. By following the similar argument as in previous chapter the MPOE optimization is considered in transmitter prefilter design in this chapter too. MPOE prefilter is designed by conditioning the filter weights on the transmitted bits [19]. In addition, a novel MRT beamforming is also developed by taking advantage of the available statistical knowledge of the channel, to improve the Bit Error Rate (BER) performance of the proposed prefilter models.

The contributions of this chapter are follows:

1. We develop MPOE/MMSE based joint prefilters by assuming only the first order and second order statistics of the channel.

2. Also we propose an individual prefiltering system model where we employ individual prefilter for each users. The prefilter coefficients are optimized using MPOE/MMSE criteria. A minimal complexity receiver is employed in all the prefiltering models.

3. The performance of the proposed prefilters are further improved by using MRT beamforming for the system having only statistical knowledge of the channel. The proposed

system considerably differs from other works on maximum ratio transmission where complete CSI has been assumed [39, 41–43, 49, 53].

3.1.1 Notations

In this chapter $\lfloor . \rfloor$ denotes floor operation and $\lceil . \rceil$ is ceiling operation. Superscript T denotes transpose and bold small letters denote sequence/vector. Superscript * and H denote complex conjugate and Hermitian transpose, respectively. Parentheses $[.]$, $(.)$ used in vector and signal arguments to denote discrete samples and continuous signals, respectively however, when used in functions they do not have any specific meanings. Superscripts I, Q denote in-phase and quadrature-phase components respectively. $E(.)$ is statistical expectation, $var(.)$ is variance, $\Re(.)$ is real part of complex number and $\Im(.)$ is imaginary part of complex number.

3.2 Signal Model

Consider a similar DS-CDMA system model of Chapter 2 as shown in Fig 2.1. By following similar steps of (2.2)-(2.9) the received signal at the uth user after matched filtering is

$$y_u[i] = \sum_{k=0}^{N-1} s_{uk} \sum_{m=0}^{L_h^u-1} h_u[m][j_1] \sum_{l=0}^{L_z-1} z[l][j_2] \sum_{v=1}^{U} A_v b_v[j_2] \tilde{s}_v[iN+k-m-l] + \sum_{k=0}^{N-1} s_{uk} \eta_u[iN+k] \tag{3.1}$$

where

$$j_1 = \left\lfloor \frac{iN+k-m}{N} \right\rfloor, \quad j_2 = \left\lfloor \frac{iN+k-m-l}{N} \right\rfloor \tag{3.2}$$

In (5.5), $\sum_{m=0}^{L_h^u-1}$ gives the Inter Symbol Interference (ISI) term due to the multipath channel while $\sum_{v=1}^{U}$ is the Multiple Access Interference (MAI) component due to multiuser transmissions. Since BPSK constellations are used for input data, the decision statistics is given by $\Re(y_u[i]) = y_u^R[i]$. In the following sections we shall derive the MPOE and MMSE algorithms for the demodulation at the uth user with the above decision statistic $(y_u^R[i])$.

3.3 Proposed Joint Prefiltering Model

In the prefilter design only the first order and second order statistics of the downlink channel are assumed at the base station.

3.3.1 MPOE based prefiltering

We first compute the conditional probability of error ($P_{E|\mathbf{B}[i]}$) conditioned on transmitted bit vector sequence $\mathbf{B}[i] = \mathbf{b}[i], \mathbf{b}[i-1], \ldots$, where $\mathbf{b}[i] = b_1[i], b_2[i], \ldots, b_U[i]$ is the vector of bits transmitted at time instant i for all the users. Let us define mean of the channel coefficient as

$$\gamma_u[m][i] = E(h_u[m][i]) \tag{3.3}$$

and the second order statistics as

$$R_u[m_1, m_2][i_1, i_2] = E\left[h_u[m_1][i_1]h_u^*[m_2][i_2]\right],\ \tilde{R}_u[m_1, m_2][i_1, i_2] = E\left[h_u[m_1][i_1]h_u[m_2][i_2]\right] \tag{3.4}$$

$$\begin{aligned} C_u[m_1, m_2][i_1, i_2] &= E\left[(h_u[m_1][i_1] - \gamma_u[m_1][i_1])(h_u^*[m_2][i_2] - \gamma_u^*[m_2][i_2])\right] \\ \tilde{C}_u[m_1, m_2][i_1, i_2] &= E\left[(h_u[m_1][i_1] - \gamma_u[m_1][i_1])(h_u[m_2][i_2] - \gamma_u[m_2][i_2])\right] \end{aligned} \tag{3.5}$$

The mean ($\mu_{y_u^R|\mathbf{B}[i]}$) of the decision statistic ($y_u^R[i]$) is given by

$$\begin{aligned} \mu_{y_u^R|\mathbf{B}[i]}[i] = E(y_u^R|\mathbf{B}[i]) = E\Bigg[\Re\Bigg(\sum_{k=0}^{N-1} s_{uk} \sum_{m=0}^{L_h^u-1} h_u[m][j_1] \sum_{l=0}^{L_z-1} z[l][j_2] \sum_{v=1}^{U} A_v b_v[j_2]\ \tilde{s}_v[iN+k-m-l] \\ + \sum_{k=0}^{N-1} s_{uk}\eta_u[iN+k]\Bigg)\Bigg] \end{aligned} \tag{3.6}$$

By using the fact that $E[\Re(a)] = \Re(E[a])$ for any a, $E(\eta_u[iN+k]) = 0$ and except $h_u[m][j_1]$, $\eta_u[iN+k]$ all other quantities are deterministic, the above equation can be written as

$$\mu_{y_u^R|\mathbf{B}[i]}[i] = \Re\left[\sum_{k=0}^{N-1} s_{uk} \sum_{m=0}^{L_h^u-1} \gamma_u[m][j_1] \sum_{l=0}^{L_z-1} z[l][j_2] \sum_{v=1}^{U} A_v b_v[j_2]\tilde{s}_v[iN+k-m-l]\right] \tag{3.7}$$

Without loss of generality we can assume that channel $h_u[.][.]$ and noise $\eta_u[.]$ follow independent distribution. Now by using the fact that $var(a+b) = var(a) + var(b)$ when a and b are independent, the conditional variance of the decision statistics ($\sigma^2_{y_u^R|\mathbf{B}[i]}$) is given by

$$\begin{aligned} \sigma^2_{y_u^R|\mathbf{B}[i]}[i] = var\left[\Re\left(\sum_{k=0}^{N-1} s_{uk} \sum_{m=0}^{L_h^u-1} h_u[m][j_1] \sum_{l=0}^{L_z-1} z[l][j_2] \sum_{v=1}^{U} A_v b_v[j_2]\tilde{s}_v[iN+k-m-l]\right)\right] \\ + var\left[\sum_{k=0}^{N-1} s_{uk}\eta_u[iN+k]\right] \end{aligned} \tag{3.8}$$

Since the receiver noises are assumed to be zero mean $i.i.d$ AWGN with equal variance (i.e, σ) and also the spreading coefficients s_{uk} is either +1 or -1 and deterministic we can write,

$$var\left[\sum_{k=0}^{N-1} s_{uk}\eta_u[iN+k]\right] = N\frac{\sigma^2}{2} \tag{3.9}$$

where we have used linearity property of variance operation over independent random variables. Let

$$\sigma^2_{\tilde{y}_u^R|\mathbf{B}[i]}[i] = var\left(\Re\left[\sum_{k=0}^{N-1} s_{uk}\sum_{m=0}^{L_h^u-1} h_u[m][j_1]\sum_{l=0}^{L_z-1} z[l][j_2]\left(\sum_{v=1}^{U} A_v b_v[j_2]\ \tilde{s}_v[iN+k-m-l]\right)\right]\right) \tag{3.10}$$

This can be rewritten as

$$\begin{aligned}\sigma^2_{\tilde{y}_u^R|\mathbf{B}[i]}[i] &= var\left(\Re\left[\sum_{k=0}^{N-1}\sum_{m=0}^{L_h^u-1}\sum_{l=0}^{L_z-1}\sum_{v=1}^{U} s_{uk}h_u[m][j_1]z[l][j_2]A_v b_v[j_2]\ \tilde{s}_v[iN+k-m-l]\right]\right)\\ &\triangleq var\left(\Re\left[\sum_{k,m,l,v} h_u[m][j_1]f_u[k,m,l,v]\right]\right)\end{aligned} \tag{3.11}$$

where $f_u[k,m,l,v] = s_{uk}z[l][j_2]A_v b_v[j_2]\ \tilde{s}_v[iN+k-m-l]$, the indices j_1, j_2 are given in (3.2) and the sum $\sum_{k,m,l,v} = \sum_{k=0}^{N-1}\sum_{m=0}^{L_h^u-1}\sum_{l=0}^{L_z-1}\sum_{v=1}^{U}$. By using the fact that $var(a) = E[a-E(a)]^2$ for any a and $f_u[k,m,l,v]$ is deterministic variable, (3.11) can be written as

$$\begin{aligned}\sigma^2_{\tilde{y}_u^R|\mathbf{B}[i]}[i] &= E\left[\left(\Re\left[\sum_{k,m,l,v}(h_u[m][j_1]-\gamma_u[m][j_1])f_u[k,m,l,v]\right]\right)^2\right]\\ &= E\left[\Re\left(\sum_{k_1,m_1,l_1,v_1}(h_u[m_1][j_{11}]-\gamma_u[m_1][j_{11}])f_u[k_1,m_1,l_1,v_1]\right).\right.\\ &\qquad\left.\Re\left(\sum_{k_2,m_2,l_2,v_2}(h_u[m_2][j_{21}]-\gamma_u[m_2][j_{21}])f_u[k_2,m_2,l_2,v_2]\right)\right]\end{aligned} \tag{3.12}$$

where,

$$j_{11} = \left\lfloor\frac{iN+k_1-m_1}{N}\right\rfloor \quad j_{21} = \left\lfloor\frac{iN+k_2-m_2}{N}\right\rfloor \tag{3.13}$$

For notational convenience let us assume

$$\begin{aligned}h_1 &= h_u[m_1][j_{11}],\ \ \gamma_1 = \gamma_u[m_1][j_{11}],\ \ f_1 = f_u[k_1,m_1,l_1,v_1]\\ h_2 &= h_u[m_2][j_{21}],\ \ \gamma_2 = \gamma_u[m_2][j_{21}],\ \ f_2 = f_u[k_2,m_2,l_2,v_2]\end{aligned} \tag{3.14}$$

Since the channel coefficients of different users are $i.i.d$, from (3.12), (5.17) we can get

$$\sigma^2_{\tilde{y}_u^R|\mathbf{B}[i]}[i] = E\left[\sum_{k_1,m_1,l_1,v_1,k_2,m_2,l_2,v_2}\Re[(h_1-\gamma_1)f_1]\Re[(h_2-\gamma_2)f_2]\right] \tag{3.15}$$

By using the fact that $\Re(a) = \frac{(a+a^*)}{2}$ for any complex number a, the above equation can be rewritten as

$$\sigma^2_{\tilde{y}_u^R|\mathbf{B}[i]}[i] = \frac{1}{4}E\left[\sum_{k_1,m_1,l_1,v_1,k_2,m_2,l_2,v_2}(h_1f_1 - \gamma_1 f_1 + h_1^* f_1^* - \gamma_1^* f_1^*)(h_2 f_2 - \gamma_2 f_2 + h_2^* f_2^* - \gamma_2^* f_2^*)\right] \tag{3.16}$$

After some algebraic manipulations on the above equation we get

$$\sigma^2_{\tilde{y}_u^R|\mathbf{B}[i]}[i] = \frac{1}{4}\sum_{k_1,m_1,l_1,v_1,k_2,m_2,l_2,v_2} E\Big[(h_1-\gamma_1)(h_2-\gamma_2)f_1f_2 + (h_1^*-\gamma_1^*)(h_2-\gamma_2)f_1^*f_2 + (h_1-\gamma_1)(h_2^*-\gamma_2^*)f_1f_2^* + (h_1^*-\gamma_1^*)(h_2^*-\gamma_2^*)f_1^*f_2^*\Big] \tag{3.17}$$

Since f_1 and f_2 are deterministic, by using (3.5) in (3.17)

$$\sigma^2_{\tilde{y}_u^R|\mathbf{B}[i]}[i] = \frac{1}{4}\left[\sum_{k_1,m_1,l_1,v_1,k_2,m_2,l_2,v_2}\tilde{C}_u f_1 f_2 + \tilde{C}_u^* f_1^* f_2^* + C_u f_1 f_2^* + C_u^* f_1^* f_2\right] \tag{3.18}$$

where $C_u = C[m_1, m_2][j_{11}, j_{21}]$ and $\tilde{C}_u = \tilde{C}[m_1, m_2][j_{11}, j_{21}]$. From (3.8), (3.9) and (3.18) the conditional variance will become

$$\sigma^2_{y_u^R|\mathbf{B}[i]}[i] = \frac{1}{4}\left[\sum_{k_1,m_1,l_1,v_1,k_2,m_2,l_2,v_2}\tilde{C}_u f_1 f_2 + \tilde{C}_u^* f_1^* f_2^* + C_u f_1 f_2^* + C_u^* f_1^* f_2\right] + N\frac{\sigma^2}{2} \tag{3.19}$$

We have derived expressions for the conditional mean (3.7) and conditional variance (3.19) of $y_u^R[i]$. The conditional probability of error of uth user as a function of above derived conditional mean and conditional variance is [54]

$$P_{E|\mathbf{B}[i]}[i] = Q\left(\frac{b_u[i]\mu_{y_u^R|\mathbf{B}[i]}[i]}{\sigma_{y_u^R|\mathbf{B}[i]}[i]}\right) \tag{3.20}$$

and the corresponding probability of correct detection is

$$Q\left(-\frac{b_u[i]\mu_{y_u^R|\mathbf{B}[i]}[i]}{\sigma_{y_u^R|\mathbf{B}[i]}[i]}\right) \tag{3.21}$$

where we have used the fact that $1 - Q(x) = Q(-x)$.

We would like to minimize the joint conditional probability of error for all users, namely,

$$P_{EJ}[i] = 1 - P[y_1^R \in \alpha_1, y_2^R \in \alpha_2, \ldots, y_U^R \in \alpha_U] \tag{3.22}$$

where $P[y_1^R \in \alpha_1]$ is the probability of correct detection for uth user, α_u is the uth user decision region for symbol detection and J denotes joint probability of error. We have dropped the conditioning markers and index i for notational ease. Since the noise vectors for all users are independent, the joint conditional probability of error becomes

$$P_{EJ}[i] = 1 - P[y_1^R \in \alpha_1]P[y_2^R \in \alpha_2] \dots P[y_U^R \in \alpha_U] \tag{3.23}$$

Using (3.21), (3.23) and since we have assumed identical distribution assumption for noise, P_{EJ} can be written in closed form as

$$P_{EJ}[i] = 1 - \prod_{u=1}^{U} Q\left(-\frac{b_u[i]\mu_{y_u^R|\mathbf{B}[i]}[i]}{\sigma_{y_u^R|\mathbf{B}[i]}[i]}\right) \tag{3.24}$$

The prefilter coefficients ($\mathbf{z}[.][i]$) of length L_z for each bit interval i is calculated by minimizing the above formulated probability of error. The proposed algorithm is adaptive in nature where the prefilter coefficients are adapted continuously. Gradient search is the simplest adaptive algorithm widely used. Therefore, we employ the gradient descent approach to adaptively calculate the prefilter coefficients as follows

$$\mathbf{z}[.][i+1] = \mathbf{z}[.][i] - \mu\frac{\partial P_{EJ}}{\partial \mathbf{z}[.][i]} \tag{3.25}$$

where μ is an appropriately chosen step-size parameter, and in general it could be adaptive.

3.3.2 MMSE based prefiltering

By following the similar procedure of Section 2.4.2 we can write the cost function for MMSE based algorithm as

$$\begin{aligned}\xi^2_{J|\mathbf{B}} &= \sum_{u=1}^{U} E\Big[((y_u^R)^2 + b_u^2 - 2y_u^R b_u)|\mathbf{B}\Big] \\ &= \sum_{u=1}^{U}\Big[E((y_u^R)^2|\mathbf{B}) + 1 - 2b_u E(y_u^R|\mathbf{B})\Big]\end{aligned} \tag{3.26}$$

Since $\sigma^2_{\tilde{y}_u^R|\mathbf{B}[i]} = E((y_u^R)^2|\mathbf{B})$ when mean is 0, the same procedure of $\sigma^2_{\tilde{y}_u^R|\mathbf{B}[i]}[i]$ can be followed to derive $E((y_u^R)^2|\mathbf{B})$ except that $R_u,\ \tilde{R}_u$ will replace $C_u,\ \tilde{C}_u$ because $C_u,\ \tilde{C}_u$ become $R_u,\ \tilde{R}_u$ when mean is 0. Therefore, $E((y_u^R)^2|\mathbf{B})$ can now be written as

$$E((y_u^R)^2|B) = \frac{1}{4}\Bigg[\sum_{k_1,m_1,l_1,u_1,k_2,m_2,l_2,u_2} \tilde{R}_u f_1 f_2 + \tilde{R}_u^* f_1^* f_2^* + R_u f_1 f_2^* + R_u^* f_1^* f_2\Bigg] \tag{3.27}$$

where $j_{11},\ j_{21}$ are given by (5.16) and $\tilde{R}_u = \tilde{R}_u[m_1, m_2][j_{11}, j_{21}]$, $R_u = R_u[m_1, m_2][j_{11}, j_{21}]$. From (3.26) and (3.27) the cost function can be written as

$$\xi^2_{J|\mathbf{B}[i]}[i] = \sum_{u=1}^{U}\left[\frac{1}{4}\Bigg(\sum_{k_1,m_1,l_1,u_1,k_2,m_2,l_2,u_2} \tilde{R}_u f_1 f_2 + \tilde{R}^*_u f^*_1 f^*_2 + R_u f_1 f^*_2 + R^*_u f^*_1 f_2\Bigg) + 1 - 2b_u[i]\mu_{y^R_u|\mathbf{B}[i]}\right] \tag{3.28}$$

where $\mu_{y^R_u|\mathbf{B}[i]}$ is given by (3.7). We follow the similar gradient descent approach as in (3.25) to compute $\mathbf{z}[.][i]$ by minimizing $\xi^2_{J|\mathbf{B}[i]}[i]$.

Note that in the statistical channel algorithm, we only need knowledge of the first order ($\gamma_u[.][.]$) and second order ($C_u[.,.][.,.], \ldots, C_u[.,.][.,.]$) statistics of the channel coefficients in designing the prefilter.

3.4 Proposed Individual Prefiltering Model

In this model the data for user u is prefiltered by a individual filter of length L^u_z with a discrete time impulse response $\mathbf{z}_u[.][i]$ as shown in Fig 2.2. The resulting prefiltered signals from all U users are added and then transmitted from the base station. The prefilters $\mathbf{z}_u[.][i]$, $u = 1, \ldots, U$ are designed such that the probability of error for that particular user is minimum at the receiver. The prefiltered signal at time instant n corresponding to user u is given by

$$x_u[n] \otimes \mathbf{z}_u[.][n] \tag{3.29}$$

Now the total signal to be transmitted, is given by

$$\sum_{u=1}^{U} x_u[n] \otimes \mathbf{z}_u[.][n] \tag{3.30}$$

If we carry out the similar formulation as in (2.2)-(2.9) by using (3.30) in place of $x[n]$, the received signal at user u after matched filtering is

$$y_u[i] = \left[\sum_{k=0}^{N-1} s_{uk} \sum_{m=0}^{L^u_h-1} h_u[m][j_1] \sum_{l=0}^{L^u_z-1} \sum_{v=1}^{U} z_v[l][j_2] A_v b_v[j_2]\ \tilde{s}_v[iN + k - m - l]\right] + \sum_{k=0}^{N-1} s_{uk}\eta_u[iN + k] \tag{3.31}$$

where j_1 and j_2 are given by (3.2). The decision statistics is $\Re(y_u[i]) = y^R_u[i]$.

3.4.1 MPOE based prefilter

The probability of error for a user u ($P^u_{E|\mathbf{B}[i]}[i]$) can be formulated in the similar way as given in (3.20), except the fact that the prefilter is different for each user. By analyzing along the

similar lines of (3.3)-(3.19) and by replacing $y_u[i]$ in (3.3)-(3.19) by (3.31), the conditional mean ($\mu_{y_u^R|\mathbf{B}[i]}$) and the conditional variance ($\sigma^2_{y_u^R|\mathbf{B}[i]}$) can be written as

$$\mu_{y_u^R|\mathbf{B}[i]}[i] = \Re\left[\sum_{k=0}^{N-1} s_{uk} \sum_{m=0}^{L_h^u-1} \gamma_u[m][j_1] \sum_{l=0}^{L_z^u-1} \sum_{v=1}^{U} z_v[l][j_2] A_v b_v[j_2]\ \tilde{s}_v[iN+k-m-l]\right] \quad (3.32)$$

$$\begin{aligned}\sigma^2_{y_u^R|\mathbf{B}[i]}[i] &= var\left(\Re\left[\sum_{k=0}^{N-1} s_{uk} \sum_{m=0}^{L_h^u-1} h_u[m][j_1] \sum_{l=0}^{L_z^u-1} \left(\sum_{v=1}^{U} z_v[l][j_2] A_v b_v[j_2]\ \tilde{s}_v[iN+k-m-l]\right)\right]\right) + N\frac{\sigma^2}{2} \\ &= \frac{1}{4}\left[\sum_{k_1,m_1,l_1,v_1,k_2,m_2,l_2,v_2} \tilde{C}_u f_1 f_2 + \tilde{C}_u^* f_1^* f_2^* + C_u f_1 f_2^* + C_u^* f_1^* f_2\right] + N\frac{\sigma^2}{2}\end{aligned} \quad (3.33)$$

where $C_u = C[m_1, m_2][j_{11}, j_{21}]$, $\tilde{C}_u = \tilde{C}[m_1, m_2][j_{11}, j_{21}]$ and

$$f_1 = f_u[k_1, m_1, l_1, v_1],\ f_2 = f_u[k_2, m_2, l_2, v_2],\ f_u[k, m, l, v] = s_{uk} z_v[l][j_2] A_v b_v[j_2]\ \tilde{s}_v[iN+k-m-l] \quad (3.34)$$

Note that $f_u[k, m, l, v]$ of individual prefiltering is different from the corresponding joint prefiltering. The cost function to be minimized to determine the prefilter coefficients ($\mathbf{z}_u[.][n]$) can be formulated, by using the above derived conditional mean and conditional variance as follows

$$P^u_{E|\mathbf{B}[i]}[i] = Q\left(\frac{b_u[i]\mu_{y_u^R|\mathbf{B}[i]}[i]}{\sigma_{y_u^R|\mathbf{B}[i]}[i]}\right) \quad (3.35)$$

Note that the probability of error at the receiver is calculated after the signal is prefiltered and transmitted through the multipath channel as shown in Fig 2.2. Therefore, the probability of error at the receiver for user u is function of all users prefiltering coefficients.

Intuitively we can see that all other users' prefilter coefficients influence the probability of error of a particular user by disturbing the orthogonality among the spreading codes as shown in (3.32) and (3.33). Hence, it is important to optimize the probability of error of a particular user by taking into account the effect caused in the received signal due to all other prefilter coefficients. Now the prefilter of length L_z^u at time instant $i+1$ for user u is calculated using gradient search method as follows

$$\mathbf{z}_u[.][i+1] = \mathbf{z}_u[.][i] - \mu\frac{\partial P_E^u}{\partial \mathbf{z}_u[.][i]}, \qquad u \in \{1, 2, \ldots, U\} \quad (3.36)$$

3.4.2 MMSE based prefiltering

By following the same arguments as that of Section 3.3.2 and Section 3.4.1 the MMSE cost function for user u is

$$\xi^2_{u|\mathbf{B}[i]}[i] = \sum_{u=1}^{U}\left(\frac{1}{4}\Bigg[\sum_{k_1,m_1,l_1,u_1,k_2,m_2,l_2,u_2} \tilde{R}_u f_1 f_2 + \tilde{R}^*_u f^*_1 f^*_2 + R_u f_1 f^*_2 + R^*_u f^*_1 f_2\Bigg] + 1 - 2b_u \mu_{y^R_u|\mathbf{B}[i]}[i]\right) \tag{3.37}$$

where f_1, f_2 are given in (3.34) and $\tilde{R}_u = \tilde{R}_u[m_1, m_2][j_{11}, j_{21}]$, $R_u = R_u[m_1, m_2][j_{11}, j_{21}]$. We follow the similar gradient descent approach as in (3.36) to compute $\mathbf{z}_u[.][i]$ by minimizing $\xi^2_{u|\mathbf{B}[i]}[i]$.

3.5 MRT Beamforming for Joint Prefilter

In MRT beamforming each user data will be transmitted through M paths with M different weights as shown in Fig 2.3. Note that in Fig 2.3 prefilter (**z**[.][.]) is common for all users and all paths. By following the same procedure in (2.33) after chip rate sampling $x_u[n]$ can be written as

$$x_u[n] = A_u b_u[n_N]\tilde{s}_u[n] \tag{3.38}$$

The uth user data at mth path will be multiplied by maximum ratio weight w_{um}. The weights w_{um} will be calculated at every bit interval and assumed to be constant over one bit interval because channel is constant over one bit interval. Now the signal transmitted for user u at mth path is

$$x'_{um}[n] = A_u b_u[n_N]\tilde{s}_u[n] w_{um}[n] \tag{3.39}$$

The beamforming weights are concatenated for user u in vector format as

$$\mathbf{w}_u[i] = \big[w_{u1}[i], w_{u2}[i], \ldots, w_{uM}[i]\big]^T \tag{3.40}$$

Assume that the wireless channel between M transmitter beamforming antennas and a mobile receiver antenna for user u is $\mathbf{h}_u[i]$ which can be represented as

$$\mathbf{h}_u[i] = \big[h_{u1}[i], h_{u2}[i], \ldots, h_{uM}[i]\big]^T \tag{3.41}$$

where $h_{um}[i]$, ($u = 1, \ldots, U,\ m = 1, \ldots, M$) is the channel coefficient between mth beamforming antenna of uth user and receiver antenna at ith bit interval.

Assume that the transmit beamforming vector for user u is $\mathbf{w}_u$, where the time index is dropped for notational convenience. The average SNR at the receiver of user u is given by $\mathbf{w}_u^H E(\mathbf{h}_u \mathbf{h}_u^H)\mathbf{w}_u$. Now, among all possible unit-norm transmit beamforming vectors $\mathbf{w}_u$, the one which maximizes the average received SNR is the dominant eigenvector of $E(\mathbf{h}_u \mathbf{h}_u^H)$. The total signal transmitted for all U users after prefiltering is

$$x'[n] = \left[\sum_{u=1}^{U}\sum_{m=1}^{M} A_u b_u[n_N]\tilde{s}_u[n]w_{um}[n]\right] \otimes \mathbf{z}[.][n] \tag{3.42}$$

By using the linearity property of convolution the above equation can be written as

$$\begin{aligned} x'[n] &= \sum_{u=1}^{U}\Big(A_u b_u[n_N]\tilde{s}_u[n]w_{u1}[n] \otimes \mathbf{z}[.][n]\Big) + \sum_{u=1}^{U}\Big(A_u b_u[n_N]\tilde{s}_u[n]w_{u2}[n] \otimes \mathbf{z}[.][n]\Big) + \ldots \\ &\quad + \sum_{u=1}^{U}\Big(A_u b_u[n_N]\tilde{s}_u[n]w_{uM}[n] \otimes \mathbf{z}[.][n]\Big) \end{aligned} \tag{3.43}$$

Now the signal transmitted from MRT beamforming antenna m is

$$x''_m[n] = \sum_{u=1}^{U}\Big(A_u b_u[n_N]\tilde{s}_u[n]w_{um}[n] \otimes \mathbf{z}[.][n]\Big) \tag{3.44}$$

The next step is to find the prefilter coefficients ($\mathbf{z}[.][i]$).

Let γ_{um} is mean, C_{um}, $\tilde{C}_{um}$, R_{um} and $\tilde{R}_{um}$ are second order statistics of $h_{um}[i]$. Then

$$\gamma_{um}[i] = E(h_{um}[i]) \tag{3.45}$$

$$\begin{aligned} C_{um_1m_2}[i_1, i_2] &= E\Big[(h_{um_1}[i_1] - \gamma_{um_1}[i_1])(h^*_{um_2}[i_2] - \gamma^*_{um_2}[i_2])\Big] \\ \tilde{C}_{um_1m_2}[i_1, i_2] &= E\Big[(h_{um_1}[i_1] - \gamma_{um_1}[i_1])(h_{um_2}[i_2] - \gamma_{um_2}[i_2])\Big] \end{aligned} \tag{3.46}$$

$$R_{um_1m_2}[i_1, i_2] = E\Big[h_{um_1}[i_1]h^*_{um_2}[i_2]\Big], \quad \tilde{R}_{um_1m_2}[i_1, i_2] = E\Big[h_{um_1}[i_1]h_{um_2}[i_2]\Big] \tag{3.47}$$

The $x[n]$ in (2.6) is replaced with (3.42) and follow the same steps of (2.7)-(2.9) to find the received signal at the receiver of uth user ($y_u[i]$)

$$\begin{aligned} y_u[i] = \sum_{k=0}^{N-1} s_{uk} \sum_{l=0}^{L_z-1} z[l][j_2] \sum_{v=1}^{U}\sum_{m=1}^{M} A_v b_v[j_2]\tilde{s}_v[iN + k - l]w_{vm}[j_2]h_{um}[j_1] \\ + \sum_{k=0}^{N-1} s_{uk}\eta_u[iN + k] \end{aligned} \tag{3.48}$$

where, since $L_h^u = 1$ j_1 and j_2 are given by

$$j_1 = \left\lfloor \frac{iN + k}{N} \right\rfloor, \quad j_2 = \left\lfloor \frac{iN + k - l}{N} \right\rfloor \tag{3.49}$$

3.5.1 MRT beamforming for MPOE joint prefilter

By following the similar steps of (3.3)-(3.19) and by using (3.48) in place of $y_u[i]$ the conditional mean and variance of the decision statistics are given by

$$\mu_{y_u^R|\mathbf{B}[i]}[i] = E(y_u^R|\mathbf{B}[i]) = \Re\left[\sum_{k=0}^{N-1} s_{uk} \sum_{l=0}^{L_z-1} z[l][j_2]\left(\sum_{v=1}^{U}\sum_{m=1}^{M} A_v b_v[j_2]\tilde{s}_v[iN+k-l].\right.\right.$$
$$\left.\left..w_{vm}[j_2]\gamma_{um}[j_1]\right)\right] \quad (3.50)$$

where j_1 and j_2 are given in (3.49).

$$\sigma^2_{y_u^R|\mathbf{B}[i]}[i] = \frac{1}{4}\left[\sum_{\substack{k_1,l_1,v_1,m_1,\\ k_2,l_2,v_2,m_2}} \tilde{C}_{um_1m_2} f_1 f_2 + \tilde{C}^*_{um_1m_2} f_1^* f_2^* + C_{um_1m_2} f_1 f_2^* + C^*_{um_1m_2} f_1^* f_2\right]$$
$$+N\frac{\sigma^2}{2} \quad (3.51)$$

where

$$C_{um_1m_2} = C_{um_1m_2}[j_{11}, j_{21}], \;\; \tilde{C}_{um_1m_2} = \tilde{C}_{um_1m_2}[j_{11}, j_{21}] \quad (3.52)$$

$$j_{11} = \left\lfloor \frac{iN+k_1}{N} \right\rfloor, \; j_{21} = \left\lfloor \frac{iN+k_2}{N} \right\rfloor \quad (3.53)$$

$$\begin{aligned} f_1 &= f_u[k_1, l_1, v_1, m_1] \\ f_2 &= f_u[k_2, l_2, v_2, m_2] \\ f_u[k,l,v,m] &= s_{uk} z[l][j_2] A_v b_v[j_2] \tilde{s}_v[iN+k-1] w_{vm}[j_2] \end{aligned} \quad (3.54)$$

For $k_1,\ l_1,\ v_1,\ m_1,\ k_2,\ l_2,\ v_2,\ m_2$ (3.11) can be revisited. Now the probability of error at particular bit period i for mth beamforming path of user u as a function of conditional mean and variance is

$$P_{E|\mathbf{B}[i]}[i] = Q\left(\frac{b_u[i]\mu_{y_u^R|\mathbf{B}[i]}[i]}{\sigma_{y_u^R|\mathbf{B}[i]}[i]}\right) \quad (3.55)$$

The joint probability of error P_{Ej} can be determined by using the similar procedure of (3.24). P_{EJ} can now be used as cost function in (3.25) to determine the prefilter coefficients.

3.5.2 MRT beamforming for MMSE joint prefilter

The same procedure of Section 3.3.2 is followed by using (3.48) in place of $y_u[i]$. The MMSE cost function is

$$\begin{aligned}\xi^2_{J|\mathbf{B}[i]}[i] &= \sum_{u=1}^{U} E\Big[(y_u^R)^2 + b_u^2 - 2y_u^R b_u)|\mathbf{B}\Big] \\ &= \sum_{u=1}^{U}\Big[E((y_u^R)|\mathbf{B})^2 + 1 - 2b_u E(y_u^R|\mathbf{B})\Big] \\ &= \sum_{u=1}^{U}\Bigg[\frac{1}{4}\Bigg(\sum_{\substack{k_1,m_1,l_1,u_1,\\ k_2,m_2,l_2,u_2}} \tilde{R}_{um_1m_2} f_1 f_2 + \tilde{R}^*_{um_1m_2} f_1^* f_2^* + R_{um_1m_2} f_1 f_2^* + R^*_{um_1m_2} f_1^* f_2\Bigg) + 1 \\ &\qquad - 2b_u \mu_{y_u^R|\mathbf{B}[i]}[i]\Bigg] \qquad (3.56)\end{aligned}$$

where j_{11}, j_{21} are same as in (3.53), $\mu_{y_u^R|\mathbf{B}[i]}$ is same as in (3.50), f_1, f_2 are given in (3.54) and $R_{um_1m_2} = R_{um_1m_2}[j_{11}, j_{21}]$, $\tilde{R}_{um_1m_2} = \tilde{R}_{um_1m_2}[j_{11}, j_{21}]$. The above formulated mean square error will be optimized by using (3.25) to determine the prefilter coefficients.

3.6 MRT Beamforming for Individual Prefilter

Each user is assumed to have M beamforming weights with an individual prefilter for each user as shown in Fig 2.4. Note that in Fig 2.4 the prefilter ($\mathbf{z}_u[.][.]$) is common for all M beamforming antennas of user u. By following the same steps of (3.42)-(3.44), the signal transmitted from beamforming antenna m is

$$x''_m[n] = \sum_{u=1}^{U}\Big(A_u b_u[n_N]\tilde{s}_u[n] w_{um}[n] \otimes \mathbf{z}_u[.][n]\Big) \qquad (3.57)$$

The individual prefilter weights can be derived by following similar analysis in Sections 3.4 and 3.5.1. By following the similar steps of (2.7)-(2.9) the received signal after matched filtering is

$$\begin{aligned}y_u[i] = \sum_{k=0}^{N-1} s_{uk} \sum_{l=0}^{L_z^u-1}\sum_{v=1}^{U}\sum_{m=1}^{M} z_v[l][j_2] A_v b_v[j_2]\tilde{s}_v[iN+k-l] w_{vm}[j_2] h_{um}[j_1] \\ + \sum_{k=0}^{N-1} s_{uk}\eta_u[iN+k] \qquad (3.58)\end{aligned}$$

3.6.1 MRT beamforming for MPOE individual prefilter

The similar analysis of (3.3)-(3.19) can be followed by substituting (3.58) in place of $y_u[i]$ to calculate the conditional mean ($\mu_{y_u^R|\mathbf{B}[i]}$) and the conditional variance ($\sigma^2_{\tilde{y}_u^R|\mathbf{B}[i]}[i]$). The condi-

tional mean and variance are given by

$$\begin{aligned}\mu_{y_u^R|\mathbf{B}[i]}[i] &= E(y_u^R|\mathbf{B}[i]) \\ &= \Re\Bigg[\sum_{k=0}^{N-1} s_{uk} \sum_{l=0}^{L_z^u-1} \sum_{m=1}^{M} \sum_{v=1}^{U} z_v[l][j_2] A_v b_v[j_2] \tilde{s}_v[iN+k-l]. \\ &\qquad .w_{vm}[j_2]\gamma_{um}[j_1]\Bigg] \end{aligned} \tag{3.59}$$

$$\sigma^2_{y_u^R|\mathbf{B}[i]}[i] = \frac{1}{4}\Bigg[\sum_{\substack{k_1,l_1,v_1,m_1,\\ k_2,l_2,v_2,m_2}} \tilde{C}_{um_1m_2} f_1 f_2 + \tilde{C}^*_{um_1m_2} f_1^* f_2^* + C_{um_1m_2} f_1 f_2^* + C^*_{um_1m_2} f_1^* f_2\Bigg] + N\frac{\sigma^2}{2} \tag{3.60}$$

where $f_1 = f_u[k_1, l_1, v_1, m_1]$, $f_2 = f_u[k_2, 1, l_2, v_2, m_2]$ and

$$f_u[k, l, v, m] = s_{uk} z_v[l][j_2] A_v b_v[j_2] \tilde{s}_v[iN + k - 1 - l] w_{vm}[j_2] \tag{3.61}$$

Now the probability of error at particular instant of time i for uth user's data is

$$P^u_{E|\mathbf{B}[i]}[i] = Q\left(\frac{b_u[i]\mu_{y_u^R|\mathbf{B}[i]}[i]}{\sigma_{y_u^R|\mathbf{B}[i]}[i]}\right) \tag{3.62}$$

$P^u_{E|\mathbf{B}[i]}$ can now be used as cost function in gradient search of (3.36) to determine the MPOE prefilter coefficients.

3.6.2 MRT beamforming for MMSE individual prefilter

The approach similar to that of Section 3.4.2 is adopted with the $y_u[i]$ of (3.58). The MMSE cost function is given by

$$\begin{aligned}\xi^2_{u|\mathbf{B}[i]}[i] &= \sum_{u=1}^{U}\Bigg(\frac{1}{4}\Bigg[\sum_{\substack{k_1,m_1,l_1,u_1,\\ k_2,m_2,l_2,u_2}} \tilde{R}_{um_1m_2} f_1 f_2 + \tilde{R}^*_{um_1m_2} f_1^* f_2^* + R_{um_1m_2} f_1 f_2^* + R^*_{um_1m_2} f_1^* f_2\Bigg] + 1 \\ &\qquad - 2b_u \mu_{y_u^R|\mathbf{B}[i]}[i]\Bigg]\Bigg) \end{aligned} \tag{3.63}$$

where j_{11}, j_{21} are given in (3.53), $\mu_{y_u^R|\mathbf{B}[i]}[i]$ is given in (3.59) and f_1, f_2 are given in (3.61). The above formulated mean square error will be the cost function in (3.36) to determine the MMSE prefilter weights.

The prefilter weights are normalized at every bit period in both the MPOE and MMSE algorithms in all proposed models to reduce the effect of power boosting.

3.7 Complexity Analysis

3.7.1 Complexity of the proposed MPOE individual prefilter algorithm

The probability of error expression for individual prefiltering model is

$$P^{u}_{E|\mathbf{B}[i]}[i] = Q\left(\frac{b_u[i]\mu_{y^R_u|\mathbf{B}[i]}[i]}{\sigma_{y^R_u|\mathbf{B}[i]}[i]}\right) \tag{3.64}$$

The filter updation equation is given by

$$\mathbf{z}_u[.][i+1] = \mathbf{z}_u[.][i] - \mu\frac{\partial P^u_E}{\partial \mathbf{z}_u[.][i]}, \qquad u \in \{1, 2, \ldots, U\} \tag{3.65}$$

Using Leibniz integral rule we can write

$$\frac{\partial P^u_E}{\partial \mathbf{z}_u[.][i]} = -\frac{1}{\sqrt{2\pi}}\exp\left(\frac{-\mu^2_{y^R_u|\mathbf{B}[i]}}{2\sigma^2_{y^R_u|\mathbf{B}[i]}[i]}\right)\frac{\partial\left(\frac{\mu_{y^R_u|\mathbf{B}[i]}}{\sigma_{y^R_u|\mathbf{B}[i]}[i]}\right)}{\partial \mathbf{z}_u[.][i]} \tag{3.66}$$

As the exponential with p digits of precision requires just O($p^{1/2}$) complexity [55], the complexity in finding filter weights essentially lies in determining the values of $\mu_{y^R_u|\mathbf{B}[i]}$ and $\sigma^2_{y^R_u|\mathbf{B}[i]}[i]$.

Complexity in determining $\mu_{y^R_u|\mathbf{B}[i]}$

The received signal in (3.31) is expanded in (3.78) to distinguish the signal component and interference component. As number of users increases interference term in (3.78) approaches Gaussian. Since $b_u[j_2]$ is either $+1$ or -1 and if we assume $A_u = 1, \forall\, u$ the complexity involved in determining $\mu_{y^R_u|\mathbf{B}[i]}$ of (3.78) is $2L_zL_h$ flops. If we include the complexity in determining the index term j_1 and j_2 the total complexity will be $20L_zL_h$ multiplications and $10L_zL_h$ additions where we have assumed division takes 4 flops [54]. Therefore, the total complexity involved in determining $\mu_{y^R_u|\mathbf{B}[i]}$ is O(L_zL_h).

Complexity in determining $\sigma^2_{y^R_u|\mathbf{B}[i]}[i]$

From (3.19)

$$\sigma^2_{y^R_u|\mathbf{B}[i]}[i] = \frac{1}{4}\left[\sum_{k_1=0}^{N-1}\sum_{m_1=0}^{L^u_h-1}\sum_{l_1=0}^{L_z-1}\sum_{v_1=1}^{U}\sum_{k_2=0}^{N-1}\sum_{m_2=0}^{L^u_h-1}\sum_{l_2=0}^{L_z-1}\sum_{v_2=1}^{U}\left(\tilde{C}_u f_1 f_2 + \tilde{C}^*_u f^*_1 f^*_2 + C_u f_1 f^*_2 + C^*_u f^*_1 f_2\right)\right] + N\frac{\sigma^2}{2} \tag{3.67}$$

As $b_u[j_2], s_{uk}$ are either $+1$ or -1 and if we assume $A_u = 1,\ \forall\ u$ then f_1 and f_2 can be directly determined. Due to the above fact the summations $\sum_{k_1=0}^{N-1}$, $\sum_{k_2=0}^{N-1}$ in (3.67) will not constitute any additional complexity. However, the terms $\sum_{v_1=1}^{U}$ and $\sum_{v_2=1}^{U}$ will introduce additional complexity since $f_1,\ f_2$ are functions of $z_u[.][.]$ as derived in (3.34). Furthermore, the second order statistics of the channel coefficients $C_u,\ C_u^*,\ \tilde{C}_u,\ \tilde{C}_u^*$ are already available. Therefore, from (3.67) the total number of multiplications involved is O($U^2L_h^2L_z^2$) and the total number of additions is O($U^2L_h^2L_z^2$). We have U such prefilters. However, since $\gamma_u[.][.]$, $C_u,\ C_u^*,\ \tilde{C}_u,\ \tilde{C}_u^*$ are given, we can see in (3.32) and (3.33) that the only component which is specific to user u is s_{uk} which is either $+1$ or -1. Therefore, with little modification the function which calculates prefilter coefficients of user u can be used to calculate the prefilter coefficients of all other users.

Hence, the total number of operations involved in calculating all the prefilter coefficients in the case of MPOE prefiltering is O($U^2L_h^2L_z^2$). Similar complexity is involved in MMSE based prefiltering models.

3.7.2 Complexity of the proposed MPOE joint prefilter algorithm

The joint probability of error is

$$P_{EJ}[i] = 1 - \prod_{u=1}^{U} Q\left(-\frac{b_u[i]\mu_{y_u^R|\mathbf{B}[i]}[i]}{\sigma_{y_u^R|\mathbf{B}[i]}[i]}\right) \tag{3.68}$$

Unlike individual prefiltering, in joint prefiltering $f_1,\ f_2$ are functions of common prefilter $z[.][.]$. Therefore, by following the similar arguments of Section 3.7.1 with new f_1 and f_2 we can conclude that the complexity involved in determining gradient of single $Q(.)$ term in (3.68) is O($L_h^2L_z^2$). We have U such terms in (3.68). Therefore, the total complexity in determining the prefilter coefficient $\mathbf{z}[.][.]$ is O($U^2L_h^2L_z^2$).

3.7.3 Complexity of other precoding algorithms

The total number of operations required in determining the cost function in the case of transmitter-based inverse filter systems proposed in [16] is O(U^2) (reference: equation (10) of [16]) and the number of operations required in calculating the prefilter coefficients is O(U^3) (reference: equation (11) of [16]). Here we have assumed multiplication of two matrices of equal size N requires N^2 operations and matrix inverse of matrix of size N requires N^3 operations. Similar complexity is required in case of Tomlinson-Harashima Precoding filter proposed in [52] though it is

single user system. The transmitter precoding system proposed in [30] requires Cholesky factorization of $L \times L$ matrix where L is the CDMA code gain. Therefore, the total complexity in the algorithm proposed in [30] is L^4. Note that in case of orthogonal CDMA system the coding gain is directly proportional to number of users. Therefore, as the number of users increases the complexity increases in power of four in [30].

Therefore, we can conclude that our proposed algorithm has much lower complexity compared to other existing algorithms and scales very well with respect to number of users.

3.8 Simulation Results

Extensive simulations have been carried out to calculate the filter coefficients and the corresponding BER for various scenarios for both MPOE and MMSE prefilters. To demonstrate the performance of the proposed algorithms BPSK modulation is considered with bits -1 and +1 being equi-probable. The spreading codes are assumed to be orthogonal and the spreading gain of N = 32 is used for the simulations. Root raised cosine chip waveform with the roll off factor of $\beta = 0.1$ is considered and the number of users is taken to be $U = 16$ except for the graph in which the number of users itself is varying. The results were averaged over at least 1000 independent channels. The channel coefficients were complex Gaussian with both real and imaginary parts are $i.i.d$ Gaussian distributed. FIR channel filter length L_h^u is taken to be 4 and the prefilter length L_z is considered to be 5 for all the models. We have carried out the optimization using numerical gradient descent approach for simulation purpose.

3.8.1 BER performance of joint and individual prefiltering

The performance of the proposed prefiltering algorithms are compared with that of completely known channel prefiltering model (complete CSI model) proposed in [48, 49] and the system without prefiltering. BER performance for various SNRs is shown in Fig 3.1. Lower bound on individual prefiltering probability of error which is derived in Appendix I, is also plotted in Fig 3.1. From Fig 3.1 it is clear that the proposed prefiltering models outperform the system without prefiltering. We can also see that the MPOE algorithms perform significantly better than that of the respective MMSE algorithms. At low SNRs both MPOE and MMSE performs very closely.

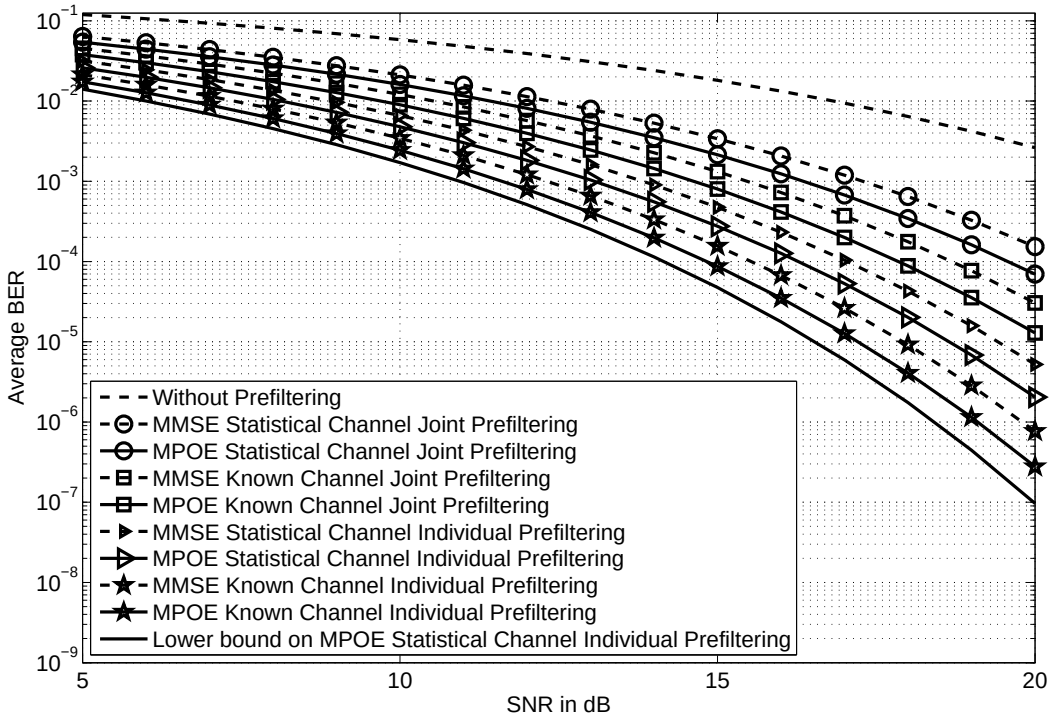

Figure 3.1: Performance of MPOE and MMSE transmitter prefiltering for various SNRs

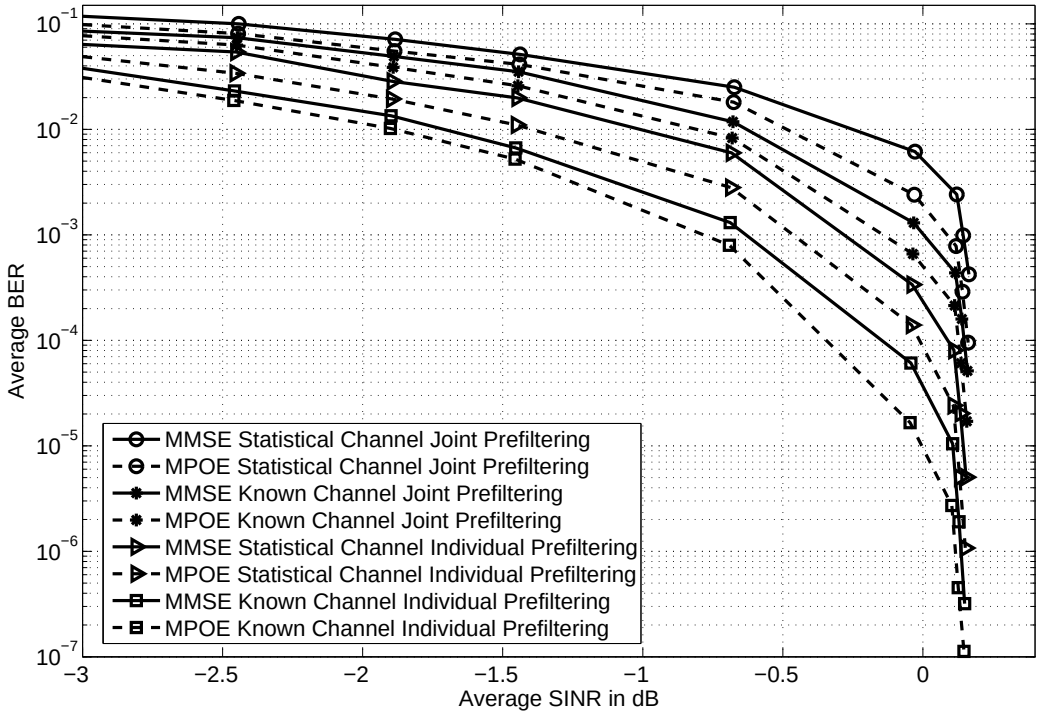

Figure 3.2: Performance of MPOE and MMSE transmitter prefiltering for various SINRs

This is because at low SNRs

$$\sigma^2_{y_u^R|\mathbf{B}[i]}[i] = var\left[\Re\left(\sum_{k=0}^{N-1} s_{uk} \sum_{m=0}^{L_h^u-1} h_u[m][j_1] \sum_{l=0}^{L_z-1} z[l][j_2] \sum_{v=1}^{U} A_v b_v[j_2] \tilde{s}_v[iN+k-m-l]\right)\right] + N\frac{\sigma^2}{2}$$
$$\approx N\frac{\sigma^2}{2} \tag{3.69}$$

$i.e.$ at low SNRs, the channel almost behaves like AWGN channel hence, the similar performance [25]. However, as the SNR increases channel variance term starts dominating the noise variance term in (3.69) hence, there is a significant performance gain at high SNRs in MPOE systems. Furthermore, from Fig 3.1 we can observe that statistical channel algorithms perform close to that of the corresponding fully known channel algorithms.

From Fig 3.1, we can also infer that individual prefiltering performs much better than that of corresponding joint prefiltering systems. This is because in joint prefiltering model there is one common prefilter for all users hence, some of the users channel may not get prefiltered properly. However, in individual prefiltering model we have U number of prefilters. Hence, effectively the length of the individual prefilter is U times that of corresponding joint prefilter and consequently this compensates for the MAI as well as ISI in a better way.

The BER performance of proposed algorithms for various SINRs (Signal to Interference and Noise Ratio) is also analyzed and the results are shown in Fig 3.2. Average SINR is calculated at each SNR (SNR varies from $5\ dB$ to $20\ dB$ to calculate SINR) using the approach presented in Appendix III. In Fig 3.2 we can observe that the average SINRs are negative (in dB) at low SNRs since the average SINR at the receiver is less in magnitude in multiuser interference environment. At high SINR the curves become steep. This is due to diminishing noise variance at high SINR (due to increase in SNR) and hence, interference term dominates which is more or less constant.

It is interesting to observe the performance of the proposed models for various spreading code correlation coefficients (correlation coefficient ρ is defined in (3.77)). For a given ρ all 16 users' spreading codes are generated such that each spreading code has correlation coefficient of ρ with all other codes. We have varied the ρ value from 0.0625 to 0.25 and generated all the users' spreading codes for each ρ. With thus generated spreading codes we have calculated the corresponding BER for a fixed SNR. Fig 3.3 shows the BER performance for various ρ and fixed SNR of $20\ dB$ for both joint and individual prefiltering model. From Fig 3.3, we can observe that as the ρ increases the performances slightly reduces due to the increasing effect of

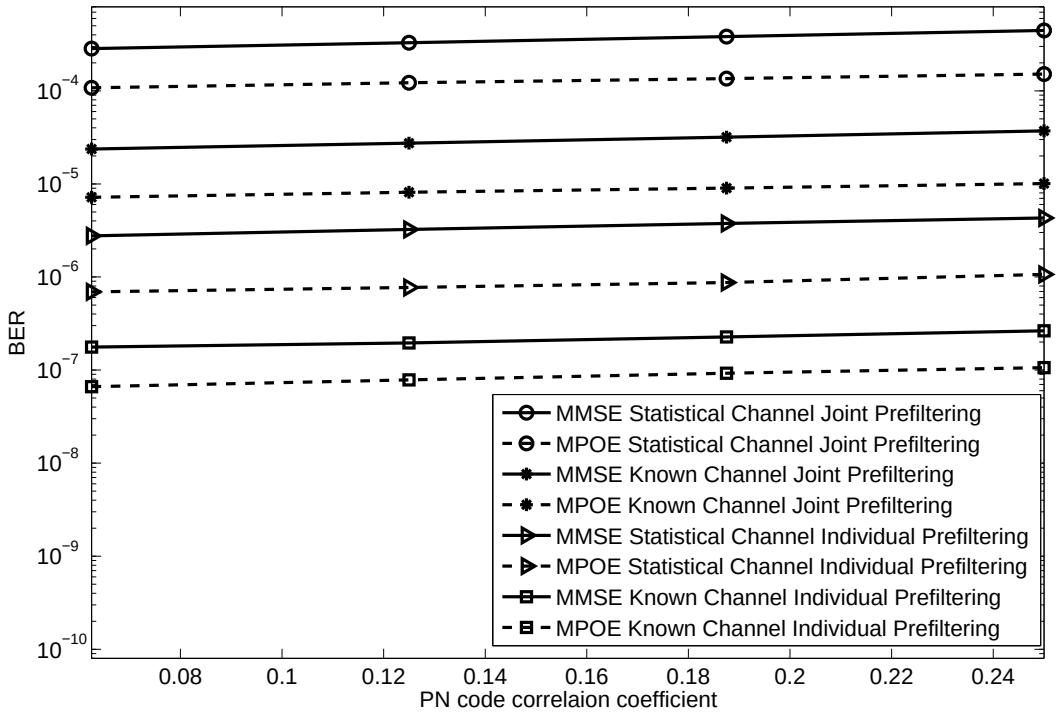

Figure 3.3: Performance of MPOE and MMSE prefilters for various ρ and fixed SNR of $20\ dB$

MAI. The impact is minimal because the prefilter is optimized to cater for this effect.

3.8.2 Proposed prefilters' performance with higher order modulations

Using the procedure explained in Appendix IV the probability of errors are formulated for higher modulations such as QPSK, 16 QAM and 64 QAM. With thus formulated probability of error MPOE prefilters (both joint and individual) are designed and their performances are plotted for various SNRs in Fig 3.4. We can observe from Fig 3.4 that BER performance reduces when the modulation order increases for a fixed transmission power. This is because in higher order modulations the constellation size reduces and also the detection region. Therefore, the BER performance reduces due to increase in detection error as the detection region reduces.

3.8.3 Performance comparison of various prefiltering algorithms

In Fig 3.5 we compare the MPOE individual filter performance with that of "transmitter-based inverse filters (INVF)" proposed in [16] and with "optimized transmitter precoding system (OTPS)" proposed in [30]. This plot shows the average BER as function of SNR in dB. The

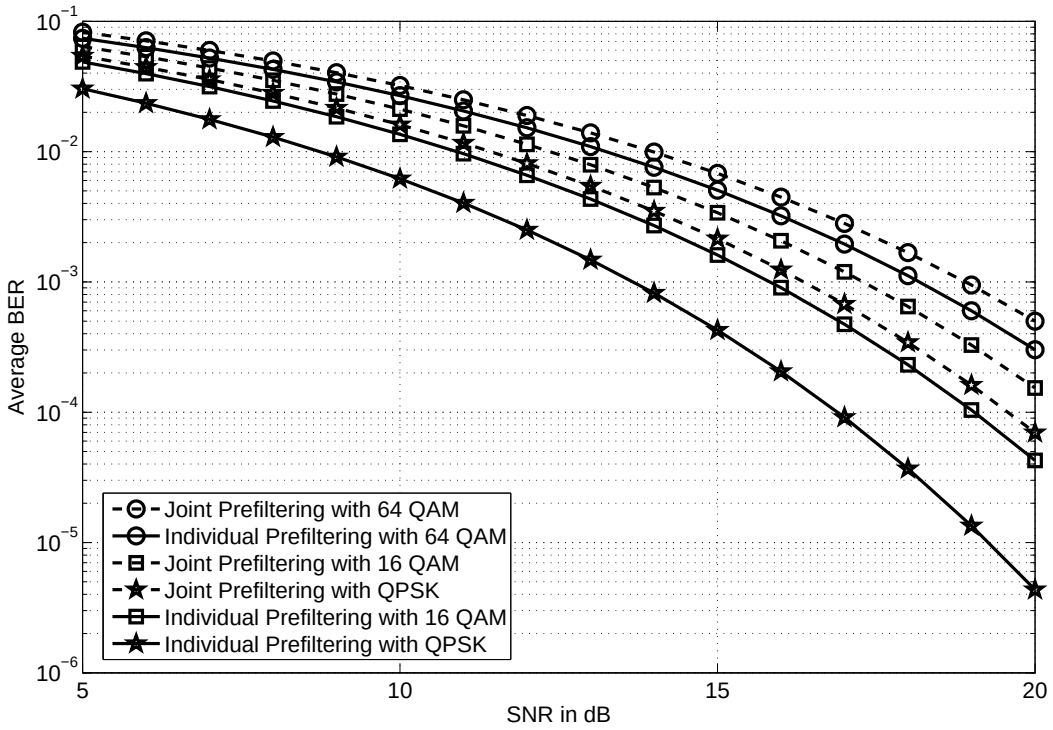

Figure 3.4: Performance of MPOE and MMSE transmitter prefiltering with higher modulations for various SNRs

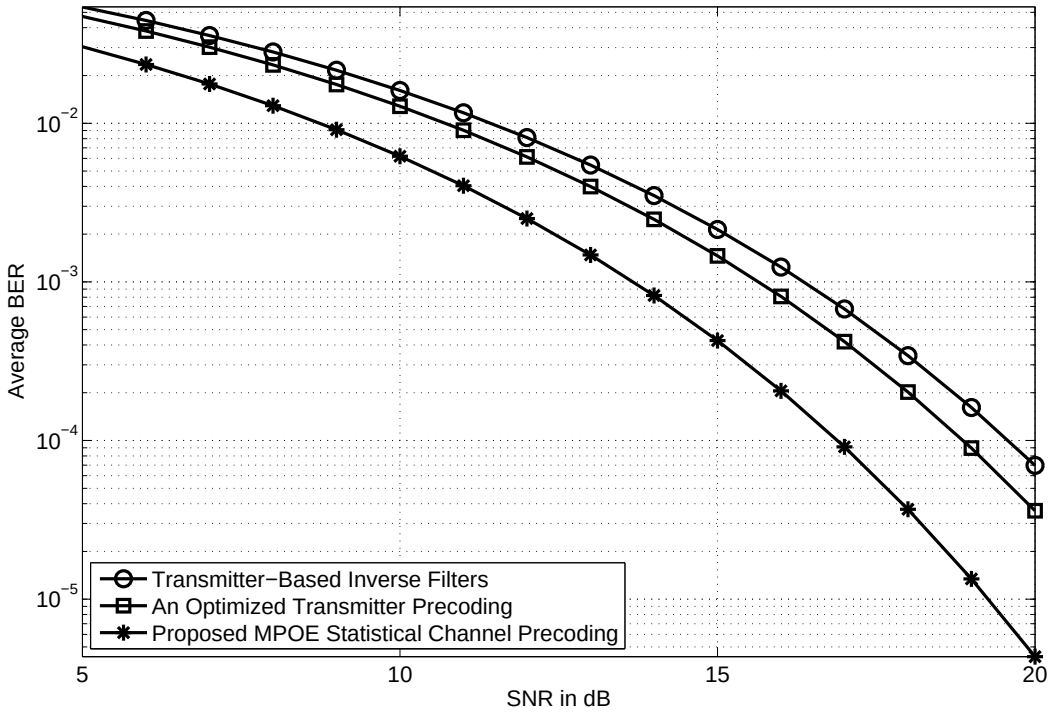

Figure 3.5: Performance comparison of MPOE individual prefiltering algorithm with other algorithms

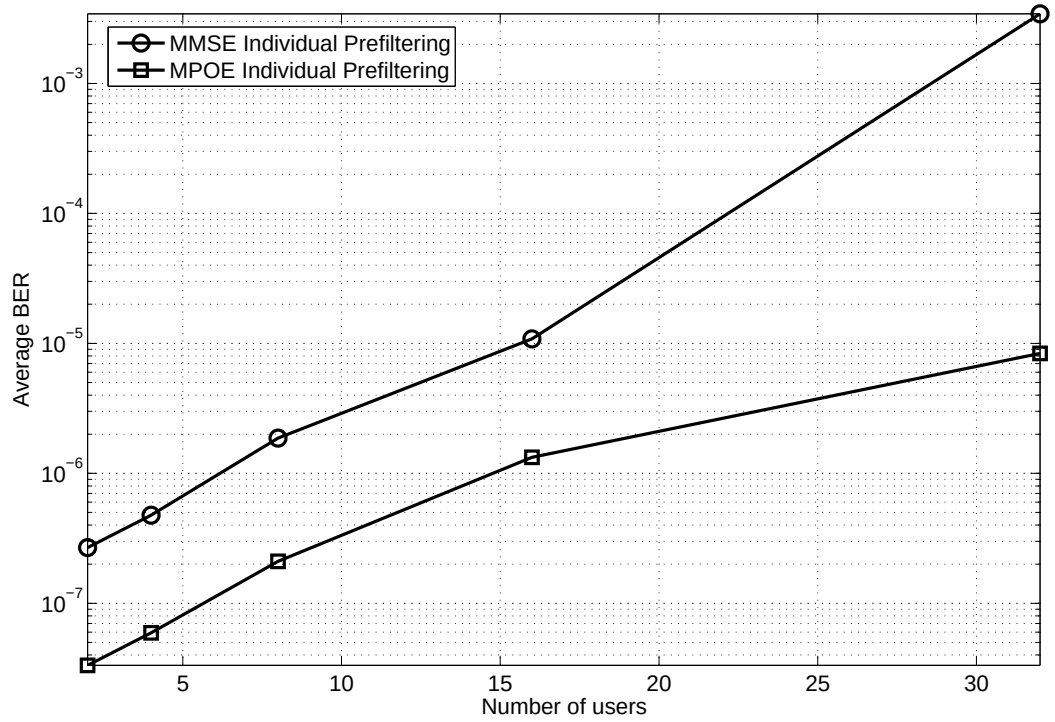

Figure 3.6: BER against number of users ($SNR = 20\ dB$)

results were obtained with number of users equal to 16. From this figure we can see that the MPOE prefilter outperforms the INVF prefilter as well as OTPS prefilters. This is because both "INVF" and "OTPS" are based on MMSE criterion and also both of them suffer from stability problem associated with the matrix inverse operations in determining prefilter coefficients.

3.8.4 Varying number of users

The effect of increasing the number of users for a fixed SNR of $20\ dB$ is shown in Fig 3.6. From Fig 3.6 we can observe that as the number of users increases the BER performance reduces. This is because as the number of users increases, the interference experienced by the system will also increase. We can also observe that the MPOE prefilter outperforms the corresponding MMSE prefilter when the number of users increases to large extend. This is because, though the interference increases with number of users MPOE prefilter still minimizes the probability of error.

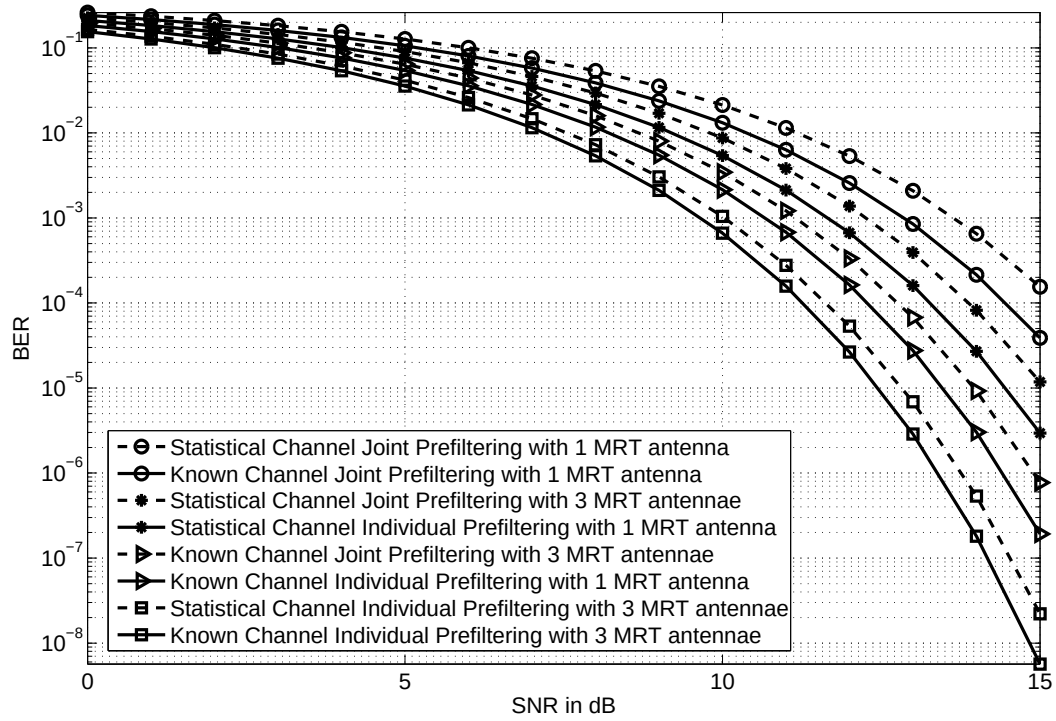

Figure 3.7: BER Performance of MPOE prefilters with MRT beamforming for various SNRs

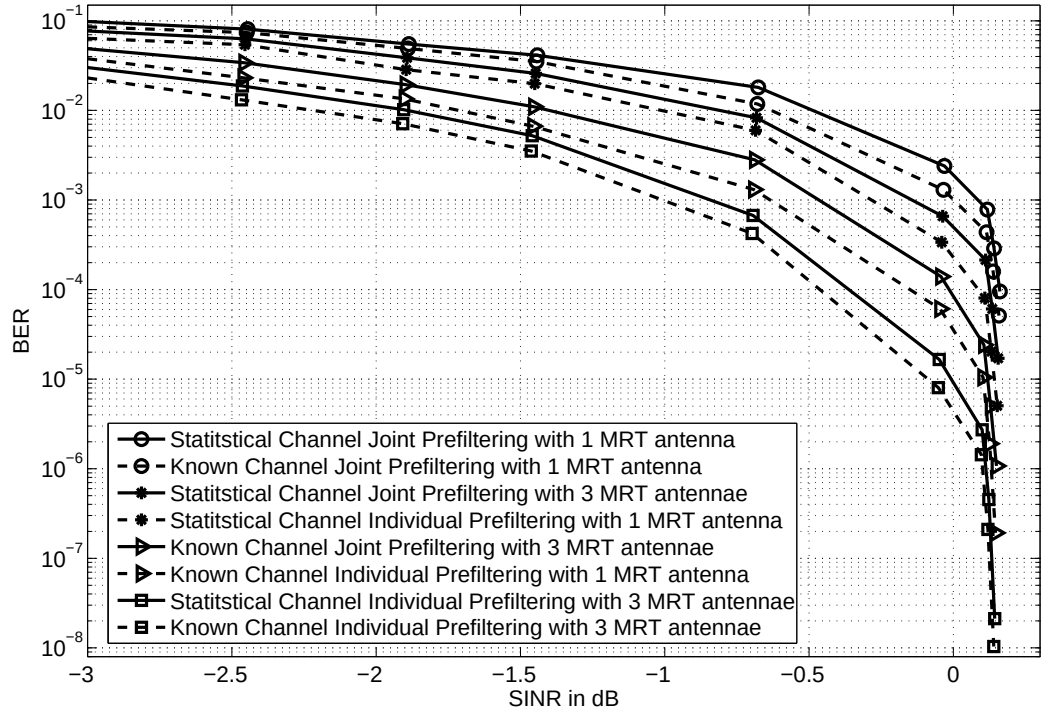

Figure 3.8: BER Performance of MPOE prefilters with MRT beamforming for various SINRs

3.8.5 MRT beamforming results and discussions

The BER performance of the proposed system models with MRT beamforming is plotted. Comparisons are made with known channel models. Results for varying SNRs and SINRs are shown in Fig 3.7 and Fig 3.8 respectively. Single and 3 beamforming antennas are assumed for each user at the base station. Since it is shown that MPOE outperforms MMSE at all SNRs, only MPOE model is considered for MRT beamforming to visualize the plots better. From Fig 3.1, Fig 3.2, Fig 3.7 and Fig 3.8 one can observe that BER performance of MPOE prefilter with beamforming is better than that of MPOE prefilter without beamforming. This can be justified as follows: since the weights are proportional to dominant eigen vector of $E(\mathbf{h}\mathbf{h}^H)$, weights will be matched to the channel coefficients itself (approximately), hence multipath effect will be better compensated.

Fig 3.8 also shows that the performance of statistical channel MRT beamforming will be slightly inferior to that of known channel beamforming. This is because the beamforming weights are calculated by maximizing the average SNR at the receiver in the case of statistical channel model, but instantaneous SNR is maximized to calculate the beamforming weights in known channel case. It is intuitively known that SNR will be maximum by maximizing instantaneous SNR than by maximizing the average SNR. Hence, the known channel beamforming performs better than that of statistical channel beamforming. Moreover, as the diversity order increases (number of beamforming antennae) the difference in BER performance between known channel and statistical reduces. This is due to beamforming diversity which combat the channel effect in statistical channel model. But the cost paid in increasing the beamforming weights is transmitter complexity. Though the number of transmitter antennas are increased for each user, MRT beamforming will not increase the transmission power at base station since the antennae weights are equal to maximum eigen vector which has unit energy.

3.9 Conclusion

In this chapter two system models have been proposed for MPOE and MMSE based prefilterings for DS-CDMA systems by assuming only the first order and second order statistical parameters of channel at the base station transmitter. Simulation results show that the performance of the statistical channel model closely matches with the system where complete channel knowledge is assumed. Furthermore, MPOE prefilters are superior to that of MMSE prefilters in terms of

BER performance and individual prefilters are superior to that of corresponding joint prefilters. The effect of MAI is also well analyzed by varying the number of users and the correlation coefficients of the spreading codes. Also the performance of the proposed MPOE/MMSE prefilterings are further enhanced by employing MRT beamforming. Therefore, we conclude that prefiltering based on statistical knowledge of the channel has high potential for practical implementations.

Appendix I

Lower bound on individual probability of error

$$P^{u}_{E|\mathbf{B}[i]}[i] = Q\left(\frac{b_u[i]\mu_{y^R_u|\mathbf{B}[i]}[i]}{\sigma_{y^R_u|\mathbf{B}[i]}[i]}\right) \tag{3.70}$$

$$\begin{aligned} b_u[i]\mu_{y^R_u|\mathbf{B}[i]}[i] &= b_u[i]\Re\left[\sum_{k=0}^{N-1} s_{uk} \sum_{m=0}^{L^u_h-1} \gamma_u[m][j_1] \sum_{l=0}^{L_z-1}\sum_{v=1}^{U} A_v b_v[j_2] z_v[l][j_2]\tilde{s}_v[iN+k-m-l]\right] \\ &\leq \left| b_u[i] \sum_{k=0}^{N-1} s_{uk} \sum_{m=0}^{L^u_h-1} \gamma_u[m][j_1] \sum_{l=0}^{L_z-1}\sum_{v=1}^{U} A_v b_v[j_2] z_v[l][j_2]\tilde{s}_v[iN+k-m-l]\right| \\ &\leq \sum_{k=0}^{N-1}\sum_{m=0}^{L^u_h-1}\sum_{l=0}^{L_z-1}\sum_{v=1}^{U} \left| s_{uk}\gamma_u[m][j_1] A_v b_v[j_2] z_v[l][j_2]\tilde{s}_v[iN+k-m-l]\right| \end{aligned} \tag{3.71}$$

Since chip sequence is having unit energy, prefilter coefficients are normalized to unit energy and if we assume $A_u = 1 \; \forall \; u$ and also perfect synchronization then the mean of the received signal is

$$\mu_{y^R_u|\mathbf{B}[i]}[i] \leq \sum_{m=0}^{L^u_h-1} \left|\gamma_u[m][j_1]\right| \tag{3.72}$$

From (3.8) and (3.19) the variance of the received signal is

$$\begin{aligned} \sigma^2_{y^R_u|\mathbf{B}[i]}[i] &= var\left[\Re\left(\sum_{k=0}^{N-1} s_{uk} \sum_{m=0}^{L^u_h-1} h_u[m][j_1] \sum_{l=0}^{L_z-1}\sum_{v=1}^{U} A_v b_v[j_2] z_v[l][j_2]\tilde{s}_v[iN+k-m-l]\right)\right] + N\frac{\sigma^2}{2} \\ &\geq N\frac{\sigma^2}{2} \end{aligned} \tag{3.73}$$

The above inequality is from the fact that $var(.) \geq 0$. From (3.70), (5.29) and (5.30) the lower bound on individual probability of error can be written as

$$P^{u}_{E|\mathbf{B}[i]}[i] \geq Q\left(\frac{\sum_{m=0}^{L^u_h-1}\left|\gamma_u[m][j_1]\right|}{\sqrt{(N\sigma^2/2)}}\right) \tag{3.74}$$

It is interesting to note that the lower bound is function of number of multipaths and SNR.

Appendix II

Lower bound on joint probability of error

The joint probability of error is

$$\begin{aligned} P_{EJ}[i] &= 1-\prod_{u=1}^{U} Q\left(-\frac{b_u[i]\mu_{y_u^R|\mathbf{B}[i]}[i]}{\sigma_{y_u^R|\mathbf{B}[i]}[i]}\right) \geq 1-max_u\, Q\left(-\frac{b_u[i]\mu_{y_u^R|\mathbf{B}[i]}[i]}{\sigma_{y_u^R|\mathbf{B}[i]}[i]}\right) \\ &= min_u\, Q\left(\frac{b_u[i]\mu_{y_u^R|\mathbf{B}[i]}[i]}{\sigma_{y_u^R|\mathbf{B}[i]}[i]}\right) \end{aligned} \tag{3.75}$$

where $max_u\, Q\left(-\frac{b_u[i]\mu_{y_u^R|\mathbf{B}[i]}[i]}{\sigma_{y_u^R|\mathbf{B}[i]}[i]}\right)$ is the maximum probability of correct detection among all users and $min_u\, Q\left(\frac{b_u[i]\mu_{y_u^R|\mathbf{B}[i]}[i]}{\sigma_{y_u^R|\mathbf{B}[i]}[i]}\right)$ is the minimum probability of error among all users. The above inequality is from the fact that $\prod_{u=1}^{U} Q\left(-\frac{b_u[i]\mu_{y_u^R|\mathbf{B}[i]}[i]}{\sigma_{y_u^R|\mathbf{B}[i]}[i]}\right) \leq max_u\, Q\left(-\frac{b_u[i]\mu_{y_u^R|\mathbf{B}[i]}[i]}{\sigma_{y_u^R|\mathbf{B}[i]}[i]}\right)$. It is an interesting observation because the lower bound for joint probability error is very similar to that of individual probability of error.

Appendix III

Determination of SINR and correlation coefficient

From (5.5) the received signal is

$$y_u[i] = \sum_{m=0}^{L_h^u-1} h_u[m][j_1] \sum_{l=0}^{L_z-1} z[l][j_2] \sum_{v=1}^{U} A_v b_v[j_2] \sum_{k=0}^{N-1} s_{uk}\tilde{s}_v[iN+k-m-l] + \sum_{k=0}^{N-1} s_{uk}\eta_u[iN+k] \tag{3.76}$$

where $\tilde{s}_v = s_{v((n)mod(N))}$ and

$$\sum_{v=1}^{U} A_v b_v[j_2] \sum_{k=0}^{N-1} s_{uk}\tilde{s}_v[iN+k-m-l] \approx \begin{cases} A_u b_u[j_2].(1) & \text{if } v=u \\ \sum_{v=1,v\neq u}^{U} A_v b_v[j_2].(\rho) & \text{if } v\neq u \end{cases}$$

where ρ is the correlation coefficient between spreading codes which is given by

$$\rho = \sum_{k=0}^{N-1} s_{uk}\tilde{s}_v[iN+k-m-l] \qquad \text{if } v\neq u \tag{3.77}$$

From (3.76) and (3.77)

$$y_u[i] \approx \sum_{m=0}^{L_h^u-1} h_u[m][j_1] \sum_{l=0}^{L_z-1} z[l][j_2] \sum_{v=1}^{U} A_v b_v[j_2] + I.(U-1).\rho + \eta = \mathrm{S} + I_{(MAI+ISI)} + \eta \quad (3.78)$$

where I is the interference factor due to amplitude gain of the interfering users, S is the signal component, $I_{(MAI+ISI)}$ is the interference component and η is the noise term. Now the SINR is given by

$$SINR = \frac{S}{I_{(MAI+ISI)} + \eta} \quad (3.79)$$

(3.79) gives instantaneous SINR for user u. However, instantaneous SINR has some random quantity ($h_u[m][j_1]$) associated with that and also the ρ is altered by the random $h_u[m][j_1]$ while signals propagate through the channel. Therefore, we work with average SINR over longer bit period.

Chapter 4

Route Discovery and Route Resilience for Multihop Cellular Networks

This chapter proposes a cross-layer routing protocol and route resilience scheme for CDMA based Multihop Cellular Network (MCN). MCN is defined as one in which the mobile node may communicate with base station or with other mobile nodes by relaying its communication through one or more neighbouring mobile nodes. This is in contrast to most deployments today where there is only a single-hop access to the base station. In this chapter in designing the routing protocol for MCN, multiple constraints are imposed on intermediate relay node selection and end-to-end path selection. The constraints on relay nodes include willingness for cooperation, *sufficient neighbourhood connectivity* and the level of interference offered on the path. Path constraints include end-to-end throughput and end-to-end delay. A facile incentive mechanism is presented to motivate the cooperation between nodes in call forwarding. In addition, we present a route resilience scheme in the event of dynamic call dropping. In particular, a fast neighbour detection scheme for route resilience is proposed. Instead of using periodic HELLO messages as in traditional ad-hoc routing, the proposed neighbour detection scheme adopts explicit handshake mechanism to reduce neighbour detection latency. We conclude the chapter by demonstrating the superior performance of the proposed routing and route resilience scheme compared with the other well known routing algorithms.

4.1 Introduction

Conventional cellular network uses a centralized networking system which has fixed infrastructure (base stations and wide-area communication), with the mobile node accessing the infrastructure in a single radio hop. In contrast, ad-hoc wireless networks consist of fully distributed wireless nodes with no dependency on fixed infrastructure. The communication within ad-hoc networks is generally a path which is formed of multiple radio hops. Recent studies [56–58] have shown that the use of multihop relaying in conventional cellular networks has several advantages such as capacity improvements, lower transmission power requirement and effective spectral re-use. It can also be of instrumental in time critical applications [59, 60]. Such a network has come to be termed as Multihop Cellular Network (MCN). In MCNs, a fundamental issue we investigate is that of finding a multihop routing path and route resilience in order to achieve satisfactory end-to-end performance. A cross layer unified routing scheme is proposed with multiple metrics in this chapter.

An established routing path in an MCN might become unusable at any time due to node mobility, energy drainage of relay nodes or poor channel quality. One straightforward solution to this problem is to repeat the normal route discovery procedure to find an alternative path. However, this solution could incur a large traffic overhead, but more importantly adds latency in re-establishing the communication path for a connection that is in progress. To solve this problem, we propose an effective on-the-fly route resilience scheme for route maintenance along with a cross layer routing protocol.

The major contributions of this chapter include:

1. A unified cross layer routing protocol is proposed with multiple constraints for CDMA MCNs. Full cooperation is not assumed in call forwarding and therefore present a facile incentive mechanism to motivate cooperation between mobile nodes acting as relays. In the routing protocol design, multiple constraints are imposed on intermediate relay node selection and end-to-end path selection. The relay node constraints include cooperation, *sufficient neighbourhood connectivity* and level of interference. Path constraints for route selection are end-to-end throughput and end-to-end delay.

   The proposed routing protocol follows a cross-layer design between network layer, MAC layer and physical layer. The end-to-end throughput is defined using physical layer parameters: received power, signal to interference and noise ratio (SINR) and probability

of successful packet delivery. The interference metric involves MAC layer and physical layer parameters, and these metrics are used in the network layer for routing protocol design.

2. A route resilience scheme is introduced in the event of dynamic call dropping. If we assume a path consists of multiple hops or links, then dynamic call dropping occurs when one of the links breaks and the path is no longer usable. Link breakage may be caused by node mobility, poor channel quality (i.e. interference) or energy drainage of a node, resulting in a non-forwarding node. In the proposed resilience scheme we bypass the non-forwarding node and route the call via one of the cooperative neighbours such that all the routing criteria are satisfied.

3. A fast neighbour detection mechanism is proposed for the route resilience scheme. The neighbour detection mechanism is localized and carried out in a distributed fashion at each node. Instead of using periodic HELLO messages, the proposed scheme adopts an explicit handshake mechanism to reduce the latency in neighbour detection.

4.2 Related Work

An MCN architecture was proposed in [56] and evaluated in [57] where shortest-path-first algorithm was adopted in route selection. An integrated Cellular and Ad-hoc Relaying (iCAR) system was presented in [58] with a set of fixed relays and fixed routes through these relays. A routing protocol for hybrid networks based on a spanning-tree was proposed in [61], and selection of relay-nodes based on finding a route that has the smallest bottleneck was presented in [62]. A charging and rewarding policy in routing for MCNs was proposed in [63, 64] where Dynamic Source Routing (DSR) is used as the routing protocol. A route selection algorithm based on call status, signal strength, battery power and round-trip time (RTT) was proposed in [59]. There are a number of power-aware ad-hoc routing protocols which use energy as the critical parameters [65–70]. Recently there has been much work on route maintenance and route recovery for ad-hoc networks. Route maintenance using local route recovery techniques was proposed in [71] and a power-aware route maintenance protocol enabled through balancing power dissipation among nodes was proposed in [72]. A route recovery scheme based on an any-cast policy was presented in [73] and a fast route recovery method for a cellular Internet

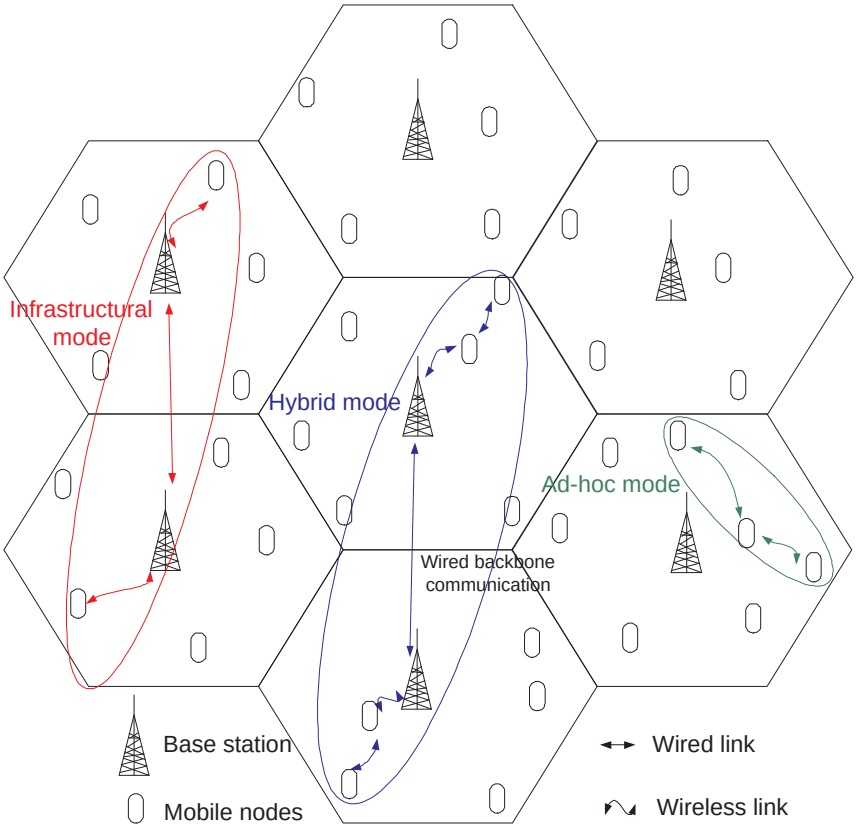

Figure 4.1: MCN hybrid architecture

Protocol (IP) access network was given in [74].

Our proposed cross-layer routing protocol introduces a new dimension to the work listed above. The resilience functionality our approach provides is similar to that proposed by Lee *et al* [75]. However, whilst Lee *et al*'s work *assumes* both full cooperation from all nodes and relies on single-hop broadcast techniques, this chapter analyzes the incentives for cooperation and uses a fast neighbour detection technique.

4.3 Hybrid Architecture for MCN

There could be three possible modes of operation for MCNs as shown in Fig 4.1.

1. Ad-hoc mode: The source-to-destination call is multihop in nature without using any infrastructure (i.e. base stations). However, the centralized base stations will have knowledge about the on-going communications through control channels as explained in Section 4.4.

2. Infrastructural mode: As in a conventional cellular mode of operation, all communication is single-hop. The major concerns about the infrastructural mode include limited user capacity, higher transmission power and communication failures when the mobile user is in a 'dead spot' or out of the coverage area.

3. Hybrid mode: This can be viewed as a combination of infrastructural and ad-hoc mode. This mode would be used where the source and destination nodes are in different cells so the source-to-destination path involves base station(s). The communication, from the source node to its base station and/or the destination node to its base station, is multihop.

In the rest of the chapter, we assume a scenario with a single cell that uses the ad-hoc mode of operation as default.

4.4 Assumptions and Proposed Ad-hoc Mode MCN Architecture

In this chapter, we assume that mobile nodes are distributed according to a two-dimensional uniform point process. The base station and the nodes use CDMA as the access method for their interconnections [76]. Perfect power control is used in this CDMA network so that all the transmitters use just the transmission power level that is required to let the receiver decode the signal with proper quality. However, the nodes transmit HELLO messages with fixed power p_{HELLO} for neighbour detection. Nodes are assumed not to transmit and receive in the same time slot to avoid primary collision at nodes [77]. The propagation channel between the mobile nodes are flat fading and $i.i.d$ Rayleigh.

The logical channel is divided into Control Channel (CCH) and Traffic Channel (TCH). CCH handles only signaling, while TCH carries speech and data traffic. Control messages, containing the source ID and the destination ID are exchanged between the nodes and base station using a CCH. Control messages are routed based on Dijkstra's algorithm, as they are very short and transmitted, only at the time of call initialization. TCHs follow the unified cross layer routing scheme proposed in Section 4.5. Fig 4.2 shows such an architecture with dashed lines for control messages and continuous lines for voice/data communications.

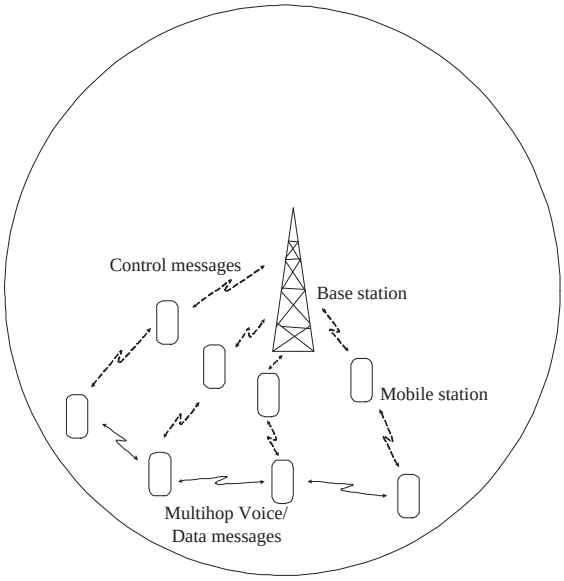

Figure 4.2: Proposed single cell system model

4.5 Proposed Cross Layer Routing Protocol

In our proposal, when a node wants to initiate transmission to a destination node, it will transmit a call initiation request or *Route Request* (RReq) packet containing the ID of the source and destination to its base station over a CCH. The base station uses the strategy proposed in this section to compute a route between the source node and the destination node. This route information is sent back to the source using a *Route Reply* (RRep) packet over the CCH. The source node then inserts the route information into its data packets and transmits these data packets.

The constraints used in the proposed routing protocol are divided into *node constraints* and *path constraints*. The constraints considered for relay node selection are:

1. Cooperation: All of the selected relay nodes must cooperate to forward the call.

2. *Sufficient neighbourhood connectivity*: The selected relay nodes must have a sufficient number of connected neighbours in order to provide resilience.

3. Interference: Interference caused in the networks due to communication between any two relay nodes in the path must be below certain threshold I_{max}.

The constraints for path selection are:

1. End-to-end throughput: End-to-end throughput in the selected path must be above certain threshold.

2. End-to-end delay: End-to-end delay in the selected path must be below certain threshold.

4.5.1 Node selection criteria

Cooperation metric and proposed incentive mechanism

An essential component in MCN is the co-operation of mobile nodes in relaying data packets from other mobile nodes. In our proposal, each node has a *willingness status* [78] flags for packet relaying as follows:

1. will_status=0 for non cooperation

2. will_status=1 for cooperation

In conventional cellular networks, mobile nodes by default do not agree for packet relaying since packet relaying consumes scarce resources such as battery power, processor time and bandwidth. Hence, the default willingness status of a node is 0 (i.e. non-cooperation for packet relaying) [78]. Therefore, it is clear that a node must be stimulated in some way to change their willingness status from 0 to 1. The proposed incentive mechanism works as follows.

Whenever a node wants to initiate a communication, it sends a RReq to the base station through CCH. Upon receiving the RReq, the base station broadcasts a *Cooperation request* (CReq) to the whole network (cell) through broadcast CCH. The CReq contains source ID, destination ID and the *incentive amount* per node that is to be 'paid' after communication. Those nodes that are interested will change their willingness status from 0 to 1 and reply to the base station using CCH. Let us assume $\bar{\Phi}(n)$ is the network of cooperating nodes (nodes with will_status=1). It makes sense that the incentives for multihop routing to be 'paid' by service providers since:

- MCN promises enormous user capacity improvement which is advantageous for the service provider [56].

- A routing path is found by the base station, which has the capability of switching to single hop when it finds multihop is inefficient and costlier.

- Mobile nodes may unintentionally be in unreachable locations (e.g. dead spots or out of coverage) and the service providers would like to keep customers satisfied by providing any time any where services.

neighbourhood connectivity and detection

In [79], it is shown that in a network of n randomly placed nodes, each node should be connected to $O(log(n))$ nearest neighbours. If a node has less than $0.074(log(n))$ connected neighbours, then the network is asymptotically disconnected with probability 1 as n increases. Furthermore, if each node is connected to more than $5.1774(log(n))$ nearest neighbours, then the network is asymptotically connected with probability approaching 1 as n increases. Hence, *sufficient neighbourhood connectivity* is an important criterion to establish communication within an MCN: it is essential to avoid dynamic call dropping as explained in Section 4.6. Therefore, the *sufficient neighbourhood connectivity* of nodes is defined as follows: If a node $m \in \bar{\Phi}(n)$ has k neighbours from $\bar{\Phi}(n)$ and if:

$$k > O(log(n)) \tag{4.1}$$

then node m satisfies *sufficient neighbourhood connectivity* criterion and consequently, it will become a eligible relay node. In our work we choose O as a function of square root of number of nodes in the network. Let us construct a subset $\hat{\Phi}(n)$ from $\bar{\Phi}(n)$ with nodes which satisfy our *sufficient neighbourhood connectivity* criterion. Every node builds its neighbour table and notifies this information to the base station. However, the MCN topology may change frequently and hence the time delay involved in neighbour detection is critical. In the following section the problem of neighbourhood detection with low delay is considered.

Proposed Neighbourhood Detection Scheme

Traditionally, ad-hoc routing protocols such as Optimized Link State Routing (OLSR) [78] detect neighbour changes through exchanging periodic HELLO messages. Although the HELLO based neighbour detection is simple to implement and robust in the presence of message loss, there have been concerns about its performance in the dynamic environments like MCNs:

1. Detection latency: The HELLO based mechanism has a relatively large delay in neighbour detection. For example, it takes around 3 seconds on an average for OLSR nodes to detect neighbour connections [78]. Such latency might lead to unnecessary packet drops due to route unavailability for route resilience, especially in high mobility networks.

2. Resource waste: Periodic HELLO messages are broadcasted even if no link changes occur, which wastes bandwidth and battery life. Smaller HELLO intervals resulting in increased frequency of HELLO messages would increase channel contention and might lead to congestion.

In our proposal, instead of relying on periodic HELLO messages, we use an explicit route handshake mechanism, which reduces the latency in neighbourhood detections and improves path availability. In particular, we propose a unicast based handshake (*UHS*) option. i.e. the handshake packets are transmitted as unicast messages between the neighbouring nodes. For example, when node A receives its first HELLO message from B, it sends ACK messages only to node B.

Outline:

Traditional ad-hoc routing protocols only use symmetric links in route calculations. The established (physical) connections would not be available for data transfer until identified as *symmetric* links by the routing protocols. Therefore, a delay in neighbour detection might lead to routing performance degradation. The neighbour detection latency of HELLO based routing protocols is caused by the periodic nature of HELLO messages. After receiving the first HELLO message from a neighbour, the node does not respond until it broadcasts its own HELLO message. Essentially, the neighbour handshake process is *implicit* through exchanging periodic HELLO messages.

In our scheme, we use *explicit* handshake messages to facilitate connectivity detection. More specifically, in addition to periodic HELLO messages, a node sends explicit handshake messages to its neighbours. The basic process is described as follows.

1. Each node broadcasts periodic HELLO messages to its neighbours.

2. When node A receives its first HELLO message from its unknown neighbour B, it creates a new entry for directed link ($B \rightarrow A$), and responds with an ACK message immediately to node B, with the status of the new link ($B \rightarrow A$).

3. When node B receives such an ACK message, it infers the existence of bi-directional link ($B \leftrightarrow A$); then node B sends immediately an ACK message to node A, confirming the symmetric link ($A \leftrightarrow B$) status between them.

4. If, for any reason, the ACK message from A to B is lost or dropped, the following periodic HELLO messages would recover such a loss and complete the neighbour detection as normal.

5. Similarly, if the ACK message from B to A is dropped, the next periodic HELLO message recovers the loss and acknowledges A.

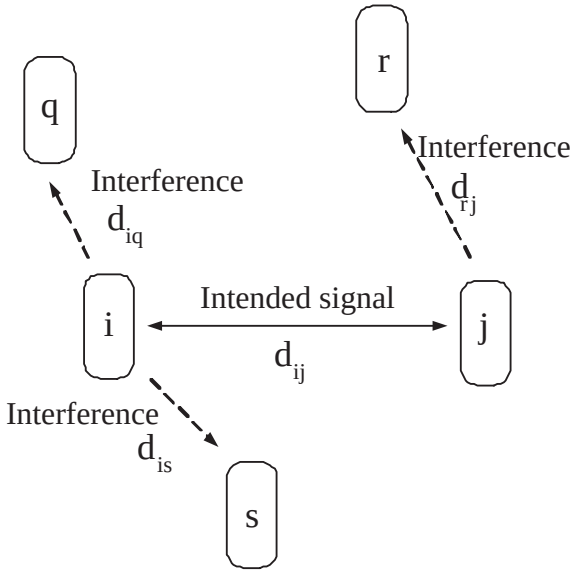

Figure 4.3: Interference metric

Additionally, to reduce control traffic overhead, we propose that nodes only transmit their neighbour table to the base station (using a CCH) when there is a change in the neighbour connectivity.

4.5.2 Interference metric

Interference reduction in CDMA networks is achieved by controlling the transmission power. However, the transmission power levels of the nodes depend on the distance of the other intermediate nodes in the route. Let us consider the communication between a particular node i and any other node j as shown in Fig 4.3. The average interference received at some node r due to transmission from node i to node j is given by:

$$\frac{\rho_{ir}^2 p_{ij}}{d_{ir}^{\gamma}} \tag{4.2}$$

where ρ_{ir} is the time-correlation between the signature waveforms of nodes i and r, γ is the path loss coefficient, d_{ir} is the distance between node i and node r, p_{ij} is the transmitted power from node i to node j. Note that the average received power in a Rayleigh flat fading channel always follows a distance-decay law [80]. To avoid channel estimation across the mobile nodes [81], we are interested in average received power in our interference calculation rather than instantaneous received power. Let us assume N is the DS-CDMA modulation processing gain. Then, the sum of the interference received in all neighbour nodes in the network due to the transmission from

i to j is given by:

$$I = \frac{1}{N}\Big(\sum_{r=1, r\neq\{i,j\}}^{n} \rho_{ir}^2 \frac{p_{ij}}{d_{ir}^{\gamma}} \Big) \tag{4.3}$$

Let us construct a subset $\ddot{\Phi}(n)$ from $\hat{\Phi}(n)$ such that the communication between any two nodes in $\ddot{\Phi}(n)$ causes interference in the network which is below certain threshold I_{max}. The nodes in $\ddot{\Phi}(n)$ are named as *potential relay nodes*.

4.5.3 Path metrics formulation

Let $\chi = \{x_1,\ x_2,\ x_3, \ldots,\ x_M\}$ denote the set of paths available between a source node and a destination node along the *potential relay nodes*. The following are the metrics used in choosing a particular path from the set χ:

1. End-to-end throughput
2. End-to-end delay

End-to-end throughput metric

End-to-end throughput is defined as the probability of successful transmission from a source node to a destination node which involves successful transmission at each and every intermediate node. The successful single hop transmission from node i to its neighbour node j ($\forall i, j \in \ddot{\Phi}(n)$) occurs when the received power at node j from node i is stronger than interference plus noise power by a factor of β (i.e $SINR \geq \beta$). The probability of successful transmission from node i to node j is:

$$\begin{aligned} \mathrm{P}(C_{i,j}) &= \mathrm{P}(SINR_{i,j} \geq \beta) = \mathrm{P}(\frac{r_{i,j}}{(I_{i,j} + \eta)} \geq \beta) \\ &= \mathrm{P}(r_{i,j} \geq \beta.(I_{i,j} + \eta)) \end{aligned} \tag{4.4}$$

where $r_{i,j}$ is the received power at node j from the intended node i, $I_{i,j}$ is the interference at node j due to other communications and η is the noise power in the receiver. Let $r_{k,j},\ k = 1, \ldots, K\ (k \neq i,\ j)$ be the received power at node j from the kth interferer and K is the total number of interferers in the network, then the interference at node j from all interferers is:

$$I_{i,j} = \frac{1}{N}\Big(\sum_{k=1, k\neq\{i,j\}}^{K} \rho_{k,j}^2 r_{k,j} \Big) \tag{4.5}$$

Erroneous detection occurs when $SINR_{i,j} < \beta$, this probability $\mathrm{P}(E_{i,j})$ is given by:

$$\mathrm{P}(E_{i,j}) = \mathrm{P}(r_{i,j} < \beta.(I_{i,j} + \eta)) \tag{4.6}$$

The propagation channel between mobile nodes is different from a conventional wireless channel. However, the envelope still follows Rayleigh distribution [82]. When the channel envelope is Rayleigh then the received power $r_{i,j}$ follows an exponential distribution. Hence:

$$\mathrm{P}(r_{i,j}) = \frac{1}{R_{i,j}} e^{\frac{-r_{i,j}}{R_{i,j}}} \tag{4.7}$$

where $R_{i,j}$ denotes the average received power $R_{i,j} = \frac{p_{i,j}}{d_{i,j}^{\gamma}}$ [80], [83].

1. Case I: number of hops > 1

   Let us say $x_m = \{1,\ 2,\ 3, \ldots, h\}$ is the path selected to relay the packets from source node 1 to the destination node h and number of hops in the communication is $h - 1$. The probability $\mathrm{P}(C_{1,h})$ that the message is successfully transmitted from source 1 to destination h is given by

   $$\mathrm{P}(C_{1,h}) = \mathrm{P}(\bigcap_{i=1}^{h-1} C_{i,i+1}) = 1 - \mathrm{P}(\bigcup_{i=1}^{h-1} E_{i,i+1}) \geq 1 - \sum_{i=1}^{h-1} \mathrm{P}(E_{i,i+1}) \tag{4.8}$$

   Let us consider a communication between node i and its closest neighbour $i + 1$ in the routing path

   $$\begin{aligned} \mathrm{P}(E_{i,i+1}) &= \mathrm{P}(SINR_{i,i+1} < \beta) \\ &= \mathrm{P}(r_{i,i+1} < \beta.(I_{i,i+1} + \eta)) \end{aligned} \tag{4.9}$$

   Now the probability of error conditioned on the interference is

   $$\begin{aligned} \mathrm{P}(E_{i,i+1})|_{I_{i,i+1}} &= \frac{1}{R_{i,i+1}} \int_0^{\beta.(I_{i,i+1}+\eta)} (e^{-\frac{r_{i,i+1}}{R_{i,i+1}}}) dr_{i,i+1} \\ &= 1 - (e^{\frac{-\beta(I_{i,i+1}+\eta)}{R_{i,i+1}}}) \end{aligned} \tag{4.10}$$

   where $I_{i,i+1}$ itself is a random quantity, therefore, the probability of error $\mathrm{P}(E_{i,i+1})$ after removing the condition on $I_{i,i+1}$ is

   $$\begin{aligned} \mathrm{P}(E_{i,i+1}) &= \mathrm{E}_{I_{i,i+1}}\left[1 - e^{-\frac{\beta(I_{i,i+1}+\eta)}{R_{i,i+1}}}\right] \\ &= \int_0^{\infty} \cdots \int_0^{\infty} \left(1 - \left(e^{-\frac{\beta[\frac{1}{N}\sum_{k=1,k\neq\{i,i+1\}}^{K} \rho_{k,i+1}^2 r_{k,i+1}+\eta]}{R_{i,i+1}}}\right)\right). \\ &\qquad \cdot \prod_{\substack{k=1, \\ k\neq\{i,i+1\}}}^{K} P(r_{k,i+1}) dr_{k,i+1} \end{aligned} \tag{4.11}$$

where $\mathrm{E}_{I_{i,i+1}}[.]$ is the expectation of [.] with the random variable being $I_{i,i+1}$. By substituting $\mathrm{P}(r_{i,j})$ from (4.7) and by invoking the independence assumption of $\mathrm{P}(r_{i,j})$, the above equation can be written as

$$\mathrm{P}(E_{i,i+1}) = 1 - \left[e^{\left(-\frac{\beta\eta}{p_{i,i+1} d_{i,i+1}^{-\gamma}}\right)} \prod_{\substack{k=1,\\ k\neq\{i,i+1\}}}^{K} \frac{1}{1 + \frac{\beta}{N} \frac{\rho_{k,i+1}^2 p_{k,i+1}}{p_{i,i+1}} (\frac{d_{i,i+1}}{d_{k,i+1}})^{\gamma}} \right] \tag{4.12}$$

From (4.8) and (4.12) the lower bound on end-to-end throughput can be written as

$$\mathrm{P}(C_{1,h}) \geq 1 - \sum_{i=1}^{h-1} \left(1 - \left[e^{\left(-\frac{\beta\eta}{p_{i,i+1} d_{i,i+1}^{-\gamma}}\right)} \prod_{\substack{k=1,\\ k\neq\{i,i+1\}}}^{K} \frac{1}{1 + \frac{\beta}{N} \frac{\rho_{k,i+1}^2 p_{k,i+1}}{p_{i,i+1}} (\frac{d_{i,i+1}}{d_{k,i+1}})^{\gamma}} \right] \right) \tag{4.13}$$

2. Case II: number of hops = 1

$$\mathrm{P}(C_{1,2}) = \mathrm{P}(r_{1,2} \geq \beta.(I_{1,2} + \eta)) \tag{4.14}$$

Now the conditional probability of correct detection is

$$\begin{aligned} \mathrm{P}(C_{1,2})|_{I_{1,2}} &= \frac{1}{R_{1,2}} \int_{\beta.(I_{1,2}+\eta)}^{\infty} (e^{-\frac{r_{1,2}}{R_{1,2}}}) dr_{1,2} \\ &= e^{\frac{-\beta.(I_{1,2})+\eta}{R_{1,2}}} \end{aligned} \tag{4.15}$$

After averaging over $I_{1,2}$ the probability of correct detection is

$$\mathrm{P}(C_{1,2}) = \left[e^{\left(-\frac{\beta\eta}{p_{1,2} d_{1,2}^{-\gamma}}\right)} . \prod_{k=1, k\neq\{1,2\}}^{K} \frac{1}{1 + \frac{\beta}{N} \frac{\rho_{k,2}^2 p_{k,2}}{p_{1,2}} (\frac{d_{1,2}}{d_{k,2}})^{\gamma}} \right] \tag{4.16}$$

From the set of paths χ, we construct a set $\{\mathbf{X}\}$ such that the constraint on end-to-end throughput is satisfied.

4.5.4 End-to-end delay metric

The major contributions to the end-to-end delay are transmission delay (queuing delay) induced by the relay nodes and propagation delay over the multihop communications. In our routing algorithm, we ensure that end-to-end delay is minimal by introducing an additional path constraint. A path that has minimal end-to-end delay and satisfies end-to-end delay constraint will be selected from set $\{\mathbf{X}\}$.

4.5.5 Summary

The summary of process involved in routing protocol design for data/voice messages is:

1. From n nodes, select a set of cooperative nodes and construct a set $\bar{\Phi}(n)$.
2. From $\bar{\Phi}(n)$ nodes, choose a set of nodes which have *sufficient neighbourhood connectivity* and build a set $\hat{\Phi}(n)$.
3. From $\hat{\Phi}(n)$ select a set of nodes which satisfy interference criterion and construct a set $\ddot{\Phi}(n)$.
4. From $\ddot{\Phi}(n)$ select source to destination paths $\{\mathbf{X}\}$ such that the lower bound on $P(C_{1,h})$ is above a certain threshold.
5. From $\{\mathbf{X}\}$ choose a source to destination path which has minimal end-to-end delay and having end-to-end delay below certain threshold.

When a node wants to start data transmission, it sends a Call Initiation Request (CIR) containing source ID and destination ID to the base station through CCH (node $\rightarrow$ base station). Upon receiving CIR the base station broadcasts within the entire network the Cooperation Request (CReq) which contains the ID of the source node, the destination node and the incentive amount offered (base station $\rightarrow$ node). After receiving CReq, those nodes that are willing to cooperate make their response, with their neighbour details to base station through the CCH (node $\rightarrow$ base station). Now the base station will find a source to destination path using *sufficient neighbourhood connectivity*, interference, end-to-end throughput and end-to-end delay constraints, and will convey the route information to the source node through CCH (base station $\rightarrow$ node).

4.6 Dynamic Call Dropping and Proposed Route Resilience Scheme

The forced termination of the call against the will of the subscriber is defined as *dynamic call dropping*. Dynamic call dropping may be caused by various reasons including mobility, energy drainage, and an emergency requirement of an intermediate node to make its own call. The proposed solution for dynamic call dropping is as follows:

Since each selected intermediate node has sufficient number of connected neighbours (*sufficient neighbourhood connectivity* criterion), whenever any of the above situations arise, the corresponding intermediate node (i.e. depleted node) notifies the base station through the CCH. The base station then picks up one of the neighbours of the depleted node as a substitute such that the constraints on all the metrics are satisfied. The depleted node will be removed from the path subsequently. This is handled without terminating the ongoing communication.

4.7 Routing Metric Analysis

Let us have a close look at the constraints used in route selection.

1. In the cooperation constraint, as the number of intermediate nodes increases, the incentive offered will also increase. Hence, the service providers will prefer having a direct link from source to destination.

2. If we look at end-to-end throughput:

   Case I: *when number of hops is very large*
   $\sum_{i=1}^{h-1} \mathrm{P}(E_{i,i+1}) \rightarrow 1$. This is from the axiom, $0 \leq \mathrm{P}(E_{i,i+1}) \leq 1$. Hence, $P(C_{1,h}) \geq 1 - \sum_{i=1}^{h-1} \mathrm{P}(E_{i,i+1}) \rightarrow 0$. This will lead to negligibly smaller end-to-end throughput.

   Case II: *when the number of hops=1*
   The end-to-end throughput is a function only of SINR. Hence, it is possible to achieve end-to-end throughput of 1 as long as the transmitted power is large enough to guarantee that $SINR > \beta$. Hence, end-to-end throughput metric also favours a direct link from source to destination.

3. As far as end-to-end delay is concerned, the delay in queuing and data propagation increases linearly with the number of intermediate nodes. Hence, the end-to-end delay constraint always favours fewer intermediate nodes, and ideally a direct path from source to destination.

In summary, all the above constraints favour direct source-to-destination paths (i.e. peer to peer communication). However, let us look at the interference constraint more closely. Assume

that the transmitted power levels at node i is adjusted such that the destination node j receives a power level of p_{ref}, i.e.:

$$p_{ij} = p_{ref} d_{ij}^{\gamma} \tag{4.17}$$

Now the interference received at neighbour nodes as a function of d_{ij} is:

$$I(d_{ij}) = \frac{1}{N}\Big(\sum_{r=1, r\neq\{i,j\}}^{n} \rho_{ir}^{2} \frac{p_{ref} d_{ij}^{\gamma}}{d_{ir}^{\gamma}} \Big) \tag{4.18}$$

where p_{ref} and d_{ir} are fixed quantities and the only variable is d_{ij}.

Therefore, the interference constraint favours a shorter hop length (d_{ij}). However, shorter hop lengths may lead to more number of relay nodes in the path. This conflicts with other constraints. Hence, it is critical to find the balance between the number of hops and the hop length such that the constraint on all metrics are satisfied.

4.7.1 Route discovery delay analysis

The delay involved in route discovery includes:

1. The delay in exchanging control messages
2. The delay in route calculation
3. The delay in neighbourhood detection

From the Section 4.5.5 each route discovery process involves exchange of 4 control messages. The computational complexity at the base station involves finding an optimal route that satisfies all the proposed metrics. Let us assume T_{CH} is the delay in exchanging one control message, $T_{computational}$ is the computational delay and $T_{neighbour}$ is the neighbour detection latency of each node. Now the total route discovery delay T_{route}:

$$\begin{aligned} T_{route} &= 4 \times T_{CH} + T_{computational} + max(T_{neighbour}) \\ &= 4 \times T_{PCH} + 4 \times T_{QCH} + T_{computational} + max(T_{neighbour}) \end{aligned} \tag{4.19}$$

where T_{PCH} is the propagation delay of control message, T_{QCH} is the queuing delay of control messages in nodes (or in base station) and $max(T_{neighbour})$ is the maximum latency in neighbour detection of any node. Generally T_{PCH} is considered negligible due to the relatively short

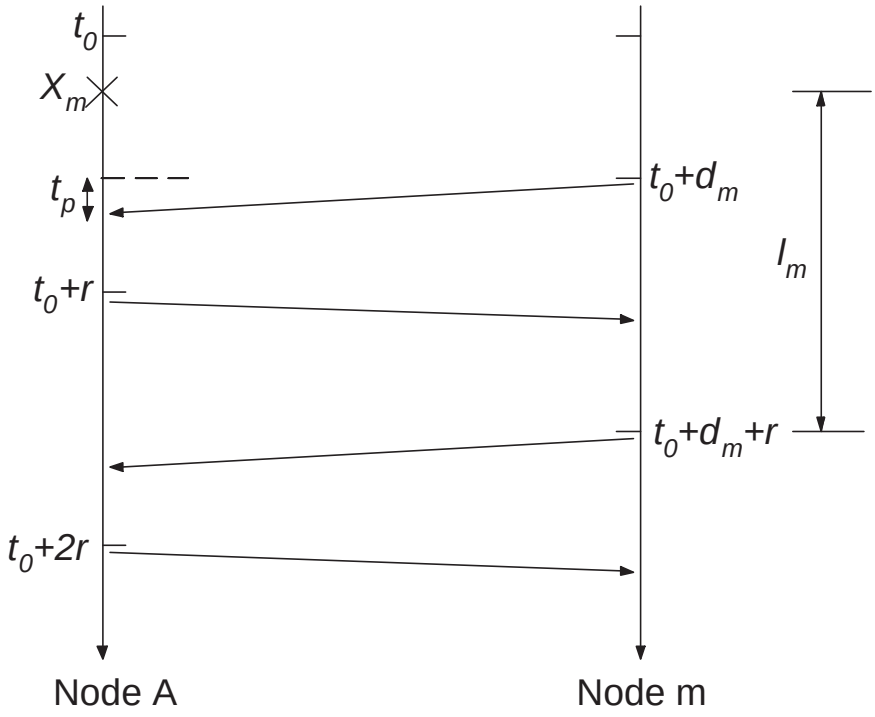

Figure 4.4: HELLO based neighbour detection

distances, and $T_{computational}$ can also be considered negligible as CPU capability is not an issue. Hence, T_{route} can be approximated as:

$$T_{route} \approx 4 \times T_{QCH} + max(T_{neighbour}) \tag{4.20}$$

4.8 Neighbourhood Detection Latency Analysis

In this section, we compare the link detection latency under HELLO based neighbour detection mechanism with that under the proposed fast neighbour detection scheme. In the following discussions, we assume that:

1. The arrival of a link establishment event is an $i.i.d$ Poisson process with arrival rate λ.
2. The delay in packet transmission and propagation (i.e. t_p) are small enough (compared with link detection latency) to be ignored.

4.8.1 HELLO based neighbour detection

Let us consider a node A and its neighbour m as shown in Fig 4.4. Assume that node A generates periodic HELLO packets at every r seconds (HELLO interval) starting from time

instant t_0, and to avoid primary collision at A, node m starts generating the periodic HELLO packets after d_m time, i.e. starting from time instant $t_0 + d_m$. Let X_m be the time when the first symmetric link is established after t_0. Then the link discovery latency of a particular link (l_m) can be approximated by:

$$\begin{aligned} l_m &= t_0 + d_m - X_m + r \\ &= r + d_m - (X_m - t_0) \end{aligned} \tag{4.21}$$

Assume a particular node A has M number of neighbours. Since the link arrivals are Poisson distributed with parameter λ, the inter-arrival time $(X_m - t_0)$ will be exponentially distributed with parameter λ [84]. Let us assume the collision avoidance offset time d_m ($1 \leq m \leq M$) for various nodes are exponentially distributed with parameter λ in the interval $(t_0, t_0 + r]$.

Now, let us calculate the total link detection latency. The total link detection latency is the sum of all the individual link detection latency values at each hop. The link detection process is assumed to be time slotted and at a given time only one link detection can occur. Then the latency involved in M link detections, (l_M), in a collision free condition is:

$$\begin{aligned} l_M &= \sum_{m=1}^{M} \Big[r + d_m - (X_m - t_0) \Big] \\ &= M \times r + \sum_{m=1}^{M} \Big[d_m - (X_m - t_0) \Big] \end{aligned} \tag{4.22}$$

Since $(X_m - t_0)$ and d_m are exponentially distributed, $\Big[d_m - (X_m - t_0) \Big]$ will also be exponentially distributed with parameter λ and $\sum_{m=1}^{M} \Big[d_m - (X_m - t_0) \Big]$ will follow $Gamma(M, \frac{1}{\lambda})$ [84].

Therefore, the statistical average link latency of total M number of link detections (L_M) in a collision free condition can be approximated by:

$$\begin{aligned} L_M = E[l_M] &= M \times r + E\Big[\sum_{m=1}^{M} \Big(d_m - (X_m - t_0) \Big) \Big] \\ &= M(r + \frac{1}{\lambda}) \end{aligned} \tag{4.23}$$

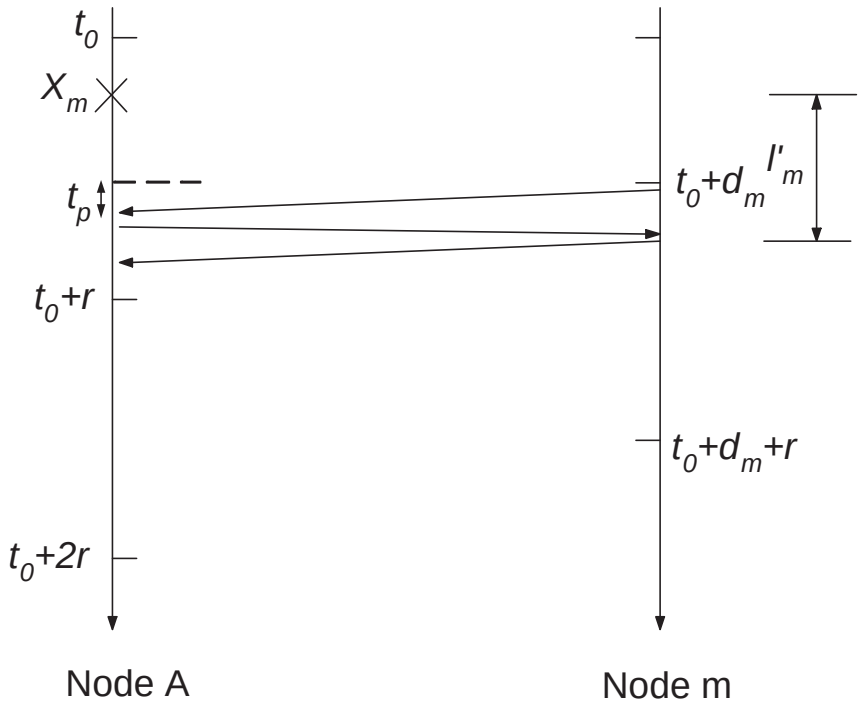

Figure 4.5: Proposed fast neighbour detection

4.8.2 Proposed fast neighbour detection scheme

As explained in Section 4.5.1, the neighbour detection consists of exchange of one HELLO message and two handshake signals as shown in Fig 4.5. Let the latency involved in a link detection is l'_m then, under our proposed scheme, the link discovery latency can be approximated by:

$$\begin{aligned} l'_m &= t_0 + d_m - X_m \\ &= d_m - (X_m - t_0) \end{aligned} \tag{4.24}$$

Now, the total link detection latency of M number of neighbours is:

$$l'_M = \sum_{m=1}^{M} \Big(d_m - (X_m - t_0) \Big) \tag{4.25}$$

By following procedures similar to the development of (4.22) and (4.23), the statistical average link detection latency of M number of neighbours (L'_M) in a collision free condition is:

$$\begin{aligned} L'_M &= E\Big[l'_M\Big] \\ &= E\Big[\sum_{m=1}^{M} \Big(d_m - (X_m - t_0) \Big)\Big] \\ &= M\frac{1}{\lambda} \end{aligned} \tag{4.26}$$

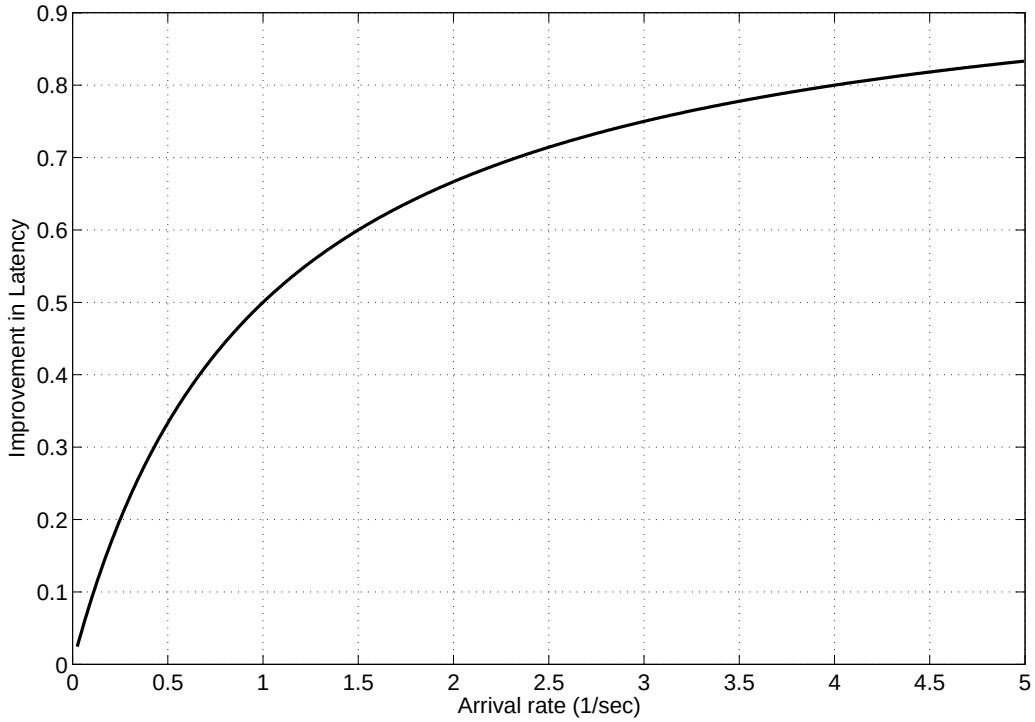

Figure 4.6: Improvement factor in latency in the case of proposed link detection compared to HELLO based link detection for a fixed HELLO interval

4.8.3 Factorial analysis

From the above discussions, we can see that the handshake scheme has a smaller link discovery latency. Smaller link discovery latency provides better route availability, which leads to better route resilience. We present now an analysis on the impacts of factors such as node density and HELLO message transmission power (p_{HELLO}) on the performance of the proposed handshake scheme. Consider the improvements of the proposed scheme on neighbour detection latency:

$$\begin{aligned} \frac{\Delta l}{L_M} &= \frac{L_M - L'_M}{L_M} \\ &= \frac{r}{(r + \frac{1}{\lambda})} \end{aligned} \tag{4.27}$$

Equation (4.27) presents a quantitative relationship between the improvements on latency and the variables of interest ($\lambda,\ r$).

Inferences drawn from the plots:

- **Rate of new link arrivals λ.** Studies on link dynamics [85] show that, the rate of new link arrivals λ increases with node velocity v, node density n and HELLO message transmission power p_{HELLO}. Fig 4.6 shows that increasing link arrival rate λ gives improvements

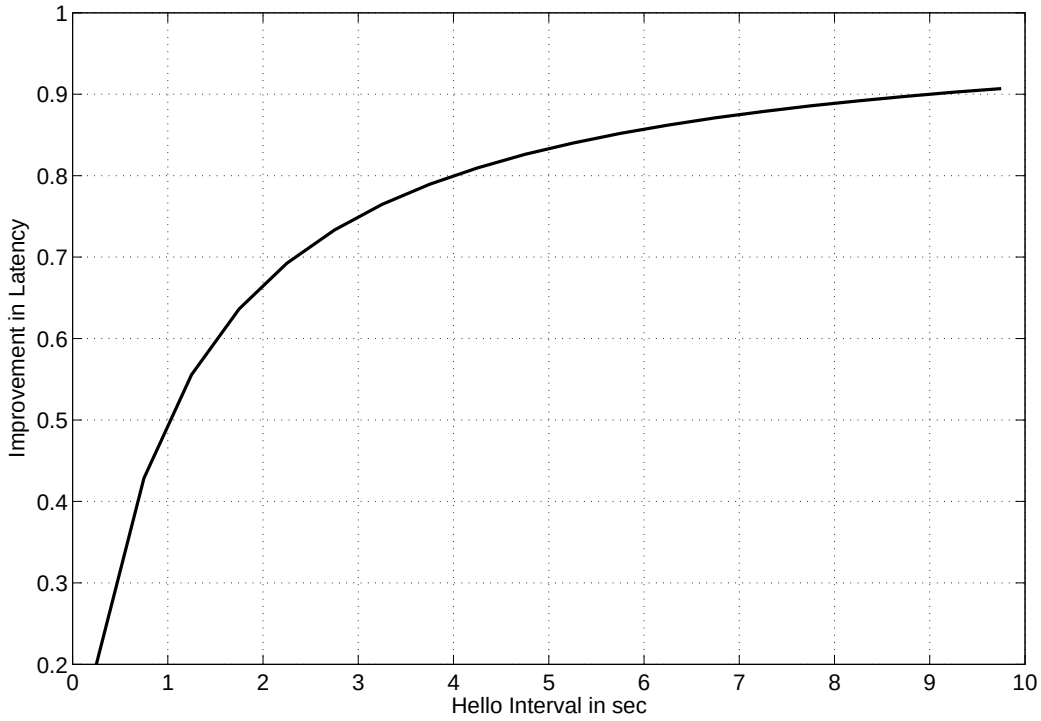

Figure 4.7: Improvement factor in latency in the case of proposed link detection compared to HELLO based link detection for a fixed link arrival rate

for link detection latency. From this we can infer that, in high-density networks with relatively higher transmission power p_{HELLO}, the proposed handshake scheme is expected to outperform the proactive neighbour detection scheme.

- **Refresh Intervals r.** From Fig 4.4 we can see that as the refresh interval r increases, the latency in HELLO based link detection will increase. However, increasing r will not have as high an impact in latency with respect to the proposed link detection scheme as we can see it from Fig 4.5. This can be seen from (4.27) and Fig 4.7 as well. Therefore, the proposed handshake scheme is expected to have a better performance in a network with large refresh interval r.

4.9 Simulations and Results

We simulate a single-cell of radius $1000m$ with nodes distributed as a two dimensional uniform processes with mean 0.5. Equal distribution of incentives for all intermediate relay nodes is assumed. The end-to-end delay threshold is considered as $100msec$, the SINR threshold (β)

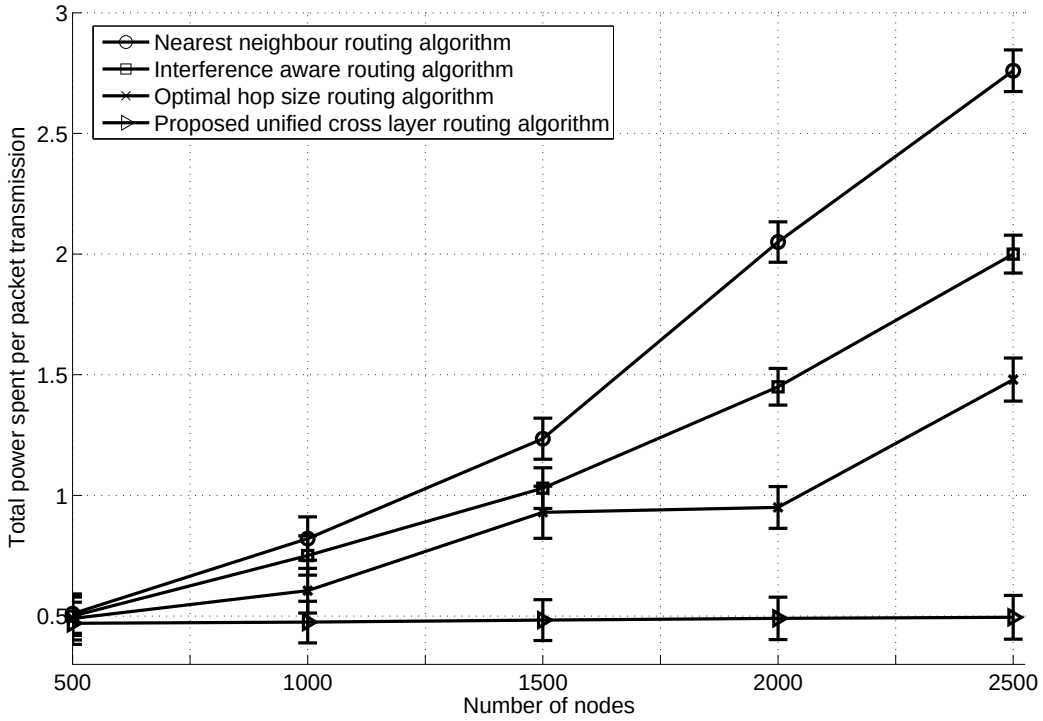

Figure 4.8: Total power spent per packet transmission versus number of nodes

for throughput calculation is taken to be $0.25dB$ and the end-to-end throughput threshold is assumed to be 0.92. The CDMA codes spreading factor (N) is taken to be 32. The Interference threshold (I_{max}) is chosen as $0dB$. To validate the performance of the proposed model, a brute-force, Monte-Carlo simulation was carried out by randomly selecting the source and destination nodes, and the results were averaged over at least 500 realizations of the node distributions. The simulation results are presented with error bars. [μ-σ,μ+σ] is the interval for error bars, where μ is the sample mean and σ is the standard deviation of the samples.

In the underlying simulation environment the proposed algorithm is compared with:

- Interference Aware Routing (IAR) proposed in [86]
- Optimum Hop Size Routing (OHSR) proposed in [76]
- Nearest neighbour routing algorithm.

4.9.1 Total power analysis

The transmission power model used for the analysis is:

$$p_{ij} = \alpha d_{ij}^4 + \lambda \tag{4.28}$$

where λ is a constant to represent minimum transmit power (p_{min}), and α is the normalization constant. For simulation purposes, let us assume $\lambda = 0.1$. The maximum transmitted power from mobile handset is assumed to be of the order of $2W$. By substituting these values, we can rewrite the above equation as:

$$p_{ij} = 1.9 \times 10^{-12} \times d_{ij}^4 + 0.1 \tag{4.29}$$

Apart from the transmission power, we also consider receive power (packet processing power) in our power analysis, since the power spent in the local oscillators and bias circuitry of the low-power transceivers will be considerable in receiving the packets [87]. A constant power of $50mW$ per packet per node in receiver circuitry is assumed in our simulations. Fig 4.8 compares the total power spent per packet transmission in various algorithms. From Fig 4.8 we can infer that the proposed routing algorithm has significantly less total power requirement per packet transmission. This is because the proposed algorithm has end-to-end delay constraint which itself acts as constraint on number of intermediate nodes. We can also observe that as the number of nodes increases the total power spent per packet transmission in the nearest neighbour algorithm and the IAR algorithm increases considerably. This is because though the single hop transmission power in both the algorithms is less, these algorithms result in many intermediate nodes as the node density increases; hence the total transmitted power and the power spent in receiving will be significantly higher. The OHSR algorithm minimizes the maximum hop length. However, most of the time it gives a path with a greater number of hops of significantly large length.

4.9.2 End-to-end throughput analysis

We assume 50 fixed nodes of uniformly distributed interferers for ongoing communications. The lower bound on end-to-end throughput is plotted by varying the number of nodes in Fig 4.9. From Fig 4.9 we can deduce that the lower bound on end-to-end throughput in the case of the proposed algorithm is considerably higher. This is because from (4.13) it is clear that lower bound on end-to-end throughput reduces as the number of hops increases. All nearest

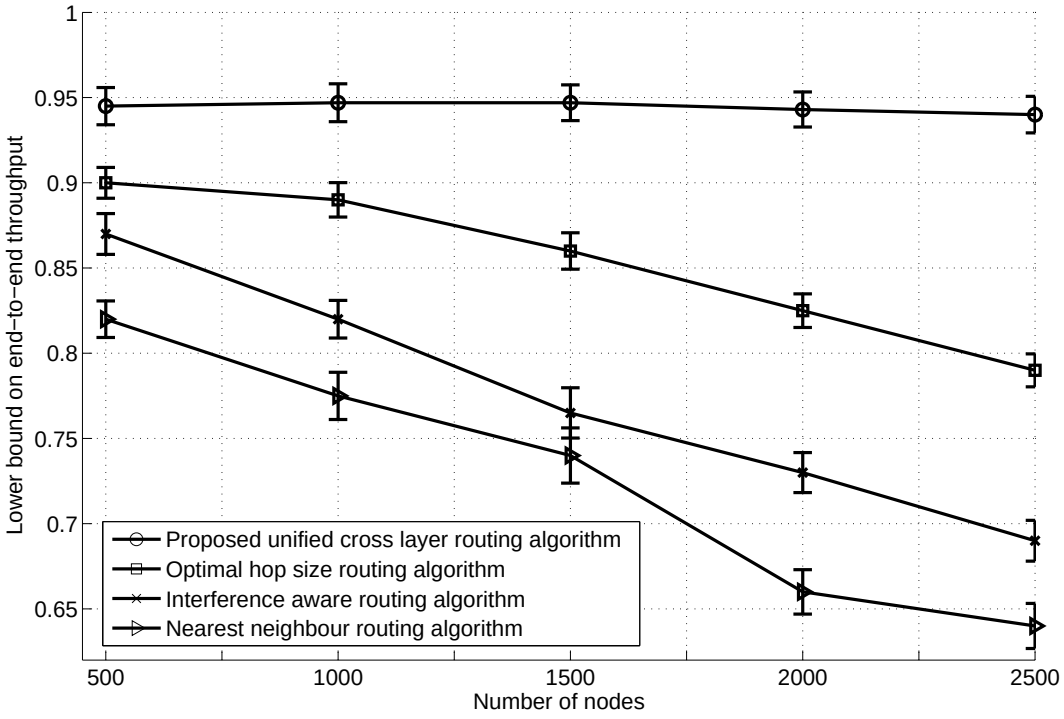

Figure 4.9: Lower bound on end-to-end throughput versus number of nodes

neighbour, IAR and OHSR algorithms result in a greater number of hops. Moreover, as the node density increases the number of hops increases in all the three algorithms. However, in our algorithm we maintain the end-to-end throughput by incorporating a constraint on it.

4.9.3 Incentives and end-to-end delay analysis

In end-to-end delay, transmission delay (queuing delay) in the intermediate nodes is a more significant component compared to the propagation delay. Therefore, as the number of intermediate nodes increases the end-to-end delay increases. Moreover, the incentives paid also increases linearly as the number of intermediate nodes increases. Hence, the algorithm behaves similar in terms of the end-to-end delay and incentives paid. A constant transmission delay (queuing delay) of $30msec$ per node is assumed in our simulation model. Fig 4.10 compares end-to-end delay. From Fig 4.10 we can infer that the end-to-end delay in case of IAR is at an intolerable level for voice communication, while the end-to-end delay in the proposed approach is around $100ms$, which is insensitive to human ears. Also, as the number of nodes increases the delay increases because as the node density increases the number of hops increases in each

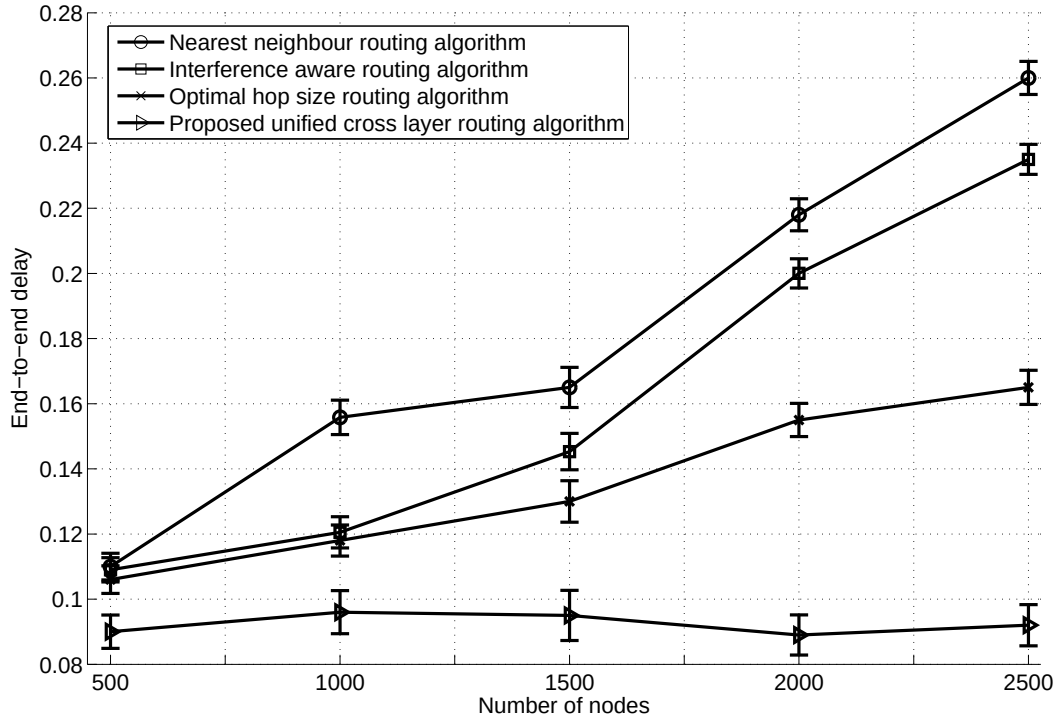

Figure 4.10: End-to-end delay versus number of nodes

of nearest neighbour, IAR and OHSR algorithms as explained above. The incentives offered will also behave like end-to-end delay.

4.10 Conclusion

We have proposed a unified cross-layer routing routing protocol for MCNs by taking all the essential performance metrics into account. The proposed algorithm is compared with the existing MCN routing algorithms such as the interference aware routing algorithm, the nearest neighbour algorithm and optimum hop size routing algorithm. We find that, compared to other algorithms, the proposed algorithm has better performance in terms of overall power consumption, end-to-end throughput, end-to-end delay and incentives paid. Also a fast neighbour detection scheme for route resilience is proposed. Instead of using periodic HELLO messages, the proposed scheme adopts an explicit handshake mechanism to reduce the latency in neighbour detection. An analytical study of the neighbour detection latency shows that the proposed scheme reduces the link detection latency compared to HELLO based neighbour detection algorithm such as OLSR.

Chapter 5

Spatial Link Scheduling for SCDMA Multihop Cellular Networks: A Cross Layer Framework

Probability of error based Spatial Code Division Multiple Access (SCDMA) scheduling algorithm is presented in this chapter to systematically reuse the orthogonal CDMA codes in a given cell for Multihop Cellular Network (MCN). We assign and reuse the CDMA codes to peer-to-peer links such that the probability of error in all scheduled links are below certain threshold. The proposed scheduling algorithm PoE-LinkSchedule involves two phases. In the first phase we present a scheduling metric "Probability of Error (PoE)" as a function of first and second order statistics of wireless channel coefficients between nodes. The second phase presents a graph theoretical as well as PoE based centralized scheduling algorithm. For a graph of network with n number of nodes, U number of links and θ thickness, the proposed scheduling algorithm has computational complexity of $\mathrm{O}(Un\log n + Un\theta)$ as opposed to $\mathrm{O}(U^U)$ in the case of exhaustive search algorithm. The performance of the proposed algorithm is evaluated in terms of *spatial reuse* and end-to-end throughput. We show that the proposed algorithm has considerably higher end-to-end throughput and higher *spatial reuse* compared to existing link scheduling algorithms.

5.1 Introduction

In MCN mobile terminals transmit packets to base stations as well as to other mobile stations using multiple hops with less transmission range. Such a system enhances the throughput, user capacity and energy efficiency [56]. This chapter addresses the problem of link scheduling for CDMA based MCN to increase the *spatial reuse*. By link scheduling, we mean assignment of proper CDMA codes to peer-to-peer links and reuse them at farther distance links such that communication over all links is successful in probability of error sense. CDMA access mechanism with orthogonal spreading codes is considered[1]. However, it can be shown that the number of orthogonal waveforms that can be designed within a given bandwidth (W) and time duration (T) is limited (O(WT)). Furthermore, since the transmissions in MCN are divided into many smaller hops, there could be many simultaneous smaller range transmissions in a given time than a conventional single hop cellular networks [88]. Therefore, it is of paramount importance to devise a scheduling strategy to reuse the orthogonal CDMA codes in a given cell to maximize the system's user capacity. Once the link scheduling information is available we can find source to destination path along the scheduled links using some routing algorithms so that the *spatial reuse* will be maximized in the network. We term the CDMA system where the CDMA codes are reused in a given cell as Spatial-CDMA (SCDMA) system. The problem of determining an optimal link schedule for a general multihop network is NP-complete [89], [90]. Hence, we present a suboptimal method for link scheduling in SCDMA MCNs. The significant contributions of this work are:

1. SNR based graph theoretical algorithms as well as brute-force computations for link scheduling in SCDMA wireless systems often lead to high probability of error in the links. To overcome this problem, we propose a link scheduling algorithm PoE-LinkSchedule for SCDMA MCN with probability of error criterion. Since the probability of error is a widely used performance metric for digital systems, it is appropriate to use it as a criterion for scheduling.

2. Peer-to-peer physical layer probability of error is formulated by assuming independent and identically distributed ($i.i.d$) Rayleigh multipath channel (frequency selective) between nodes. Only the statistical knowledge of the channel coefficients between mobile nodes is assumed in the probability of error formulation instead of complete channel

[1]Orthogonal CDMA codes are considered since it gives tight bounds on resources

knowledge. The above formulated physical layer probability of error will be used as a criterion in MAC layer link scheduling. Hence, we have a cross layer scheduling scheme.

3. We introduce *spatial reuse* as an important performance metric and argue that a high value of *spatial reuse* directly translates to higher throughput over many links.

5.2 Related Work

A Spatial Time Division Multiple Access (STDMA) link scheduling is reported in [89], shows that the tree networks can be scheduled optimally and oriented graphs can be scheduled near-optimally. Link scheduling algorithms under the physical interference model are derived in [91] and [92]. In [93], the authors investigate the time complexity of scheduling a set of communication requests in an arbitrary network. A general framework for the max-min scheduling problem in static wireless networks is proposed in [94]. A cross layer framework for multiple access problem in a contention based wireless network is derived in [95]. The design of simple distributed dynamic routing algorithms and scheduling policies based upon link state information is proposed in [96]. The problem of determining the jointly optimal end-to-end communication rates, routing, power allocation and transmission scheduling for wireless networks is considered in [97]. A code reuse scheme based on a heuristic method is proposed in [98]. Variable Spreading Factor (VSF) code allocation protocol for maximizing throughput in CDMA based ad-hoc networks is analyzed in [99]. Our proposed algorithm PoE-LinkSchedule is considerably different from all the above work. It is a cross layer approach with physical layer probability of error used as metric.

5.3 Scheduling Metric Formulation

Consider a single cell CDMA-MCN system with U transmitting links. All the nodes are assumed to transmit at same power P. Multipath channel is considered for wireless links between nodes. Partial channel knowledge, namely the first order and second order statistics of the channel between nodes are assumed to be available at the base station. Logical channel is divided into Control Channels (CCH) and Traffic Channels (TCH). CCH handles only signaling, while TCH carries speech and data traffic. Base station is the centralized scheduler. Scheduling information is transmitted from base station to the nodes through CCH. We formulate the

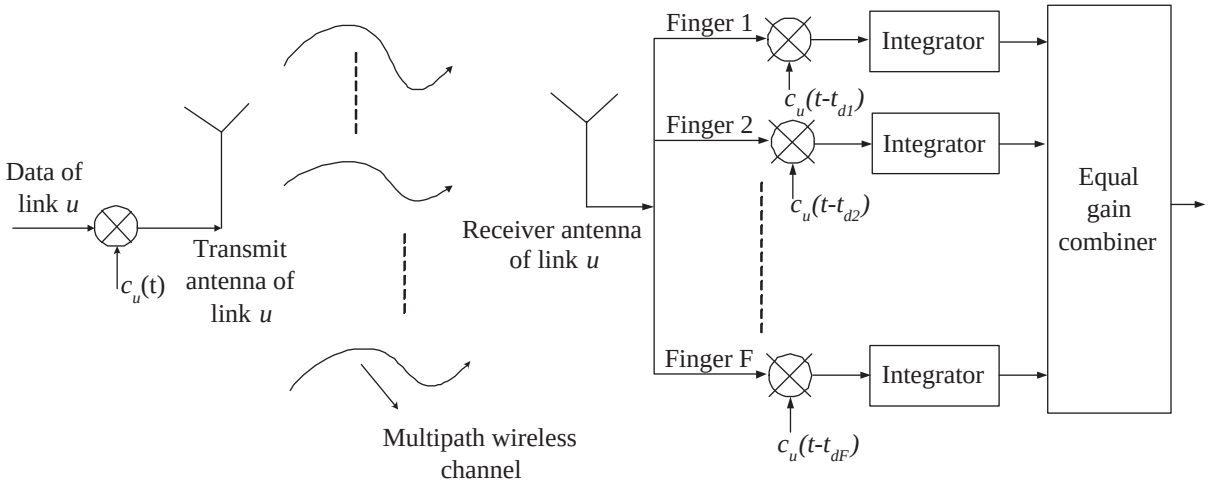

Figure 5.1: Proposed system model for communication between links.

scheduling metric $i.e.$ link (peer-to-peer) probability of error by conditioning on the transmitted bits at the link. The transmit node of link u transmits Binary Phase Shift Keying (BPSK) bit $b_u(i)$, with amplitude A_u, in ith interval. The length of signaling interval for each link is T_{bit}. Assume that transmit node of link u is assigned with a spreading waveform $c_u(.)$ and $\mathbf{s}_u = [s_{u0}, s_{u1}, \ldots, s_{uN-1}]^T$ denotes the corresponding spreading sequence. Then,

$$c_u(t) = \sum_{k=0}^{N-1} s_{uk} rect(t - kT_c), \qquad u = 1, 2, \ldots, U$$

where, T_c is the chip period, $rect(t)$ is a rectangular waveform with unit amplitude in [$0,\ T_c$] and N is the processing gain of the system. The baseband signal for the uth link in the ith bit interval can now be expressed as

$$x_u(t) = A_u b_u(i) c_u(t - iT_{bit}), \qquad iT_{bit} \leq t < (i+1)T_{bit} \tag{5.1}$$

Assume that $x_u(t)$ is sampled $(x_u[n])$ at T_c, then

$$x_u[n] = A_u b_u(n_N) \tilde{s}_u[n] \tag{5.2}$$

where $n_N = \lfloor \frac{n}{N} \rfloor$ because of chip rate sampling (note that $NT_c = T_{bit}$) and $\tilde{s}_u[n] = s_{u((n)mod(N))}$. The multipath wireless channel is modeled as Finite Impulse Response (FIR) filter. The channel gain for the uth link at the ith bit interval is denoted as $\mathbf{h}_u[.][i]$ which is of length L_h^u for all i. The elements of the channel FIR filter ($h_u[l][n]$) are assumed to be complex Gaussian with both real and imaginary parts following the $i.i.d$ Gaussian distribution. The noise ($\eta_u[n]$) is assumed to be $i.i.d.$ zero mean Additive White Gaussian Noise (AWGN). The received signal

at the receiver node of link u can now be written as

$$r_u[n] = \sum_{v=1}^{U} \mathbf{h}_v[.][n] \otimes x_v[n] + \eta_u[n] \tag{5.3}$$

where $\otimes$ denotes convolution operation and $\mathbf{h}_v[.][n]$ $(v \neq u)$ is the channel coefficient between any other node (interfering nodes) to the receiver of link u. Converting $r_u[n]$ into a parallel stream of N samples (number of chips), we obtain $\mathbf{r}_u[n] = [r_u[iN], \ldots, r_u[iN + N - 1]]^T$. Rake receiver is used in the link's receiver as shown in Fig. 5.1. The received signal after rake receiver filtering is

$$y_u[i] = \sum_{f=1}^{F} \mathbf{s}_u^{(f)T} \mathbf{r}_u[i] = \sum_{f=1}^{F} \sum_{k=0}^{N-1} s_{uk}^{(f)} r_u[iN + k] \tag{5.4}$$

where F is the number of fingers in the rake receiver and $s_{uk}^{(f)}$ is the sampled version of CDMA code corresponding to fth finger. From (5.3) and (5.4)

$$y_u[i] = \sum_{f=1}^{F} \sum_{k=0}^{N-1} s_{uk}^{(f)} \sum_{m=0}^{L_h^u - 1} \sum_{v=1}^{U} h_v[m][j] A_v b_v[j] \tilde{s}_v[iN + k - m] + \sum_{f=1}^{F} \sum_{k=0}^{N-1} s_{uk}^{(f)} \eta_u[iN + k] \tag{5.5}$$

where

$$j = \left\lfloor \frac{iN + k - m}{N} \right\rfloor \tag{5.6}$$

In (5.5), $\sum_{m=0}^{L_h^u - 1}$ gives the Inter Symbol Interference (ISI) term due to the multipath channel while $\sum_{v=1}^{U}$ is the Multiple Access Interference (MAI) component due to loss of spreading code orthogonality in a multipath environment with multiple link transmissions. Since BPSK constellations are used for input data, the decision statistics is given by $\Re(y_u[i]) = y_u^R[i]$. We compute the conditional probability of error ($P_{E|\mathbf{B}[i]}$) conditioned on transmitted bit vector sequence $\mathbf{B}[i] = \mathbf{b}[i], \mathbf{b}[i-1], \ldots$, where $\mathbf{b}[i] = \Big[b_1[i], b_2[i], \ldots, b_U[i]\Big]^T$ is the vector of bits transmitted at bit period i in links 1,2,…,U. The mean of the mth channel coefficient at ith bit interval of uth link is defined as

$$\gamma_u[m][i] = E\Big[h_u[m][i]\Big] \tag{5.7}$$

and the second order statistics of the channel coefficients are

$$C_{u,v}[m_1, m_2][i_1, i_2] = E\left[\Big(h_u[m_1][i_1] - \gamma_u[m_1][i_1]\Big)\Big(h_v^*[m_2][i_2] - \gamma_v^*[m_2][i_2]\Big)\right]$$

$$\tilde{C}_{u,v}[m_1, m_2][i_1, i_2] = E\left[\Big(h_u[m_1][i_1] - \gamma_u[m_1][i_1]\Big)\Big(h_v[m_2][i_2] - \gamma_v[m_2][i_2]\Big)\right] \tag{5.8}$$

where * denotes complex conjugate. The conditional mean ($\mu_{y_u^R|\mathbf{B}[i]}$) of the decision statistic ($y_u^R[i]$) is given by

$$\mu_{y_u^R|\mathbf{B}[i]}[i] = E\Bigg[\Re\Bigg(\sum_{f=1}^{F}\sum_{k=0}^{N-1} s_{uk}^{(f)} \sum_{m=0}^{L_h^u-1}\sum_{v=1}^{U} h_v[m][j]A_v b_v[j]\tilde{s}_v[iN+k-m] + \sum_{f=1}^{F}\sum_{k=0}^{N-1} s_{uk}^{(f)}\eta_u[iN+k]\Bigg)\Bigg] \tag{5.9}$$

By using the fact that $E[\Re(a)] = \Re(E[a])$ for any a, $E(\eta_u[iN+k]) = 0$ and except $h_u[m][j]$, $\eta_u[iN+k]$ all other quantities are deterministic, the above equation can be written as

$$\mu_{y_u^R|\mathbf{B}[i]}[i] = \Re\Bigg(\sum_{f=1}^{F}\sum_{k=0}^{N-1} s_{uk}^{(f)} \sum_{m=0}^{L_h^u-1}\sum_{v=1}^{U} \gamma_v[m][j]A_v b_v[j]\tilde{s}_v[iN+k-m]\Bigg) \tag{5.10}$$

Note that $\mu_{y_u^R|\mathbf{B}[i]}[i]$ is conditioned on transmitted bit and it is a function of mean of the channel coefficient ($\gamma_u[m][j]$).

Without loss of generality we can assume that channel $h_u[.][.]$ and noise $\eta_u[.]$ follow independent distribution. Now by using the fact that $var(a+b) = var(a) + var(b)$ when a and b are independent, the conditional variance of the decision statistics ($\sigma^2_{y_u^R|\mathbf{B}[i]}$) can be written as

$$\sigma^2_{y_u^R|\mathbf{B}[i]}[i] = var\Bigg[\Re\Bigg(\sum_{f=1}^{F}\sum_{k=0}^{N-1} s_{uk}^{(f)} \sum_{m=0}^{L_h^u-1}\sum_{v=1}^{U} h_v[m][j]A_v b_v[j]\tilde{s}_v[iN+k-m]\Bigg)\Bigg] + var\Bigg[\sum_{f=1}^{F}\sum_{k=0}^{N-1} s_{uk}^{(f)}\eta_u[iN+k]\Bigg] \tag{5.11}$$

Since the receiver noises are assumed to be zero mean $i.i.d$ AWGN with equal variance (i.e, σ) and also the spreading coefficient s_{uk} is either +1 or -1 and deterministic, we can get

$$var\Bigg[\sum_{f=1}^{F}\sum_{k=0}^{N-1} s_{uk}^{(f)}\eta_u[iN+k]\Bigg] = N \times F\frac{\sigma^2}{2} \tag{5.12}$$

where we have used linearity property of variance operation over independent random variables. Let

$$\sigma^2_{\tilde{y}_u^R|\mathbf{B}[i]}[i] = var\Bigg[\Re\Bigg(\sum_{f=1}^{F}\sum_{k=0}^{N-1} s_{uk}^{(f)} \sum_{m=0}^{L_h^u-1}\sum_{v=1}^{U} h_v[m][j]A_v b_v[j]\tilde{s}_v[iN+k-m]\Bigg)\Bigg] \tag{5.13}$$

This can be rewritten as

$$\sigma^2_{\tilde{y}_u^R|\mathbf{B}[i]}[i] = var\Bigg[\Re\Bigg(\sum_{\substack{f,k,\\ m,v}} h_v[m][j]\psi_u[f,k,m,v]\Bigg)\Bigg] \tag{5.14}$$

where $\psi_u[f,k,m,v] = s_{uk}^{(f)} A_v b_v[j]\ \tilde{s}_v[iN+k-m]$, the index j is given in (5.6) and the sum $\sum_{\substack{f,k,\\m,v}} = \sum_{f=1}^{F}\sum_{k=0}^{N-1}\sum_{m=0}^{L_h^u-1}\sum_{v=1}^{U}$. By using the fact that $var(a) = E[a-E(a)]^2$ for any a and $\psi_u[f,k,m,v]$ is deterministic variable, (5.14) can be written as

$$\begin{aligned}\sigma^2_{\tilde{y}_u^R|\mathbf{B}[i]}[i] &= E\left[\left(\Re\left[\sum_{\substack{f,k,\\m,v}}(h_v[m][j]-\gamma_v[m][j])\psi_u[f,k,m,v]\right]\right)^2\right] \\ &= E\Bigg[\Re\Bigg(\sum_{\substack{f_1,k_1,\\m_1,v_1}}(h_{v_1}[m_1][j_1]-\gamma_{v_1}[m_1][j_1])\psi_u[f_1,k_1,m_1,v_1]\Bigg). \\ &\qquad .\Re\Bigg(\sum_{\substack{f_2,k_2,\\m_2,v_2}}(h_{v_2}[m_2][j_2]-\gamma_{v_2}[m_2][j_2])\psi_u[f_2,k_2,m_2,v_2]\Bigg)\Bigg]\end{aligned} \tag{5.15}$$

where,

$$j_1 = \left\lfloor \frac{iN+k_1-m_1}{N} \right\rfloor \quad j_2 = \left\lfloor \frac{iN+k_2-m_2}{N} \right\rfloor \tag{5.16}$$

For notational convenience let us assume

$$\begin{aligned} h_1 &= h_{v_1}[m_1][j_1],\ \ \gamma_1 = \gamma_{v_1}[m_1][j_1],\ \ \psi_1 = \psi_u[f_1,k_1,m_1,v_1] \\ h_2 &= h_{v_2}[m_2][j_2],\ \ \gamma_2 = \gamma_{v_2}[m_2][j_2],\ \ \psi_2 = \psi_u[f_2,k_2,m_2,v_2] \end{aligned} \tag{5.17}$$

Since the channel coefficients of different links are $i.i.d$, from (5.15), (5.17) we can get

$$\sigma^2_{\tilde{y}_u^R|\mathbf{B}[i]}[i] = E\left[\sum_{\substack{f_1,k_1,m_1,v_1,\\f_2,k_2,m_2,v_2}} \Re[(h_1-\gamma_1)\psi_1]\Re[(h_2-\gamma_2)\psi_2]\right] \tag{5.18}$$

By using the fact that $\Re(a) = \frac{(a+a^*)}{2}$ for any complex number a, the above equation can be rewritten as

$$\sigma^2_{\tilde{y}_u^R|\mathbf{B}[i]}[i] = \frac{1}{4}E\left[\sum_{\substack{f_1,k_1,m_1,v_1,\\f_2,k_2,m_2,v_2}} \Big(h_1\psi_1-\gamma_1\psi_1+h_1^*\psi_1^*-\gamma_1^*\psi_1^*\Big)\Big(h_2\psi_2-\gamma_2\psi_2+h_2^*\psi_2^*-\gamma_2^*\psi_2^*\Big)\right] \tag{5.19}$$

Since ψ_1 and ψ_2 are deterministic the above equation will become

$$\sigma^2_{\tilde{y}_u^R|\mathbf{B}[i]}[i] = \frac{1}{4}\left[\sum_{\substack{f_1,k_1,m_1,v_1,\\f_2,k_2,m_2,v_2}} \tilde{C}_{v_1,v_2}\psi_1\psi_2 + \tilde{C}^*_{v_1,v_2}\psi_1^*\psi_2^* + C_{v_1,v_2}\psi_1\psi_2^* + C^*_{v_1,v_2}\psi_1^*\psi_2\right] \tag{5.20}$$

where $C_{v_1,v_2} = C_{v_1,v_2}[m_1, m_2][j_1, j_2]$ and $\tilde{C}_{v_1,v_2} = \tilde{C}[m_1, m_2][j_1, j_2]$ can be calculated using (5.8). From (5.11), (5.12), (5.13) and (5.20) the conditional variance will become

$$\sigma^2_{y_u^R|\mathbf{B}[i]}[i] = \frac{1}{4}\left[\sum_{\substack{f_1,k_1,m_1,v_1,\\ f_2,k_2,m_2,v_2}} \tilde{C}_{v_1,v_2}\psi_1\psi_2 + \tilde{C}^*_{v_1,v_2}\psi_1^*\psi_2^* + C_{v_1,v_2}\psi_1\psi_2^* + C^*_{v_1,v_2}\psi_1^*\psi_2\right] + N \times F\frac{\sigma^2}{2} \tag{5.21}$$

We have derived expressions for the conditional mean (5.10) and conditional variance (5.21) of $y_u^R[i]$. The conditional probability of error of uth link as a function of above derived conditional mean and conditional variance is [19]

$$P^u_{E|\mathbf{B}[i]}[i] = Q\left(\frac{b_u[i]\mu_{y_u^R|\mathbf{B}[i]}[i]}{\sigma_{y_u^R|\mathbf{B}[i]}[i]}\right) \tag{5.22}$$

Let us denote the conditional probability of error of uth link between nodes i and j as $P_{E_{ij}}$. The code assignment and reuse will be done such that $P_{E_{ij}} < \beta \; \forall i, j \in n$ where β is the probability of error threshold and n is the number nodes in the network.

5.4 System Model and Proposed Link Schedule Algorithm

Let us consider a SCDMA MCN network $\Phi(\mathcal{V}, \mathcal{E})$ with n nodes, where $\mathcal{V} = \{v_1, v_2, \ldots, v_n\}$ is the set of vertices/nodes and $\mathcal{E}$ is the set of edges/links between nodes. A link schedule for the SCDMA network is denoted by $\Psi(\mathbf{C}, \mathcal{M}_1, \cdots, \mathcal{M}_C)$, where

- **C** = $\{c_i\}$ set of CDMA codes available for link schedule
- $|\mathbf{C}|$:= size of **C**, $|\mathcal{E}|$:= U size of $\mathcal{E}$, $|\mathcal{V}|$:= n size of $\mathcal{V}$
- $\mathcal{M}_i$= set of transmitter-receiver pairs which can communicate concurrently using same CDMA code c_i i.e. $\{t_{i,1} \rightarrow r_{i,1}, \cdots, t_{i,|\mathcal{M}_i|} \rightarrow r_{i,|\mathcal{M}_i|}\}$
- $|\mathcal{M}_i|$:= size of $\mathcal{M}_i$

If node v_k is within node v_j's *communication range*, then there is a *communication edge* from v_j to v_k, denoted by $v_j \xrightarrow{c} v_k$. Thus, the mapping from network $\Phi(\cdot)$ to communication network $\mathcal{G}_c(\mathcal{V}_c, \mathcal{E}_c)$ can be described as follows:

$$D(j,k) \leq R_c \;\; \Rightarrow \;\; v_j \xrightarrow{c} v_k \in \mathcal{E}_c, \;\; v_k \xrightarrow{c} v_j \in \mathcal{E}_c \tag{5.23}$$

where R_c is the communication range [100] and $D(j,k)$ is the distance between nodes v_j and v_k. i.e., $\mathcal{G}_c(\mathcal{V}_c, \mathcal{E}_c)$ consists of nodes which has communication link with atleast one of its neighbour. The schedule $\Psi(\cdot)$ is then designed from the graph $\mathcal{G}_c(\cdot)$. The scheduling problem is to assign CDMA code to nodes such that the communication over links are successful and simultaneously maximize the *spatial reuse* of the CDMA codes in the network. Specifically, an SCDMA link scheduling algorithm is equivalent to assigning a unique color to every communication edge in the graph, such that source-destination pairs corresponding to $communication\ edges$ with the same CDMA code can transmit simultaneously in a particular time slot.

Algorithm 1 PoE-LinkSchedule

input: Given network $\Phi(\cdot)$ and its associated communication graph $\mathcal{G}_c(\cdot)$
output: Set of colors $\mathbf{C}$ which ensures successful communication in all links, $\mathbf{C} : \mathcal{E}_c \rightarrow \{1, 2, \ldots\}$
Label the vertices of $\mathcal{G}_c$ randomly using uniform distribution
Use *successive breadth first searches* algorithm to partition $\mathcal{G}_c$ into out and in oriented graphs g_i, $1 \leq i \leq k$
for $i \leftarrow 1$ to k **do**
  for $j \leftarrow 1$ to n **do**
    if g_i is out-oriented **then**
      let $\lambda = (s, d)$ be such that $Label(d) = j$
    else
      let $\lambda = (s, d)$ be such that $Label(s) = j$
    end if
    $\mathbf{C}(\lambda) \leftarrow$ PoE-LinkColor(λ)
  end for
end for

5.4.1 PoE-LinkSchedule algorithm

We use graph coloring approach for scheduling of CDMA codes among links. The term "colors" in graph coloring approach represents available CDMA codes. The proposed PoE-LinkSchedule algorithm is described in Algorithm 1. We use physical layer probability of error as metric in scheduling algorithm. Probability of error is formulated based only on first and

second order statistics of the channel.

Step-1: In first step of our PoE-LinkSchedule algorithm at Line 3, we label all the vertices (nodes) randomly using uniform distribution.

Step-2: After the labeling step, communication graph $\mathcal{G}_c(\cdot)$ obtained in Section. 5.4 (equation (5.23)) is decomposed into k number of out-oriented and in-oriented graphs $g_1, g_2, \ldots, g_k$ in Line 4 [89]. This decomposition is achieved by partitioning graph $G_c(\cdot)$, the undirected equivalent of $\mathcal{G}_c(\cdot)$ into undirected forests. To reduce intensive computations, a *successive breadth first searches* is used to decompose $G_c(\cdot)$ into undirected forests. Each undirected forest is further mapped to two directed forests. In one forest, the edges (links) in every connected component point away from the root and every vertex has at most one incoming edge, thus producing an out-oriented graph. In the other forest, the edges in every connected component point toward the root and every vertex has at most one outgoing edge, thus producing an in-oriented graph. An in-oriented graph is also constructed by Algorithm 1 in [92] to determine a link schedule in a power-controlled STDMA network.

Step-3: In last step Lines 5-14, the oriented graphs are considered sequentially. For each oriented graph, vertices are considered in increasing order by label and the unique edge associated with each vertex is colored using the PoE-LinkColor function. In essence, the edges are considered in a random order for scheduling, since labeling is random. In Line 8 and 10 $Label(.)$ is the re-labeling function which assigns number j to nodes which are randomly considered for re-labeling. The PoE-LinkColor function is explained in Algorithm 2. In Algorithm 1 the $communication\ edge$ between nodes s and d ($s \rightarrow d$) is denoted as $\lambda(s, d)$. We choose the first color such that the resulting probability of error at the receiver of λ and the receivers of all co-colored edges are below the threshold β. If no such color is found, we assign a new color to λ.

5.5 Complexity Analysis

5.5.1 Complexity of the probability of error scheduling metric

As the $Q(.)$ function value can be found from look-up table, the complexity in determining probability of error (5.22) essentially lies on determining the values of $\mu_{y_u^R|\mathbf{B}[i]}$ and $\sigma^2_{y_u^R|\mathbf{B}[i]}[i]$.

Algorithm 2 PoE-LinkColor($\hat{\lambda}$)

input: Given network $\Phi(\cdot)$ and its associated communication graph $\mathcal{G}_c(\cdot)$

output: A color which ensures successful communication in a given link

$\mathcal{C} \leftarrow$ set of existing colors

$\mathcal{C}_c \leftarrow \{C(h) : h \in \mathcal{E}_c$, h is colored, $\hat{\lambda}$ and h interferes each other and hence PoE $\geq \beta$ in both $\hat{\lambda}$ and h $\}$

$\mathcal{C}_{cf} = \mathcal{C} \setminus \mathcal{C}_c$ i.e., $\mathcal{C}_{cf}$ is nothing but $\mathcal{C}$ except $\mathcal{C}_c$

for $i \leftarrow 1$ to $|\mathcal{C}_{cf}|$ **do**

  $r \leftarrow i^{th}$ color in $\mathcal{C}_{cf}$

  $E_r \leftarrow \{h : h \in \mathcal{E}_c, \mathbf{C}(h) = r\}$

  $\mathbf{C}(\hat{\lambda}) \leftarrow r$

  if probability of error at all receivers of $E_r \cup \{\hat{\lambda}\}$ lower than β **then**

    return r

  end if

end for

return $|\mathcal{C}| + 1$

Complexity in determining $\mu_{y_u^R|\mathbf{B}[i]}$

The received signal in (5.5) is expanded in the following equation with the assumption of perfect synchronization

$$y_u[i] = \sum_{f=1}^{F} \sum_{k=0}^{N-1} s_{uk}^{(f)} \sum_{m=0}^{L_h^u-1} h_u[m][j] \Big(A_u b_u[j] \tilde{s}_u[iN + k - m] \Big) + \sum_{f=1}^{F} \sum_{k=0}^{N-1} s_{uk}^{(f)} \eta_u[iN + k] \tag{5.24}$$

Since $b_u[j]$ is either $+1$ or -1 and if we assume $A_u = 1, \ \forall \ u$ the computational complexity in determining $\mu_{y_u^R|\mathbf{B}[i]}$ of (5.24) is $2L_h$ flops. If we include the complexity in determining the index term j the total complexity will be $10L_h$ multiplications and $4L_h$ additions where we have assumed division takes 4 flops [54]. Therefore, the total complexity involved in determining $\mu_{y_u^R|\mathbf{B}[i]}$ is O(L_h).

Complexity in determining $\sigma^2_{y_u^R|\mathbf{B}[i]}[i]$

From (5.21)

$$\sigma^2_{y_u^R|\mathbf{B}[i]}[i] = \frac{1}{4}\Bigg[\sum_{\substack{f_1,k_1,m_1,v_1,\\ f_2,k_2,m_2,v_2}} \tilde{C}_{v_1,v_2}\psi_1\psi_2 + \tilde{C}^*_{v_1,v_2}\psi_1^*\psi_2^* + C_{v_1,v_2}\psi_1\psi_2^* + C^*_{v_1,v_2}\psi_1^*\psi_2\Bigg] + N \times F\frac{\sigma^2}{2} \tag{5.25}$$

As $b_u[j], s_{uk}$ are either $+1$ or -1 and if we assume $A_u = 1,\ \forall\ u$ then ψ_1 and ψ_2 can be directly determined. Due to the above fact the summations $\sum_{k_1=0}^{N-1}$, $\sum_{k_2=0}^{N-1}$ in (5.25) will not constitute any additional complexity. Furthermore, the second order statistics of the channel coefficients $C_u,\ C_u^*,\ \tilde{C}_u,\ \tilde{C}_u^*$ are already available. Therefore, the terms which constitute complexity are $\sum_{m_1=0}^{L_h^u-1}$, $\sum_{m_2=0}^{L_h^u-1}$ as ψ_us are functions of m and also the terms $\sum_{v_1=1}^{U}$, $\sum_{v_2=1}^{U}$ as C_us are functions of u. Hence, the total number of operations involved in determining the $\sigma^2_{y_u^R|\mathbf{B}[i]}[i]$ O($U^2L_h^2$).

After analyzing the complexity involved in determining $\mu_{y_u^R|\mathbf{B}[i]}$ and $\sigma^2_{y_u^R|\mathbf{B}[i]}[i]$ we can conclude that the number of operations required to determine probability of error metric for a particular link is O($U^2L_h^2$).

5.5.2 Complexity of the proposed scheduling algorithm

In this section, we derive upper bounds on the running time complexity (computational complexity) of the PoE-LinkSchedule algorithm. Let us assume θ as thickness of the communication graph $\mathcal{G}_c(\mathcal{V}, \mathcal{E}_c)$ i.e., minimum number of graphs into which the undirected equivalent of $\mathcal{G}_c(\cdot)$ can be partitioned.

Lemma 5.1 *An oriented graph g can be colored with no more than $\mathrm{O}(n)$ colors using PoE-LinkSchedule.*

Since an oriented graph with n vertices has at most n edges, the edges of g can be colored with at most n colors.

Lemma 5.2 *For an oriented graph g, the running time of PoE-LinkSchedule is $\mathrm{O}(n^2)$.*

Assuming that an element can be chosen randomly and uniformly from a finite set in unit time (Chapter 1, [101]), the running time of Phase 1 can be shown to be $\mathrm{O}(n)$. Since there is only one oriented graph, Phase 2 runs in time $\mathrm{O}(1)$. In Phase 3, the unique edge associated with the vertex under consideration is assigned a color using PoE-LinkColor algorithm. From

Lemma 5.1, the size of the set of colors to be examined $|\mathcal{C}_c \cup \mathcal{C}_{cf}|$ is $\mathrm{O}(n)$. In PoE-LinkColor algorithm, the probability of error is checked only once for every colored edge in the set $\bigcup_{i=1}^{|\mathcal{C}_{cf}|} E_i$ and at most n times for the edge under consideration λ. With a careful implementation, PoE-LinkColor algorithm runs in time $\mathrm{O}(n)$. So, the running time of Phase 3 is $\mathrm{O}(n^2)$. Thus, the total running time is $\mathrm{O}(n^2)$.

Theorem 5.3 *For an arbitrary graph $\mathcal{G}$, the running time of PoE-LinkSchedule is* $\mathrm{O}(Un \log n + Un\theta)$.

Assuming that an element can be chosen randomly and uniformly from a finite set in unit time [101], the running time of Phase 1 can be shown to be $\mathrm{O}(n)$. For Phase 2, the optimal partitioning technique of [102] based on Matroids can be used to partition the communication graph $\mathcal{G}_c$ into at most 6θ oriented graphs in time $\mathrm{O}(Un \log n)$. Thus, $k \leq 6\theta$ holds for Phase 3. From Lemma 5.2, it follows that the first oriented graph g_1 can be colored in time $\mathrm{O}(n^2)$. However, consider the coloring of the j^{th} oriented graph g_j, where $2 \leq j \leq k$. When coloring edge λ from g_j using PoE-LinkColor algorithm, conflicts can occur not only with the colored edges of g_j, but also with the edges of the previously colored oriented graphs $g_1, g_2, \ldots, g_{j-1}$. Hence, the worst-case size of the set of colors to be examined $|\mathcal{C}_c \cup \mathcal{C}_{cf}|$ is $\mathrm{O}(U)$. Note that in PoE-LinkColor algorithm, the probability of error is checked only once for every colored edge in the set $\bigcup_{i=1}^{|\mathcal{C}_{cf}|} E_i$ and at most U times for the edge under consideration λ. With a careful implementation, PoE-LinkColor algorithm runs in time $\mathrm{O}(U)$. Hence, any subsequent oriented graph g_j can be colored in time $\mathrm{O}(Un)$. Thus, the running time of Phase 3 is $\mathrm{O}(Un\theta)$. Therefore, the overall running time of PoE-LinkSchedule is $\mathrm{O}(Un \log n + Un\theta)$. This complexity is comparable to that of ArboricalLinkSchedule algorithm of [89] and much lower than that of TruncatedGraphSchedule algorithm of [91]. Furthermore, this complexity is much lower than that of exhaustive search algorithm which has complexity of $\mathrm{O}(U^U)$.

5.6 Effect of Channel on the PoE Metric

The numerator term of the $Q(.)$ function of probability of error metric derived in (5.22) is

$$b_u[i]\mu_{y_u^R|\mathbf{B}[i]}[i] = \Re\left[b_u[i]\sum_{f=1}^{F}\sum_{k=0}^{N-1} s_{uk}^{(f)} \sum_{m=0}^{L_h^u-1}\sum_{v=1}^{U} \gamma_v[m][j]A_v b_v[j]\tilde{s}_v[iN+k-m]\right] \tag{5.26}$$

By using the inequality that $\Re(a) < |a|$ for any complex number a (5.26) can be written as

$$b_u[i]\mu_{y_u^R|\mathbf{B}[i]}[i] \leq \left| b_u[i] \sum_{f=1}^{F} \sum_{k=0}^{N-1} s_{uk}^{(f)} \sum_{m=0}^{L_h^u-1} \sum_{v=1}^{U} \gamma_v[m][j] A_v b_v[j] \tilde{s}_v[iN+k-m] \right| \tag{5.27}$$

By using the assumption of $i.i.d$ distribution of channel and simple algebraic manipulation (5.27) can be further written as

$$b_u[i]\mu_{y_u^R|\mathbf{B}[i]}[i] \leq \sum_{f=1}^{F} \sum_{k=0}^{N-1} \sum_{m=0}^{L_h^u-1} \sum_{v=1}^{U} \left| s_{uk}^{(f)} \gamma_v[m][j] A_v b_v[j] \tilde{s}_v[iN+k-m] \right| \tag{5.28}$$

Since the chip sequence is having unit energy and if we assume $A_u = 1 \; \forall \; u$, perfect synchronization and the chip waveforms matched with rake receiver fingers are independent then (5.28) will become

$$b_u[i]\mu_{y_u^R|\mathbf{B}[i]}[i] \leq F \sum_{m=0}^{L_h^u-1} \left| \gamma_u[m][j] \right| \tag{5.29}$$

From (5.11) and (5.12) the variance term (denominator) of the probability of error metric (5.22) can be written as

$$\begin{aligned} \sigma^2_{y_u^R|\mathbf{B}[i]}[i] &= \left(var\left[\Re\Big(\sum_{f=1}^{F} \sum_{k=0}^{N-1} s_{uk}^{(f)} \sum_{m=0}^{L_h^u-1} h_u[m][j] \sum_{v=1}^{U} A_v b_v[j] \tilde{s}_v[iN+k-m] \Big) \right] + N \times F \frac{\sigma^2}{2} \right) \\ &\geq N \times F \frac{\sigma^2}{2} \end{aligned} \tag{5.30}$$

The above inequality is from the fact that $var(.) \geq 0$. From (5.22), (5.29) and (5.30) the lower bound on individual probability of error can be written as

$$P_{E|\mathbf{B}[i]}[i] \geq Q\left(\frac{\sqrt{F} \sum_{m=0}^{L_h^u-1} \left| \gamma_u[m][j] \right|}{\sqrt{(N\sigma^2/2)}} \right) \tag{5.31}$$

From (5.31) we can see that the lower bound on probability of error in a link increases when the channel mean, number of multipaths reduce and receiver noise increases. Therefore, we can conclude that the *spatial reuse* which is defined in (5.32) will increase when the mean of the channel, number of multipath increases and the receiver noise reduces.

5.7 Simulations and Results

5.7.1 Performance metric-I: Spatial reuse

The *spatial reuse* of the schedule is defined as the average number of successfully received packets per CDMA code in the SCDMA schedule. The transmission from transmit node i using

CDMA code c at tth time slot is successful at receiving node j only if $P_{E_{i,j}} \leq \beta$. Thus

$$\textit{spatial reuse} = \tau = \frac{\sum_{c=1}^{|\mathbf{C}|} \sum_{k=1}^{|\mathcal{M}_c|} I(P_{E_{i,j}} < \beta)}{|\mathbf{C}|} \tag{5.32}$$

where $I(A)$ denotes the indicator function for event A, i.e., $I(A) = 1$ if event A occurs, $I(A) = 0$ if event A does not occur. From (5.32) we can see that large value of τ implies that there are many simultaneous successful communications.

5.7.2 Performance metric-II: End-to-End throughput

End-to-end throughput is defined as the probability of successful transmission from source node to destination node, which involves successful transmission at each and every intermediate hop. The closed form expression for the end-to-end throughput is derived as follows

- Case I: Number of hops > 1

  Let us say $x_m = \{1,\ 2,\ 3, \ldots, h\}$ is the path selected to relay the packets from source node 1 to the destination node h using some routing algorithms and number of hops in the routing path is $h-1$. The probability $\mathrm{P}(S_{1,h})$ that the message is successfully transmitted from source 1 to destination h is given by:

$$\mathrm{P}(S_{1,h}) = \mathrm{P}(\bigcap_{i=1}^{h-1} S_{i,i+1}) = 1 - \mathrm{P}(\bigcup_{i=1}^{h-1} E_{i,i+1}) =\geq 1 - \sum_{i=1}^{h-1} \mathrm{P}(E_{i,i+1}) \tag{5.33}$$

  where $\mathrm{P}(E_{i,i+1})$ is the probability of error in the link $i, i+1$ as derived in (5.22).

- Case II: Number of hops = 1, $\mathrm{P}(S_{1,h}) = 1 - \mathrm{P}(E_{1,h})$

For simulations a single circular cell of radius $R = 1000\ m$ is considered with nodes distributed as stationary distribution derived from Random Waypoint (RWP) mobility model [103]. The radial distribution of nodes as a function of radial distance r from the center is given by

$$f(r) = \frac{12}{73}\Big(27r - 35r^3 + 8r^5\Big) \tag{5.34}$$

All the nodes are assumed to transmit with a constant power P. The value of R_c is considered to be $500\ m$. From the nodes' distribution we construct $\Phi(\cdot)$ and then map network $\Phi(\cdot)$ to the graph $\mathcal{G}_c(\cdot)$ using (5.23). The PoE-LinkSchedule is computed using the proposed algorithm. Once the link schedule is computed, the *spatial reuse* is calculated using (5.32). The

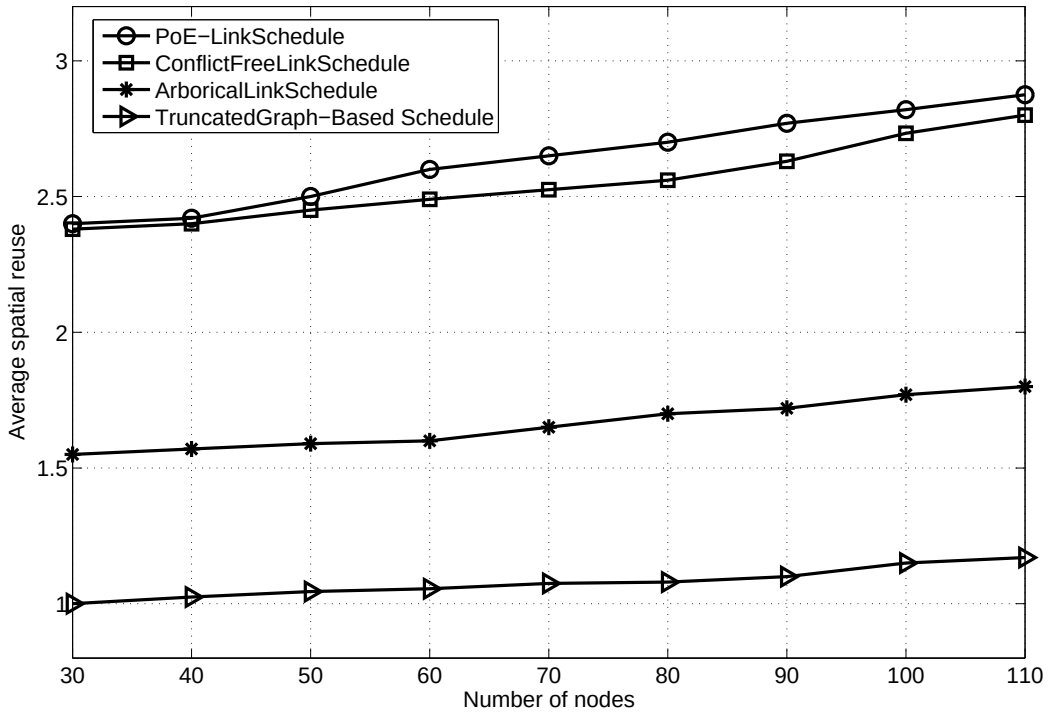

Figure 5.2: Spatial reuse versus number of nodes

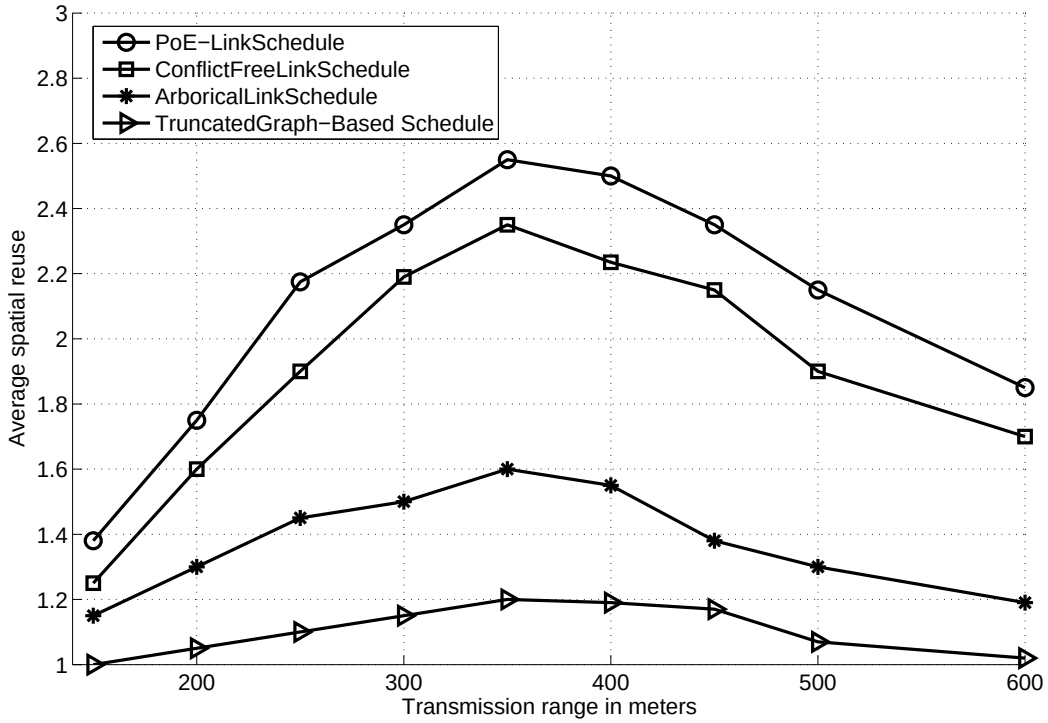

Figure 5.3: Spatial reuse versus transmission range

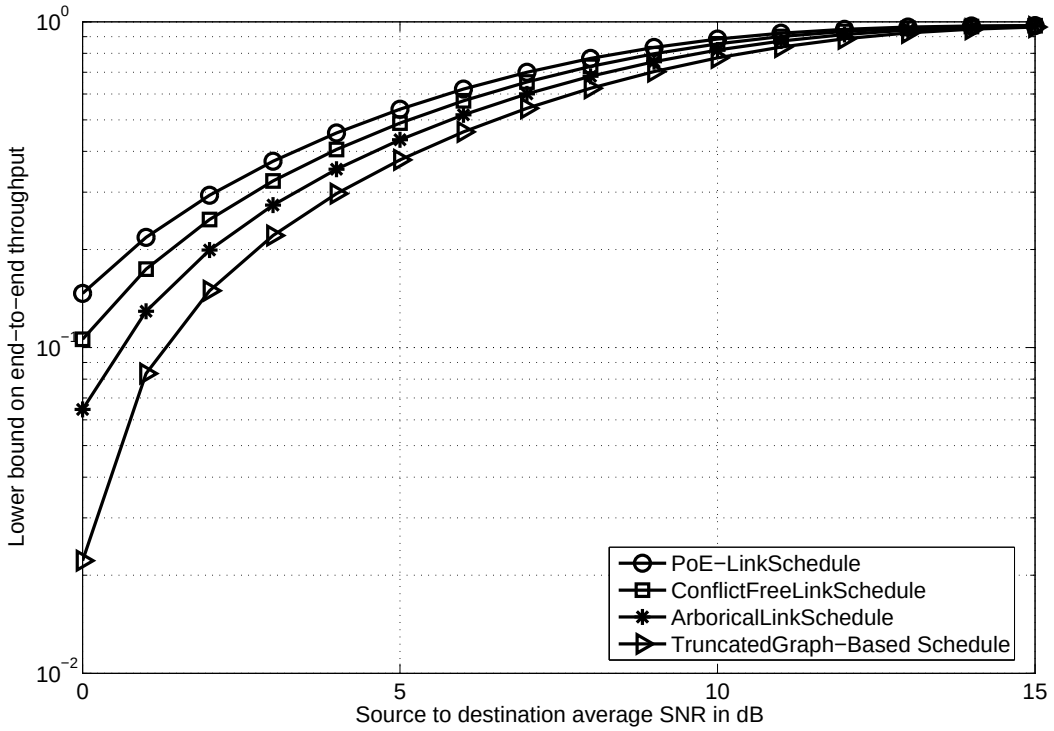

Figure 5.4: End-to-end throughput versus SNR

spatial reuse is averaged over 100 nodes' distributions. In the underlined simulation environment with the SCDMA network the *spatial reuse* is calculated using the algorithms ArboricalLinkSchedule proposed in [89], TruncatedGraphSchedule algorithm of [91] and also ConflictFreeLinkSchedule of [100]. The *spatial reuse* is plotted against the varying number of nodes in Fig. 5.2. We can observe that the PoE-LinkSchedule has higher *spatial reuse* compared to all other algorithms. This is because PoE-LinkSchedule has probability of error as scheduling metric while all the other algorithms have SNR as schedule metric. Hence, the *spatial reuse* which is the function of probability of error is higher in the proposed PoE-LinkSchedule.

The *spatial reuse* is also plotted against the transmission range for a fixed node density. From Fig. 5.3, we can see that the *spatial reuse* increases for increasing transmission range (transmission power) till it reaches the maximum range. However, after it reaches the maximum, it starts decreasing. This is because at lower transmission ranges the received signal strength will be minimum and receiver noise dominates the received signal. Therefore, as we increase the transmission range received signal strength will also increase and so does the *spatial reuse*. However, after some level of transmission range, the interference dominates the received signal. Hence, the *spatial reuse* decreases as shown in Fig. 5.3.

We have also plotted the lower bound on end-to-end throughput by selecting a random source and random destination and using minimum hop count routing algorithm. The lower bound on end-to-end throughput is calculated using (5.33) and averaged over atleast 100 different source-destination pairs. Thus obtained lower bound on end-to-end throughput is plotted in Fig. 5.4 for various SNRs. We can conclude from Fig. 5.4 that the proposed algorithm has better end-to-end throughput. This is because the end-to-end throughput metric is defined as a function of probability of error and the proposed algorithm has lower probability of error in all links due to probability of error constraint.

5.8 Conclusion

In this work, we have developed PoE-LinkSchedule algorithm for SCDMA MCNs. An empirical modeling shows that, on an average, our algorithm achieves higher *spatial reuse* and end-to-end throughput compared to the ConflictFreeLinkSchedule, ArboricalLinkSchedule and TruncatedGraphSchedule algorithms. Furthermore, PoE-LinkSchedule algorithm has complexity comparable to that of ArboricalLinkSchedule algorithm and much lower than that of TruncatedGraphSchedule algorithm. Since the statistics of the channel varies slower than the channel coefficients itself, computing PoE metric and scheduling the links offline in a centralized fashion is feasible. Thus, in cognizance of *spatial reuse* and end-to-end throughput PoE-LinkSchedule is a good candidate for efficient link scheduling algorithm. Once the scheduling information is available the source to destination path for multihop voice/data communication can be established through the scheduled links using some standard routing algorithms.

Chapter 6

On Optimal Transmission Range for Multihop Cellular Networks

In this chapter analytical relationship between transmission range and network connectivity is obtained as a function of number of nodes for CDMA based Multihop Cellular Network (MCN). We show that for a network of n uniformly distributed nodes in a single cell of unit radius, the transmission range r should be sufficiently larger than $\sqrt{\frac{2\ln n}{n-1}}$ to achieve asymptotic full connectivity. The distribution of the nodes may not be uniform in case of mobility. In such case a mobility model dependent lower bound on transmission range is obtained. We show that for Random Waypoint (RWP) model the lower bound for the nodes which lie completely inside the cell is same as the corresponding uniform node distribution case. However, for nodes on boundary the transmission range lower bound is $\left(\frac{\ln n}{n}\right)^{1/3}$ which is larger than the corresponding uniform node distribution case. Our findings show that more transmission range is required at the boundary to establish better connectivity and hence, a variable transmission range control mechanism is necessary. In addition to the lower bound, we also propose a method to choose the optimal value of transmission range using a scheduling mechanism and ensure that the optimal value is always greater than the lower bound. Thus obtained transmission range could be used to select the transmission power of the nodes in a meaningful way and hence, the nodes' isolation could be avoided and the spectral efficiency can be increased. We demonstrate empirically, that the proposed transmission range control mechanism increases the network connectivity as well as $spatial\ reuse$ of the resources.

6.1 Introduction

In Multihop Cellular Network (MCN) mobile terminals transmit packets to base stations as well as to other mobile stations using multiple hops with less transmission range. Such a system enhances the throughput, user capacity and energy efficiency [56]. However, the issue of optimal selection of the transmission range in MCN is yet to be addressed. In MCN, obtaining optimal transmission range assumes quite significance due to many multiple short range transmissions instead of single long range transmission [88]. This chapter addresses the transmission range control problem for CDMA based MCN. The motivation and main contributions of this chapter are

1. In CDMA-MCN to obtain high $spatial\ reuse$ of resources the transmission range of mobile nodes have to be decreased. While, the transmission range is decreased beyond certain threshold the connectivity of the network will become questionable [79]. We derive an analytical relationship between transmission range and connectivity as a function of number of nodes in the network and thus obtain a lower bound on transmission range as a function of number of nodes.

2. For better connectivity of the nodes the transmission range of the nodes has to be increased well above the lower bound. However, more the transmission range more the interference seen in the systems and hence, less $spatial\ reuse$ of the resources. We propose an optimal choice for the transmission range using $spatial\ reuse$ metric in the case of MCN. When the optimal range is below the connectivity lower bound then the closest suboptimal value, which satisfies lower bound as well as provides $spatial\ reuse$ close to the maximum, will be chosen. With thus obtained transmission range, the transmission power of the mobiles could be better controlled to reduce the interference [104] as well as to achieve high connectivity.

3. We also derive the minimum required transmission range as well as optimal transmission range in case of nodes' mobility. RWP mobility model is used for illustration. The results show that the transmission range in case of RWP model is same as that of uniform node distribution when the nodes lie completely inside the cell. However, it is higher than the corresponding uniform node distribution scenario when the node lies in the boundary regions.

6.2 Related Work

A transmission range strategy to maximize throughput for a direct-sequence spread-spectrum multihop packet radio network is proposed in [105]. An individual variable-range transmission power control on the physical and network connectivity, network capacity and power savings of wireless multihop networks is presented in [106]. For uniformly distributed nodes the required transmission range that creates an almost surely k connected topology for a given node density is proposed in [107]. A transmission range assignment scheme for wireless sensor node such that a multihop communication path exists between each sensor node and a super node (base station) is derived in [108]. A heuristic approach based on interference efficient topology control is proposed for wireless ad-hoc networks in [109]. [110] presents a method to adjust the powers of mobile stations to control/improve the topology of the packet radio network. [111] proposes a transmission range selection method by considering the channel fading effect. We considerably differ from all the above work by considering the boundary as well as non boundary scenarios and also the mobility in the network which is prevalent in the case of MCN.

6.3 Lower Bound on Transmission Range

We derive the lower bound on transmission range such that the network is fully connected. Disconnectivity is defined as probability of at least one node being out of coverage region of all other nodes in a given cell. Consider a single cell with unit radius and n nodes distributed as uniform point process and a single node m with transmission range r ($r < 1$) at the boundary of the cell. The scenario of node m being isolated is shown in Fig. 6.1. We wish to find the lower bound on value of r to avoid the node's isolation. The probability of node m being in isolation could be found by calculating the intersection of area of circle of radius 1 and circle of radius r.

Now the area of sector ABC which is shown with dotted lines in Fig. 6.2 is given by

$$A_{ABC} = \Big(\frac{\pi}{2} - \frac{\theta}{2}\Big)r^2 \tag{6.1}$$

Therefore, the area of shaded region A_{shaded}= Area of sector AOC centered at O- Area of OABC (two back to back triangle with OB as common side) which is given by

$$A_{shaded} = \frac{1}{2} \times 2\theta - 2 \times \frac{1}{2} \times r \times cos\Big(\frac{\theta}{2}\Big) \tag{6.2}$$

from (6.1), (6.2) the area of portion of cell within the transmission range of node m (A_r) is

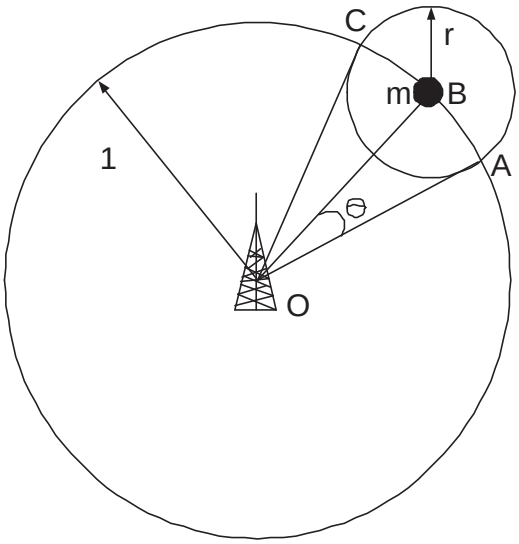

Figure 6.1: An extreme case scenario where a node m lies at boundary of a cell

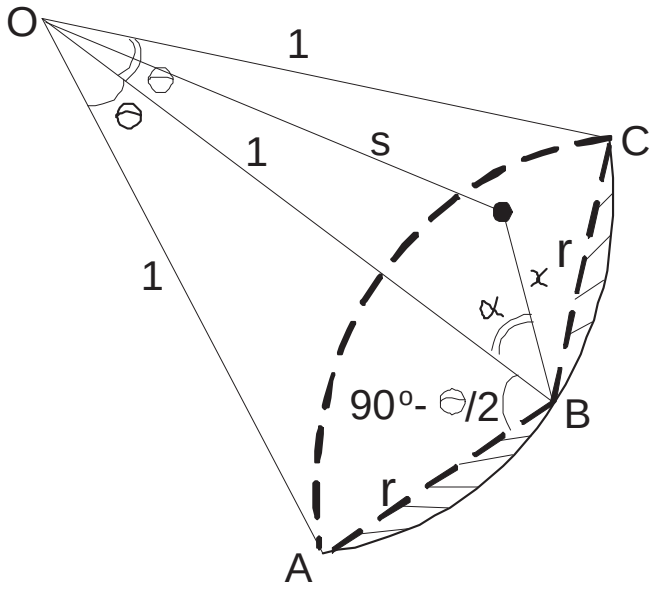

Figure 6.2: A zoomed view of the cell to look at the covered region

given by

$$A_r = \theta - r\cos\left(\frac{\theta}{2}\right) + (\frac{\pi}{2} - \frac{\theta}{2})(r^2) \tag{6.3}$$

Now consider first and second term in the RHS of above equation. As r is less than 1 in MCN we can neglect the area of shaded region of Fig. 6.2. This is because of the reason that θ being small, $\cos\theta$ tends to 1 and θ tends to r. Hence, both of these terms vanish and we can obtain the following approximation

$$A_r \approx \left(\frac{\pi}{2} - \frac{\theta}{2}\right)r^2 \tag{6.4}$$

Therefore, probability of a particular node i among n nodes being isolated (P_i) is given by probability that all $n-1$ nodes lie in uncovered region. As we have assumed uniform distribution of nodes,

$$P_i = \left(\frac{A - A_r}{A}\right)^{n-1} = \left(1 - \frac{A_r}{A}\right)^{n-1} \tag{6.5}$$

where $A = \pi$ is the area of circle of radius 1. Therefore, from (6.4), (6.5)

$$P_i = \left(1 - \left(\frac{1}{2} - \frac{\theta}{2\pi}\right) \times r^2\right)^{n-1} \tag{6.6}$$

Now, the probability of at least one node being isolated (P_i^1) is given by $P_i^1 = \bigcup_{i=1}^{n} P_i$. Upper bound on P_i^1 could be obtained by using the union bound property as

$$P_i^1 = \bigcup_{i=1}^{n} P_i \leq \sum_{i=1}^{n} P_i = \sum_{i=1}^{n} (1 - k \times r^2)^{n-1} \tag{6.7}$$

where, $k = \frac{1}{2} - \frac{\theta}{2\pi}$. Since $\theta \leq \pi$, $k < 0.5$. For dense network (i. e large n) using Poisson approximation [103]

$$P_i^1 \leq \sum_{i=1}^{n} e^{-(n-1)k\times r^2} = n \times e^{-(n-1)k\times r^2} \tag{6.8}$$

We define the probability of disconnection (P_D) as probability of at least one node being isolated (P_i^1). Therefore, from (6.8)

$$P_D \leq n \times e^{-(n-1)k\times r^2} = e^{\ln n - (n-1)k\times r^2} \tag{6.9}$$

Finally,

$$P_D \leq e^{\ln n\left(1 - \frac{(n-1)kr^2}{\ln n}\right)} = e^{\ln n\left(1 - k\times\left(\frac{r}{\sqrt{\frac{\ln n}{(n-1)}}}\right)^2\right)} \tag{6.10}$$

In the above expression if r decreases slower than, $\sqrt{\frac{\ln n}{k(n-1)}}$, then P_D will asymptotically approach zero. Hence, the network will become fully connected for sufficiently large n. As

$k < 0.5$ we can further say that $r > \sqrt{\frac{2lnn}{(n-1)}}$ in order to achieve asymptotic connectivity. This result is in agreement with a landmark result by Gupta and Kumar [112] which states that when $\pi r^2(n) = \frac{\ln n + C(n)}{n}$ then the network is connected with probability 1 provided that, for $n \to \infty$, $C(n) \to \infty$.

In case the mobile node is completely inside the cell as shown in Fig. 6.3 then in (6.5) A_r/A will become r^2 hence k will become 1. Therefore, the lower bound on transmission range for the node completely inside the cell is $\sqrt{\frac{\ln n}{(n-1)}}$. For dense network this lower bound can be approximated as

$$\sqrt{\frac{\ln n}{n}} \tag{6.11}$$

6.3.1 Lower bound on transmission range due to mobility

RWP model is a commonly used model for mobility in ad-hoc networks. Uniform distribution for nodes' location may not be true in case of mobility of nodes. The distribution of the nodes will dependent on the mobility model chosen. For instance in case of RWP model under steady state conditions the probability density function of nodes is shown in Fig. 6.4. The occurrence of node at a distance s from the origin with RWP model is given by the mean-square error approximation [113]

$$f(s) = \frac{6}{73\pi}(27 - 35s^2 + 8s^4) \tag{6.12}$$

We can find the probability density function of node occurrence in a ring of radius s with reference to the origin by multiplying the above equation by $2\pi s$:

$$f_S(s) = \frac{12s}{73}(27 - 35s^2 + 8s^4) \tag{6.13}$$

Above distribution is used for the connectivity analysis in the subsequent section.

Lets look at the worst case scenario for the isolation of node with RWP model which, again, should be looked at boundary of the cell. We can still neglect the shaded region in Fig. 6.2 and consider sectoral area ABC. Lets define a polar coordinate system (x, α) with B as center and OB as the axis in Fig 6.2. For $r < 1$, radial distance of any point in the sector from O can be stated as

$$s = \sqrt{1 + x^2 - 2xcos\alpha} \tag{6.14}$$

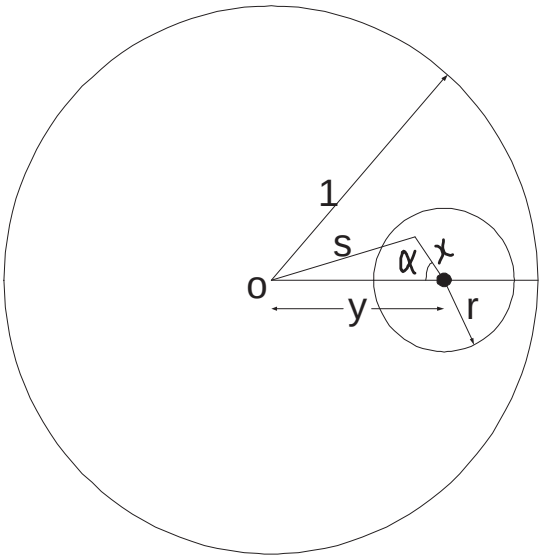

Figure 6.3: General case of a node lying completely in the cell at distance y from the origin

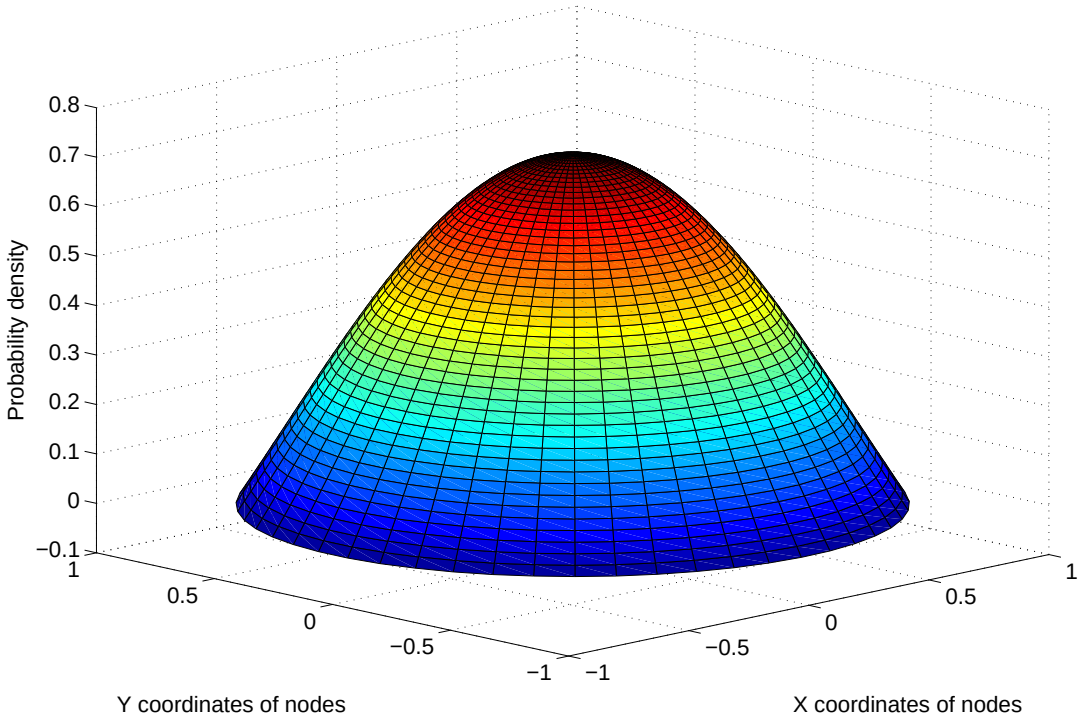

Figure 6.4: Steady state probability density of the nodes in the circular cell of radius 1 with RWP mobility model

Using this in (6.12) the probability density function of RWP model can be stated as

$$^{1}f(x,\alpha) = \frac{6}{73\pi}(38xcos\alpha - 19x^2 + 32x^2cos^2\alpha - 32x^3cos\alpha + 8x^4) \tag{6.15}$$

Now the probability that a node lies within the sector ABC of Fig. 6.2 is,

$$p = 2\int_0^{\frac{(\pi-\theta)}{2}} \int_0^r f(x,\alpha)xdxd\alpha \tag{6.16}$$

On solving with approximations (considering $sin\theta \approx \theta \approx r$ and neglecting terms of r with degree higher than 4) above equation yields

$$p \approx \frac{76r^3}{73\pi} - \frac{9r^4}{292} \approx \frac{76r^3}{73\pi} \tag{6.17}$$

Now, the mean number of nodes within the transmission range can be given as np (Poisson approximation for large n [103]), so that the probability for no node lying within the range of a given node i is

$$P_i = e^{-np} \tag{6.18}$$

Hence, in this case by union bound

$$P_D < nP_i \tag{6.19}$$

substituting p from (6.17) in (6.18) and then using (6.18) in (6.19)

$$P_D < e^{\ln n\left(1-k\left(\frac{r}{\sqrt[3]{\frac{\ln n}{n}}}\right)^3\right)} \tag{6.20}$$

where $k = \frac{76}{73\pi}$. Comparing with (6.10) this result suggests us that the transmission range value at boundary should be greater than $\left(\frac{\ln n}{n}\right)^{1/3}$.

In case when the node completely lies in the cell

$$p = \int_0^{2\pi} \int_0^r f(x,\alpha)xdxd\alpha \tag{6.21}$$

In order to look at the transmission range requirement near center, lets generalize the analysis considering that node is located at distance y from origin, where, $r \leq y \leq 1-r$ as shown in Fig. 6.3. Clearly, the substitution required for this case (as in (6.14)) is

$$s^2 = x^2 + y^2 - 2xycos\alpha \tag{6.22}$$

[1]here it is defined only for the region covered by node

Hence, calculating required $f(x, \alpha)$ and using (6.21), the following general probability expression can be obtained

$$p = \frac{1}{3}[(162 - 210y^2 + 48y^4)r^2 + (96y^2 - 105)r^4 + 16r^6] \tag{6.23}$$

For $y = r$, this probability of coverage converges to

$$p = \frac{1}{73}[162r^2 - 315r^4 + 160r^6] \tag{6.24}$$

which suggests that near center the transmission range can be chosen of the order of $\sqrt{\frac{\ln n}{n}}$. This result matches with the case for uniform node distribution as shown in (6.11). For $y = 1 - r$ the expression for p has minimum degree 3 confirming that lower bound on transmission increases at the boundary for high probability of connectivity.

6.4 Variation of Connectivity with Transmit Energy

Monte Carlo simulations have been performed to observe the effect of transmit range variation on the connectivity of a network. A 1000m radius circular area with 1000 uniformly distributed nodes have been considered. For illustration purpose hop count is taken as routing metric to select a path between a source node and destination node. However, the algorithm is routing independent. Source and destination nodes are selected using uniform distribution from the set of nodes. The probability of end-to-end connectivity (that is probability of establishing a path between any two nodes using a minimum hop count routing) is calculated for a given node transmission range. A plot is obtained between average connectivity versus transmission range. The experiment is repeated for various number of hop counts to understand the relationship between connectivity and hop count. Fig. 6.5 illustrates the plots. Note that the probability of connectivity is getting higher when hop count increases. This is because as the hop count increases we can establish the path with multiple smaller hops even though the transmission range is less.

In the second phase nodes are assumed to be distributed according to RWP model which is carried out by an inverse mapping of cumulative distribution function corresponding to probability density given in (6.13) on to cumulative distribution for uniform distribution in circular area. Fig. 6.6 shows the steady state nodes distribution for RWP mobility model and its corresponding uniform distribution. The probability of connectivity in case of RWP model is shown in Fig. 6.7 against transmission range for various hop counts.

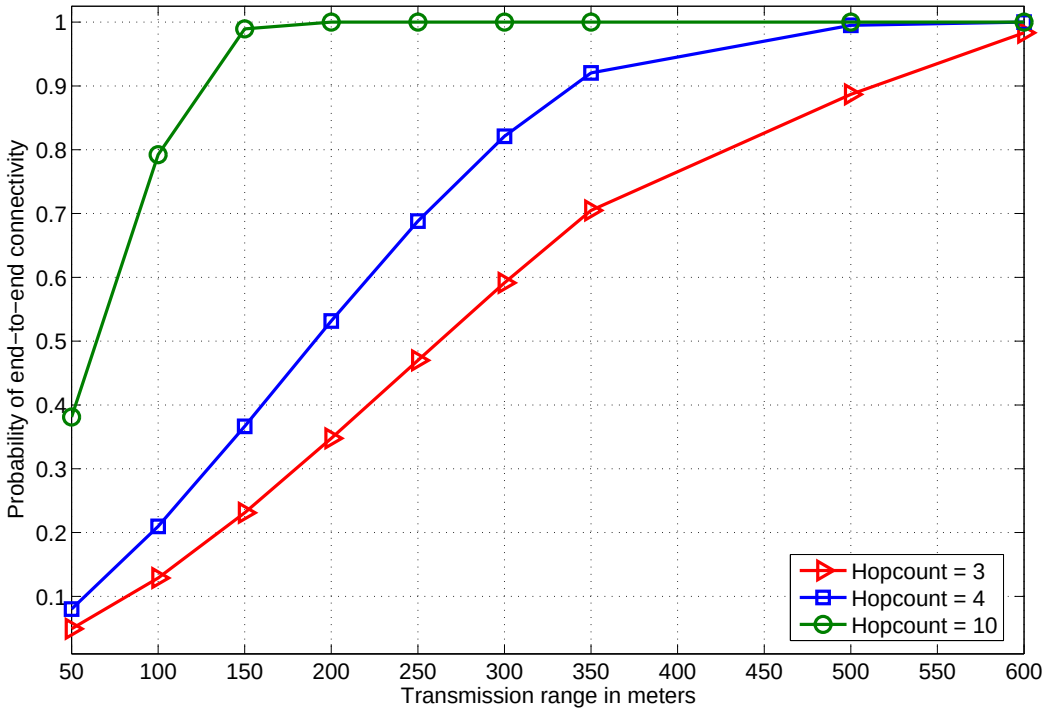

Figure 6.5: Connectivity analysis with uniformly distributed nodes

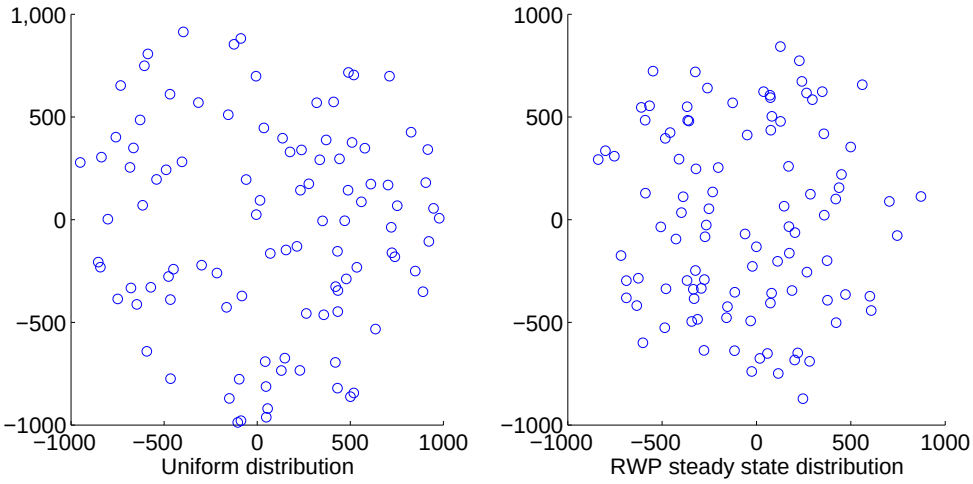

Figure 6.6: Scatter plots of node distribution for uniform distribution and the corresponding RWP model

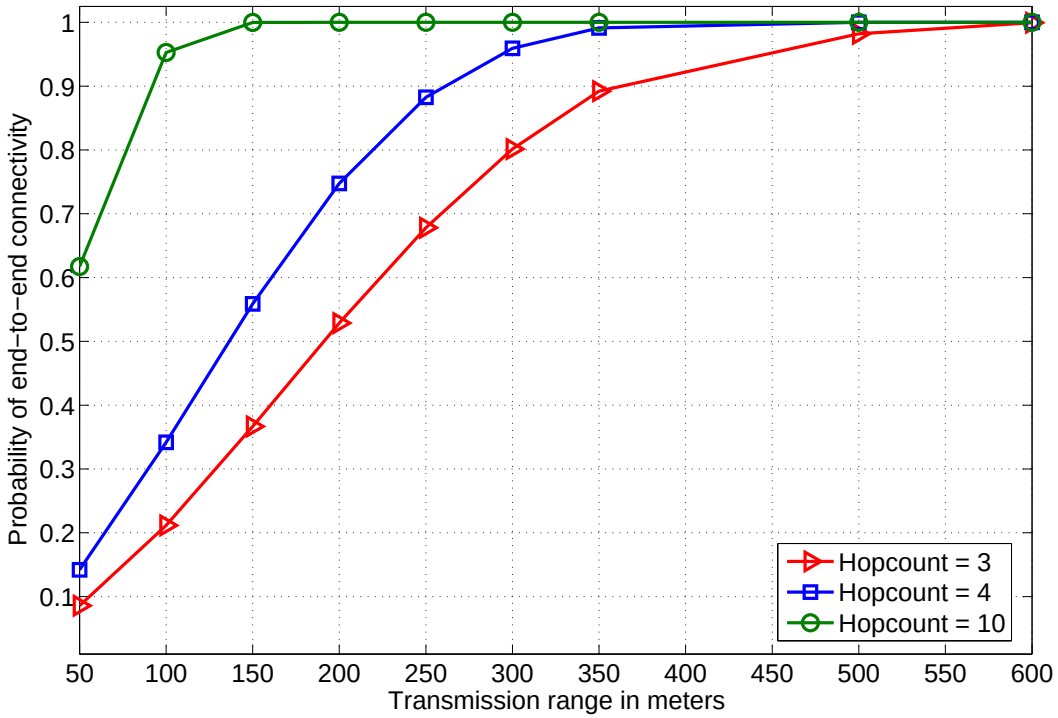

Figure 6.7: Connectivity analysis with RWP mobility model

6.4.1 Inferences drawn from the plots

We observe the effect of hop count on our analysis. For 1000 nodes, the minimum transmission range should be well above 0.08m, where we have not considered the limit on number of hops for transmission. Therefore, simulation results, considering maximum hop constraint show that a higher transmission range will be required for achieving high probability of connectivity. If we make the network more delay tolerant (in terms of hop counts), a lesser transmission range lower bounded by threshold value will be required. For same hop count, average connectivity of RWP model is found to be higher than the uniform model.

6.5 Optimal Value of Transmission Range

We have seen that the connectivity increases with the transmission range. However, it is essential that the transmit range of each user in MCN-CDMA systems must be reduced to limit interference so that the $spatial\ reuse$ can be increased. To evaluate the performance of the MCN-CDMA systems with respect to transmission range, we define the *spatial reuse* metric in

the same way as in (5.32) i.e., the average number of successfully received packets per time slot. However, we repeat it here for continuity. The transmission from node $t_{i,j}$ using CDMA code i at jth time slot is successful at receiving node $r_{i,j}$ only if $P_{E_{r_{i,j}}} \leq \beta$ where β is probability of error threshold and $P_{E_{r_{i,j}}}$ is the probability of error at receiver $r_{i,j}$. Thus

$$\textit{spatial reuse}= \sigma = \frac{\sum_{i=1}^{C} \sum_{j=1}^{M_i} I(P_{E_{r_{i,j}}} < \beta)}{C} \tag{6.25}$$

where $I(A)$ denotes the indicator function for event A, i.e., $I(A) = 1$ if event A occurs, $I(A) = 0$ if event A does not occur and C is total number of available orthogonal CDMA codes and M_i is the number of transmit and receive pairs which can successfully communicate in a given time slot using the same CDMA code i. The essence of MCN-CDMA is to have a reasonably large number of concurrent and successful transmissions. From (6.25) we can see that transmission range (power) of each node must be reduced to limit interference, however, the range (power) should be sufficient enough to maintain the probability of error at the desired receiver for a satisfactory call quality as well as to maintain the connectivity in the network. Therefore, the optimal transmission range should be chosen such that the lower bound on transmission range is satisfied as well as the $spatial\ reuse$ (which is a function of probability of error) is increased.

We consider a single circular cell of radius $R = 1000m$ with 1000 nodes distributed as uniform point process as well as distribution of RWP model. All the nodes are assumed to transmit with a constant power P. Our aim is to find the optimal transmit range for each node. Spatial reusing of CDMA codes is carried out using the PoE-LinkSchedule algorithm proposed in Chapter 5. Once the reusing strategy is planned, the $spatial\ reuse$ metric is computed using (6.25). The $spatial\ reuse$ is plotted against the transmission range in Fig. 6.8 after averaging over 100 nodes distributions. From Fig. 6.8 we can see that the $spatial\ reuse$ increases for increasing transmission range (transmission power) till it reaches the maximum range. However, after it reaches the maximum it starts decreasing. This is because at lower transmission ranges the received signal strength will be minimum and receiver noise dominates the received signal. Therefore, as we increase the transmission range received signal strength will also increase and hence, the $spatial\ reuse$. However, after some level of transmission range the interference will start dominating the received signal. Hence, the $spatial\ reuse$ will start decreasing as shown in Fig. 6.8. In case of dense network the optimal transmission range corresponding to maximum $spatial\ reuse$ will always be greater than the lower bound. However, in sparse network it may

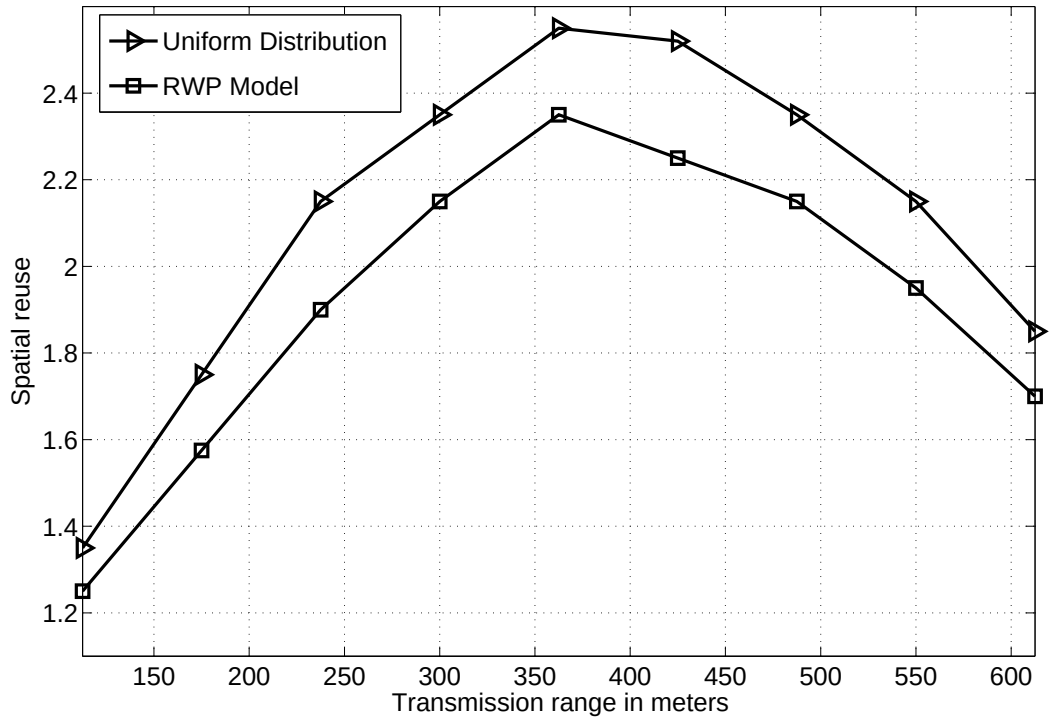

Figure 6.8: *Spatial reuse* versus transmission range

not true. In such case a suboptimal value which is greater than the lower bound and in the neighbourhood of the optimal transmission range will be selected.

6.6 Conclusion

In this work we have analyzed the relationship between connectivity and transmission range for both uniform distribution as well as RWP distribution of nodes for MCN. We have observed that with a given hop count there exists a minimum transmit energy above which the connectivity increases significantly. Later, we have also proposed a selection strategy for optimal transmission range to increase both the $spatial\ reuse$ of the resources as well as the network connectivity. Employing such a transmission range, the communication link can be better established between any pair of nodes using multiple hops with improved network capacity.

Chapter 7

Access Mechanism for Multihop Cellular Networks

A CDMA-OFDM access mechanism is proposed for Multihop Cellular Networks in this chapter. Source node, destination node and intermediate relay nodes constitute a group and a CDMA spreading sequence is assigned to each such group. In a particular group, a single OFDM carrier is assigned to each intermediate hop, hence the proposed OFDM is FDMA in nature. The sub carriers assigned to the intermediate hops in a given group are mutually orthogonal and also the CDMA codes assigned to different groups. The sub carriers and transmit power levels to the relay nodes are assigned in such a way as to maximize the end-to-end throughput. The end-to-end throughput is formulated by assuming a Rayleigh flat fading channel between nodes. Simulation results show that the proposed access mechanism achieves better end-to-end throughput and Bit Error Rate (BER) performance compared to standard access mechanisms like CDMA and OFDM-FDMA. Furthermore, the BER performance with multiple transmit sources is also considerably higher in the case of the proposed access mechanism.

7.1 Introduction

This chapter addresses the issue of access mechanism for Multihop Cellular Networks (MCN). The primary objectives of the MCN wireless systems are efficient bandwidth utilization, low implementation complexity and higher data rates. To achieve these objectives, the two primary contending technologies are

- Orthogonal Frequency-Division Multiplexing (OFDM), which has higher spectral efficiency and very low implementation complexity.
- Code Division Multiple Access (CDMA), which promises higher data rate.

The combination of CDMA and OFDM is a promising candidate for MCN. We will derive the mechanisms for using OFDM-CDMA in multihop cellular networks in the subsequent sections of this chapter.

The main contributions of this chapter are as follows:

1. We propose a strategy to use CDMA-OFDM access mechanism in multihop cellular networks. Our proposed OFDM is FDMA in nature. We propose a sub carrier allocation scheme to the intermediate hops such that the end-to-end throughput is maximized with the constraint that the interference is maintained below certain threshold.
2. The end-to-end throughput is formulated by assuming an $i.i.d$ Rayleigh flat fading propagation channel between nodes instead of the commonly encountered distance-decay law in literature.

7.2 Related Work

There has been a significant amount of research work going on in access mechanism design for MCN. MC-CDMA access mechanism is proposed for MCN in [114]; however, the system model assumes fixed relays and the proposed algorithm is only for uplink communications. Sub carrier allocation scheme to maximize the information theoretic capacity of an OFDM based multihop network is proposed in [115]. An OFDM relaying scheme by taking into account the propagation channel is proposed in [116]. Optimal number of sub-carriers into which the bandwidth should be split in order to maximize the throughput of the OFDM based MCN is analyzed in [117]. There are many literature on CDMA based MCN [118–120]. However, to the best of our knowledge, there is no literature available on CDMA-OFDM for MCN with generic system model and Rayleigh fading channel to maximize the end-to-end throughput.

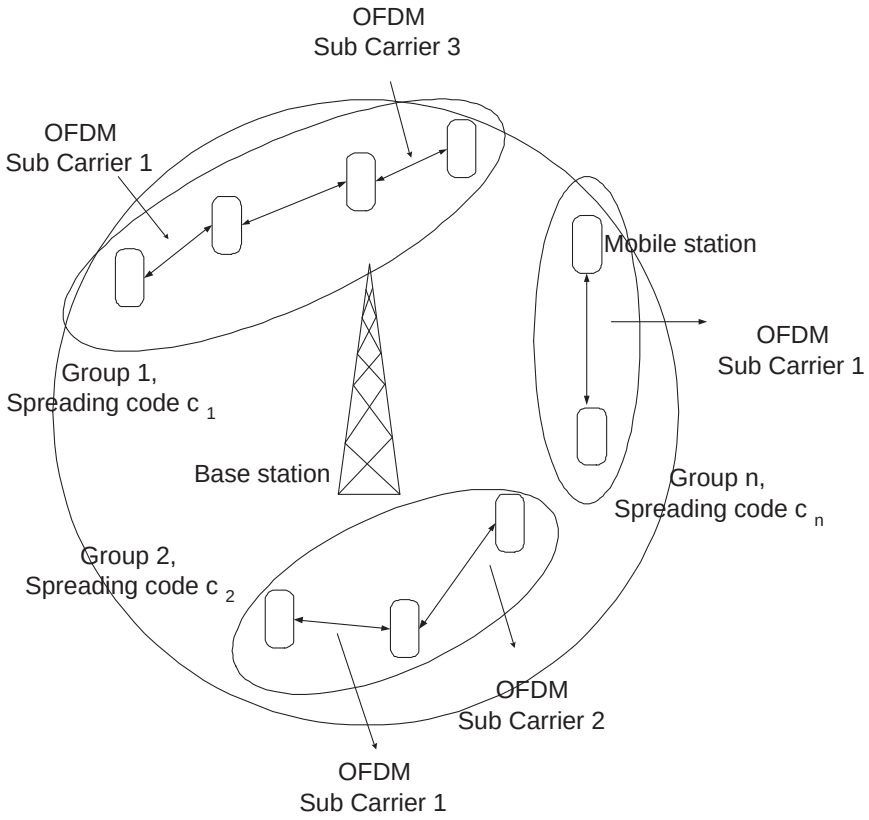

Figure 7.1: Proposed access mechanism

7.3 Proposed Access Mechanism and System Model

7.3.1 Proposed access mechanism

The underlying system model is shown in Fig 7.1. Let us assume that the source node, destination node and intermediate relay nodes in the routing form a single group as shown in Fig 7.1. There could be many such groups in a cell. Each group is assigned with a CDMA spreading code and the spreading codes assigned to different groups are orthogonal. In a particular group each node uses a single OFDM sub carrier to forward the call. Hence, the proposed OFDM is FDMA in nature. Moreover, FDMA based OFDM has higher throughput than TDMA based OFDM [115]. The receiver is a simple matched filter receiver in order to reduce the complexity. The message packets are CDMA spreaded and OFDM modulated at the source node. The relay nodes are assumed to be of demodulate and forward type; i.e., relay nodes demodulate the OFDM packet and modulate them again with a different OFDM carrier and forward it to the next node in the path. Note that CDMA spreading/despreading will be done only at the source node and/or destination node (end nodes) and not at the relay nodes (intermediate nodes).

7.3.2 System model

We consider an CDMA-OFDM system with G groups transmitting at a given instant. Assume Binary Phase Shift Keying (BPSK) constellation for generating the input bits with equal probability for bits +1 and -1. Let us consider a group g consisting of source node, destination node and set of intermediate relay nodes. Assume that source u is assigned with a spreading waveform $c_g(.)$ whose support is [$0,\ T_{bit}$] and $\mathbf{s}_g = [s_{g0}, s_{g1}, \ldots, s_{gN-1}]$ denotes the corresponding spreading sequence with spreading gain N. Then,

$$c_g(t) = \sum_{n=0}^{N-1} s_{gn} rect[t - nT_c], \tag{7.1}$$

where $rect(t)$ is a rectangular waveform with unit amplitude in [$0,\ T_c$] and T_c is the chip period. Let us assume $b_g(i)$ is transmitted bit in group g. The kth relay node in group g transmits bit $b_g(i)$ with amplitude A_{kg} in ith bit interval and the length of signaling interval for each user is T_{bit}. The baseband signal of the kth transmitting node in gth group can now be expressed as

$$x_{kg}(t) = A_{kg} b_g(i) exp\left(\frac{j2\pi kt}{T_{bit}}\right) c_g(t - iT_{bit}), \quad iT_{bit} \leq t < (i+1)T_{bit}, \tag{7.2}$$

Processing at relay nodes

Assume perfect synchronization at the relay nodes in the underlying CDMA-OFDM model and there are G number of groups communicating simultaneously. The received signal at any relay node l from any other node k in group g at any instant t is given by

$$\hat{y}_{kl}(t) = A_{kg} b_g(i) c_g(t - iT_{bit}) + \sum_{\mathcal{G}=1, \mathcal{G} \neq g}^{G} A_{\nu\mathcal{G}} b_{\mathcal{G}}(i) c_{\mathcal{G}}(t - iT_{bit}) + \eta(t) \tag{7.3}$$

where $\sum_{\substack{\mathcal{G}=1 \\ \mathcal{G} \neq g}}(.)$ is the signal received at node l from some node ν of group $\mathcal{G}$ which uses same carrier as that of node k and $\eta(t)$ is zero mean Additive White Gaussian Noise (AWGN). Once the OFDM demodulation is complete the signals are again OFDM modulated with a different carrier and transmitted to the next relay node.

Processing at end nodes

The processing at the end node consists of OFDM demodulation and CDMA despreading. Let us assume d is the end node which receives signal from node m. The OFDM demodulated

signal $\hat{y}_{md}(t)$ at node d can also be derived in a similar fashion as $\hat{y}_{ul}(t)$. After matched filtering and despreading of $\hat{y}_{md}(t)$, the received symbol $y_d[i]$ in bit interval i at node d can be written as,

$$y_d[i] = \rho A_{mg} b_g(i) + \sum_{\mathcal{G}=1 \mathcal{G} \neq g}^{G} A_{\nu \mathcal{G}} b_{\mathcal{G}}(i) \rho_{\mathcal{G}g} + \eta \tag{7.4}$$

where $\rho_{\mathcal{G}g} = \int_{t=0}^{T_{bit}} c_{\mathcal{G}}(t - iT_{bit}) c_g(t - iT_{bit}) dt$ is the correlation factor due to loss in spreading codes' orthogonality between group g and group $\mathcal{G}$, ρ is the correlation factor due to synchronization loss of waveform c_g and η is the noise added to the symbol over one bit interval.

7.4 Resources Allocation

7.4.1 Sub carrier and power allocation

We allocate the sub carriers and transmit powers to the intermediate nodes such that the end-to-end throughput is maximized with the condition that the interference caused to other nodes in the network is bounded. The end-to-end throughput is defined as the probability of successful transmission of packets from source to destination. We follow the similar procedures of (4.8)-(4.16). However, we repeat the same here for continuity. Successful transmission from source to destination involves successful transmission at each and every intermediate nodes. A node throughput is defined as the probability of successfully transmitting its packet in a given slot to its immediate neighbour in the path. The successful single hop transmission from node l to its neighbour node m occurs when the received power at node m from node l (r_{lm}) is stronger than interference plus noise power by a factor of β (i.e $SINR \geq \beta$). The probability of successful transmission from node l to node m is

$$\begin{aligned} \mathrm{P}(C_{lm}) &= \mathrm{P}(SINR_{lm} \geq \beta) \\ &= \mathrm{P}(\frac{r_{lm}}{(I_{lm} + \eta)} \geq \beta) \\ &= \mathrm{P}(r_{lm} \geq \beta.(I_{lm} + \eta)) \end{aligned} \tag{7.5}$$

where I_{lm} is the interference at node m from other communicating entities, $SINR_{lm}$ is the signal to interference plus noise ratio at link between l and m, β is the $SINR$ threshold and η is the noise power. Let $r_{\mathcal{G}m},\ \mathcal{G} = 1, \ldots, G\ (\mathcal{G} \neq g)$ be the received power at node m from the interferer in group $\mathcal{G}$. The total interference at node m from the interferers in all $G - 1$ groups

which use the same carrier as the hop between l and m is given by

$$I_{lm} = \frac{1}{N}\Big(\sum_{\mathcal{G}=1,\mathcal{G}\neq g}^{G} \rho_{\mathcal{G}g}^2 r_{\mathcal{G}m} \Big) \tag{7.6}$$

Erroneous detection occurs when $SINR_{lm} < \beta$, and this probability $\mathrm{P}(E_{lm})$ is given by

$$\mathrm{P}(E_{lm}) = \mathrm{P}(r_{lm} < \beta.(I_{lm} + \eta)) \tag{7.7}$$

The propagation channel between mobile node to mobile node is different from the conventional wireless channel. However, the envelope still follows Rayleigh distribution [82]. Using the fact that if Y is Rayleigh distributed and X=Y^2, then X will follow exponential distribution, we can conclude that r_{lm} follows exponential distribution. Hence, the probability density function of r_{lm} is given by

$$\mathrm{P}(r_{lm}) = \frac{1}{R_{lm}} e^{\frac{-r_{lm}}{R_{lm}}} \tag{7.8}$$

where R_{lm} denotes the average received power $R_{lm} = \frac{p_{lm}}{d_{lm}^{\gamma}}$, p_{lm} being the transmitted power from node l to node m and γ is the path loss coefficient [83]. Let $\chi_m = \{1,\ 2,\ 3, \ldots, h\}$ be the path selected to relay the communication from source node 1 to the destination node h in group g, with $h-1$ number of hops. The probability $\mathrm{P}(C_{1h})$ that the message is successfully transmitted from source 1 to destination h is given by

$$\begin{aligned} \mathrm{P}(C_{1h}) &= \mathrm{P}(\bigcap_{i=1}^{h-1} C_{ii+1}) \\ &= 1 - \mathrm{P}(\bigcup_{i=1}^{h-1} E_{ii+1}) \\ &\geq 1 - \sum_{i=1}^{h-1} \mathrm{P}(E_{ii+1}) \end{aligned} \tag{7.9}$$

where the last inequality is obtained by using the union bound. Note that $\mathrm{P}(C_{ii+1})$ is dependent on correct detection of all its previous nodes. Let us consider the communication between node i and $i+1$ in group g.

$$\begin{aligned} \mathrm{P}(E_{ii+1}) &= \mathrm{P}(SINR_{ii+1} < \beta) \\ &= \mathrm{P}(r_{ii+1} < \beta.(I_{ii+1} + \eta)) \\ &= \frac{1}{R_{ii+1}} \int_0^{\beta.(I_{ii+1}+\eta)} (e^{-\frac{r_{ii+1}}{R_{ii+1}}}) dr_{ii+1} \\ &= 1 - (e^{\frac{-\beta(I_{ii+1}+\eta)}{R_{ii+1}}}) \end{aligned} \tag{7.10}$$

where I_{ii+1} itself is a random variable, therefore, by analyzing along the similar lines of [83], $\mathrm{P}(E_{ii+1})$ can be written as

$$\mathrm{P}(E_{ii+1}) = \int_0^\infty \cdots \int_0^\infty \left(1 - \left(e^{-\frac{\beta\left[\frac{1}{N}\Sigma_{\mathcal{G}=1\mathcal{G}\neq g}^{G}\rho_{\mathcal{G}g}^2 r_{\mathcal{G}i+1}+\eta\right]}{R_{ii+1}}}\right)\right) \times \prod_{\mathcal{G}=1\mathcal{G}\neq g}^{G} P(r_{\mathcal{G}m})dr_{\mathcal{G}m} \tag{7.11}$$

By substituting $\mathrm{P}(r_{\mathcal{G}i+1})$ from (7.8) and by invoking independence of $\mathrm{P}(r_{\mathcal{G}i+1})$ the above equation can be written as

$$\mathrm{P}(E_{ii+1}) = 1 - \left[e^{\left(-\frac{\beta\eta}{p_{ii+1}d_{ii+1}^{-\gamma}}\right)} . \prod_{\mathcal{G}=1\mathcal{G}\neq g}^{G} \frac{1}{1+\frac{\beta}{N}\frac{\rho_{\mathcal{G}i+1}^2 p_{\mathcal{G}i+1}}{p_{ii+1}}(\frac{d_{ii+1}}{d_{\mathcal{G}i+1}})^\gamma}\right] \tag{7.12}$$

Using (7.9) and (7.12), the lower bound on end-to-end throughput ($\mathrm{P}_l(C_{1h})$) can be written as

$$\mathrm{P}(C_{1h}) \geq 1 - \sum_{i=1}^{h-1}\left(1 - \left[e^{\left(-\frac{\beta\eta}{p_{ii+1}d_{ii+1}^{-\gamma}}\right)} \prod_{\mathcal{G}=1,\mathcal{G}\neq g}^{G} \frac{1}{1+\frac{\beta}{N}\frac{\rho_{\mathcal{G}i+1}^2 p_{\mathcal{G}i+1}}{p_{ii+1}}(\frac{d_{ii+1}}{d_{\mathcal{G}i+1}})^\gamma}\right]\right) \tag{7.13}$$

Now the sub carriers and power allocation function $f(.)$ is derived as follows

$$\begin{aligned} f(c_1, c_2, \ldots, c_{h-1}, p_{12}, p_{23}, \ldots, p_{h-1h}) &= Max\ \mathrm{P}_l(c_{1h}) \\ &S.T \\ I_{ij} &< I_{max}\ \forall i,j \in h \end{aligned} \tag{7.14}$$

7.5 Simulation and Results

We simulate a single cell system with the simulation parameters presented in Table 7.1. To validate the performance of the proposed model, a Monte-Carlo simulation was carried out by randomly selecting the source and destination nodes, and the results were averaged over at least 100 realizations of the nodes distribution. We employ Genetic Algorithm (GA) to solve the constrained optimization of (7.14) [121]. Chromosome values of GA are generated from uniformly distributed random number generator. Maximum transmit power (maximum value of chromosomes) from any node is assumed to be $1\ watt$. We use 0.95 as $\mathrm{P}_l(c_{1h})$ threshold. The mean square error between the value of $\mathrm{P}_l(c_{1h})$ obtained by substituting chromosomes' values of GA and 0.95 is taken as fitness function. Cross over probability is assumed to be 0.5 while mutation probability is 0.01.

Table 7.1: Simulation Parameters to show the effectiveness of the proposed access mechanism

Parameters	Value
Cell radius	1 Km
Number of nodes in the cell	1000
Propagation loss exponent (γ)	4
SINR threshold (β)	0.25 dB
Interference threshold (I_{max})	-80 dB
Spreading factor (N)	32
Thermal noise at receiver	-90 dB
Antenna Gain in MT	0 dB (Omni directional)

7.5.1 BER performance

BER performances of various access mechanisms is compared in Fig 7.2. For comparison purpose we consider a CDMA access mechanisms which has similar correlation properties as that of our proposed CDMA-OFDM mechanism. We also consider a OFDM-FDMA access mechanism proposed in [115]. We allow 50 number of randomly placed groups to transmit at the same time i.e., $G = 50$. We examine a single group communication and assume a matched filter receiver at the end node as explained in (7.4). From Fig 7.2 we can infer that the proposed CDMA-OFDM access mechanism has better BER performance compared to other algorithms. This is because the interference in the network in the case of proposed access mechanism is much lower compared to remaining access mechanisms due to two level of orthogonal modulations. Therefore, the BER performance is much better in the case of proposed access mechanism.

7.5.2 Multiple access interference analysis

The effect of increasing the number of active groups (transmitting groups) in the system for a SNR of $20\ dB$ at each node is shown in Fig 7.3. It is evident that more the number of active groups (G), more the interference in the system. Therefore, as the number of active groups increases the BER performances of the access mechanisms reduce as shown in Fig 7.3. However, in the proposed algorithm due to the two levels of orthogonal modulations (OFDM and

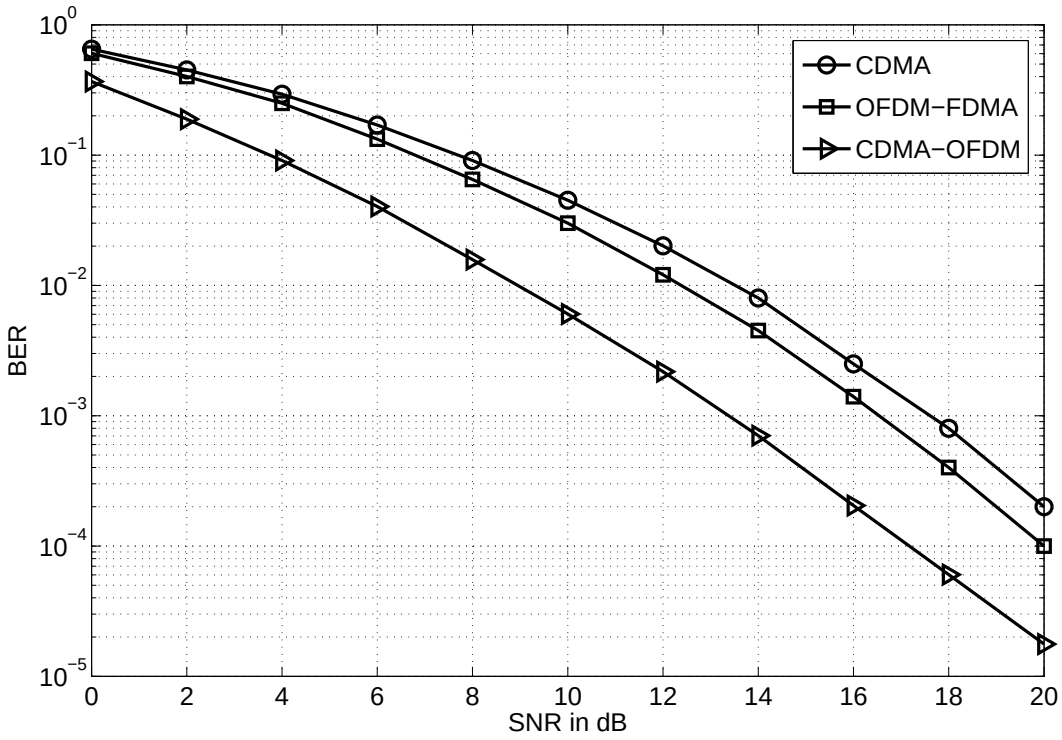

Figure 7.2: BER performance comparison

CDMA), interference at the nodes will be at tolerable level. Hence, the performance is significantly better in the proposed algorithm compared to CDMA and OFDM-FDMA algorithms.

7.5.3 End-to-end throughput analysis

We have plotted lower bound on end-to-end throughput by varying the number of active groups in Fig 7.4. From (7.13) it is clear that the end-to-end throughput is a function of transmit powers of nodes (p_{ii+1}). In the proposed algorithm the power levels are optimized such that the end-to-end throughput is maximized. Therefore, the minimum guaranteed throughput in the case of proposed algorithm is considerably higher compared to other algorithms as shown in Fig 7.4. Moreover, as the number of active group increases the end-to-end throughput reduces due to increase in interference in the system.

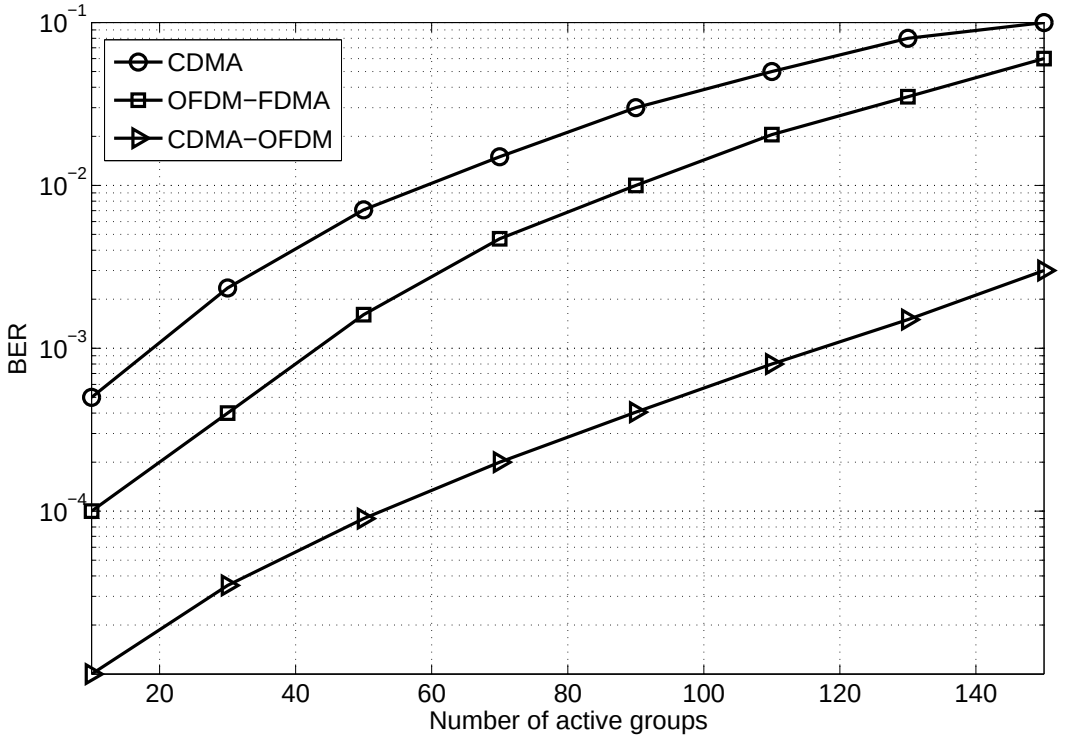

Figure 7.3: BER performance against number of active groups (G) for a fixed SNR of 20 dB

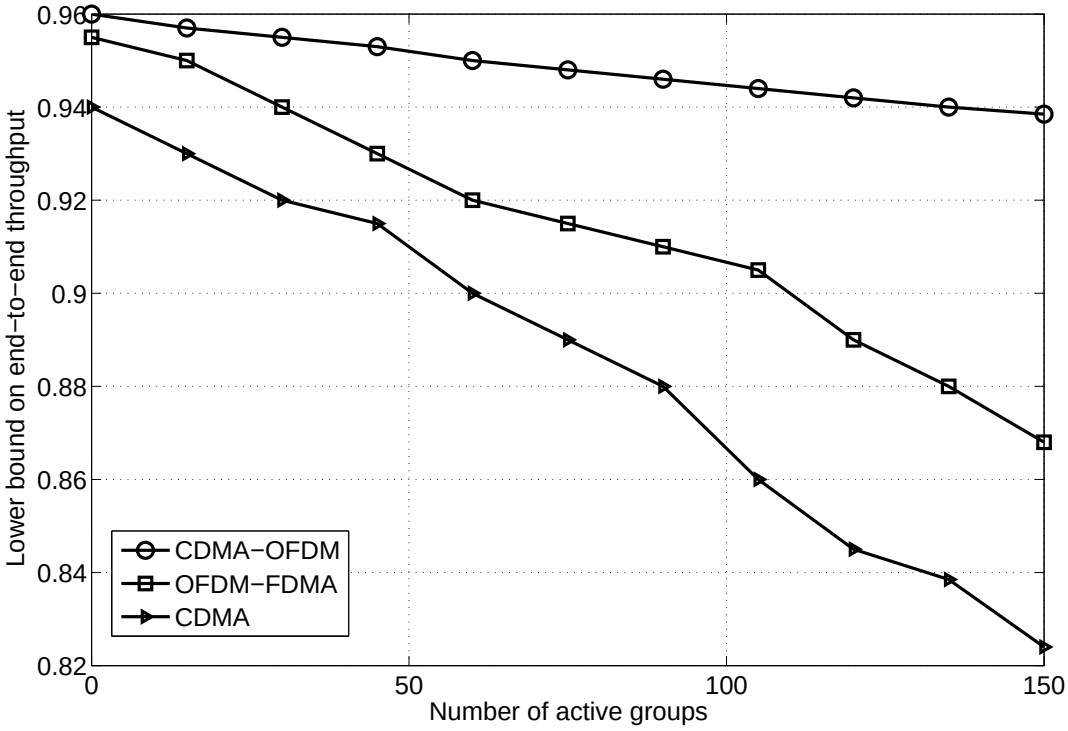

Figure 7.4: End-to-end throughput versus number of active groups (G)

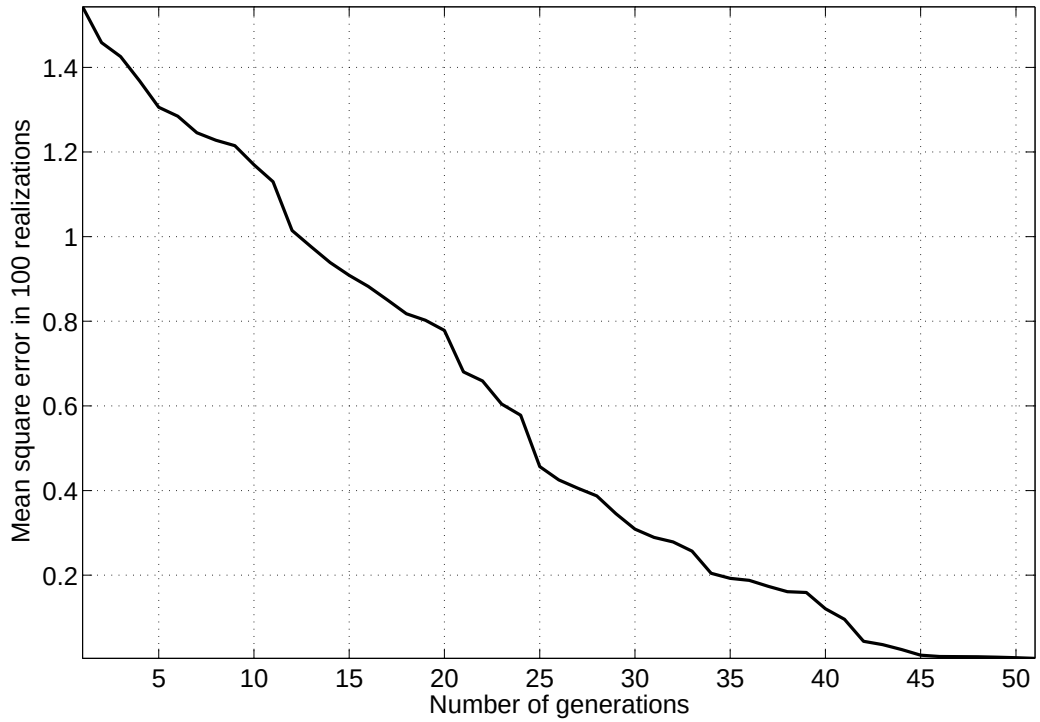

Figure 7.5: Convergence of Genetic algorithm in power and sub-carrier allocations

7.5.4 Convergence analysis

The mean square convergence of GA in power and sub carrier optimization of (7.14) is shown in Fig 7.5. From Fig 7.5 we can deduce that the GA converges to a mean square error of about 10^{-3} within 50 generations.

7.6 Conclusion

We have proposed a novel CDMA-OFDM access mechanism for MCN. We have used a simple Genetic algorithm to solve the constrained optimization of power and sub carrier allocation. Our proposed algorithm is simple in implementation and has better BER and throughput performance compared to the CDMA and OFDM-FDMA.

Chapter 8

Conclusions: Summary and Future Work

8.1 Summary

Multiuser transmission techniques and multihop communications enhance the performance of cellular systems. In this work, we have proposed two entirely new multiuser transmission algorithms. We have employed the simplest possible receiver structure and a new optimization criterion for finding the filter weights at the transmitter. We have considered the most general channel conditions with both ISI and MAI effecting the system.

- The problem of channel estimation at the transmitter was solved using the statistical estimates for the channel rather then actual channel coefficients. This greatly reduces the control overhead and saves bandwidth as well as power at the receiver (which is expended in estimating the channel and then communicating it back to the transmitter) both of which are deficient in a mobile wireless system.

- To reduce the computational complexity the conditional joint probability of error and conditional joint norm were minimized. This also gives the optimal filter for each scenario rather than the best filter for the average case. The statistical channel model based algorithms provide acceptable performance as compared to the fully known channel case even when the channel variations are large.

- We have simulated both the MPOE and the MMSE algorithms for extremely fast fading channels and observed the performance to be much better than the case without the presence of prefiltering. The MPOE algorithms performed significantly better than the MMSE algorithms as expected.

On the basis of this work, it is cogent that transmitter based prefiltering is a promising direction to explore in order to improve the performance on the downlink of wireless communication systems. Prefiltering techniques are used in many wired systems (e.g. DSL) and even in FM broadcasting (pre-emphasis, de-emphasis). This work is a step forward in their logical extension to wireless systems. In fact, the results from the statistical channel model algorithms prove that an extensive potential exists in transmitter based prefiltering techniques for application to real-life practical systems.

In addition to prefiltering we have also explored the option of establishing multihop relay communications in cellular network. Relaying has potential to reduce transmitted power and subsequent interference in the network by breaking longer communication path into a number of smaller hops. A conventional cellular approach, however, prevents capacity gains due to interference, as all traffic must be routed through the BS (Base Station). A network topology where traffic may be routed between users, without requiring the BS to take part in all calls, may avoid the capacity limits resulting from all calls routing via a single BS transceiver.

In multihop cellular networks (MCN) finding an optimal source to destination path is an important issue to be addressed. Routing based solely upon minimizing path loss/distance is unable to achieve these potential capacity gains. A novel routing algorithm based upon cross layer parameters is presented in this thesis. The proposed routing protocol was shown to increase end-to-end throughput and reduce the end-to-end delay and interference in the network.

Resource scheduling is the another method of further mitigating interference. The ad-hoc nature of the proposed architecture means that we cannot guarantee successful transmissions over all the links if all of them are simultaneously involved in calls. To mitigate this problem we have proposed a scheduling scheme where CDMA codes can be reused in a given cell with the constraint that at a given instant, communications over all transmitting links are successful in the probability of error sense. The proposed MPOE based scheduling scheme increases the spatial reuse and also the end-to-end throughput.

We have also derived the lower bound on transmission range under various conditions and proposed a method to choose optimal transmission range so that the network is fully connected simultaneously maximizing the spatial reuse.

In addition to routing, resource scheduling and transmission range control we have also proposed an OFDM-CDMA access mechanism for multihop communications in the cellular network. From the throughput and interference analysis, we can see that the proposed access

mechanism contributes not only power reductions but also increases the number of users to attain a high throughput.

Our proposed solutions solve most of the issues which can occur while incorporating multihop feature in cellular network. Therefore, we can conclude that multihop communications in cellular network can successfully be established. We further summarize from our findings that multihop communications increase spatial reuse reduce interference and also ensure end-to-end communication with minimum delay and sufficiently high throughput. Also due to reduced transmission range and high spatial reuse multihop relaying can increase the user capacity to large extent and reduce the transmission power expenditures. On the basis of this work, it can be stated without apprehension that multihop relaying has tremendous potential to be considered as candidate for future generation cellular communications.

8.2 Future Work

The following are some future work suggestions which may be worthy of further exploration in the case of prefiltering system:

- In the prefiltering model the deployment of the statistical channel algorithm in a real-life system will depend on the channel statistics and the ratio between the channel mean and the channel variance. A proper mathematical characterization of this relationship will surely help in taking decisions about systems in which the statistical channel model can be used.

- In prefiltering system, the extension of the analysis to a MIMO prefiltering system may also be investigated.

- For a given mean and variance of the channel, finding the optimum prefilter length L_z depends on the balance of MAI and ISI in the system. This trade-off could be studied further so as to gain a deeper understanding of the role of the transmitter prefilter. Using this understanding, a better demodulation scheme could be suggested which treats both the MAI as well as the ISI in the system separately thereby improving performance.

The following are some of the issues which need further attention in the case of multihop cellular networks:

- In the MCN model most of the scenarios examined are static user population. Mobility between users will cause changes in the metrics. More importantly, routing based upon metrics that have changed is likely to show impaired performance. The impact of mobility upon the various algorithms presented for MCN is currently an area for investigation.

- The concept of relaying enables a greater number of communication links permutations than has previously been possible in centralized CDMA network. The formulation of simultaneous routing, resource allocation and power control for FDMA and TDMA are well analyzed in the literature. This approach with regard to MCN in a mobile environment with OFDM-CDMA access mechanism is an area for future research.

- Cooperative diversity is an another area which can be well utilized in the MCN to maximize the end-to-end performance. However, MCN has heterogeneous and dynamic environment. Therefore, cooperative diversity in such an environment with the goal of effective resource utilization is a major challenge to be addressed.

Publications out of this Thesis

Journals:

1. **G. Kannan**, Mohit Garg, S. N. Merchant, U. B. Desai, "MPOE based prefiltering and MRT beamforming with matched filter receiver for DS-CDMA systems", *Wireless personal communications (Springer)*, no 46, pp. 199-222, 2008.

2. **G. Kannan**, Mohit Garg, S. N. Merchant, U. B. Desai, "Minimum probability of error prefiltering and maximum ratio beamforming for statistical channel model in DS-CDMA systems", *EURASIP Journal on Wireless Communications and Networking* [*under review after first revision*].

3. **G. Kannan**, Yangcheng Huang, Saleem Bhatti, S. N. Merchant and U. B. Desai, "Route discovery and route resilience for multihop cellular networks: A cross layer approach", *IET Commun.* [*under review*].

International Conferences:

1. **G. Kannan**, S. N. Merchant and U. B. Desai, "On high spatial link scheduling for SCDMA multihop cellular networks: A cross layer framework", *The 28th Conference on Computer Communications, IEEE-INFOCOM 2009* [*under review*].

2. Ravi Shankar Ojha, **G. Kannan**, S. N. Merchant and U. B. Desai, "On optimal transmission range for multihop cellular networks", *IEEE Global Communications Conference, GLOBECOM 2008*, New Orleans, USA.

3. Yangcheng Huang, **G. Kannan**, Saleem Bhatti, S. N. Merchant and U. B. Desai, "Route duration statistics of proactive ad-hoc networks routing protocol", in *Proc. Wireless Telecommunications Symposium WTS 2008*, California, USA, pp. 236-242.

4. **G. Kannan**, S. N. Merchant and U. B. Desai, "Access mechanisms for multihop cellular networks", in *Proc. IEEE 66th Vehicular Technology Conference VTC 2007-Fall*, Baltimore, USA, pp. 279-283.

5. **G. Kannan**, Mohit Garg, S. N. Merchant and U. B. Desai, "MPOE prefiltering with statistical channel model for DS-CDMA systems", in *Proc. IEEE International Conference on Communications ICC 2007*, June-2007, Glasgow, UK, pp. 2822-2828.

6. **G. Kannan**, S. N. Merchant and U. B. Desai, "Cross layer routing for multihop cellular networks", in *Proc. The 21st IEEE International Conference on Advanced Information Networking and Applications Workshops AINA 2007*, May-2007, Niagara Falls, vol 2, pp. 165-170 [**Received Nokia Travel Grant Award**].

7. **G. Kannan**, S. N. Merchant and U. B. Desai, "MRT beamforming and MPOE prefiltering for DS-CDMA systems", in *Proc. IEEE Asia Pacific Conference on Circuits and Systems, APCCAS 2006*, Dec-2006, Singapore, pp. 1188-1191.

8. Mohit Garg, **G. Kannan**, S. N. Merchant and U. B. Desai, "Minimum probability of error based prefiltering for DS-CDMA systems", in *Proc. 2006 IEEE Mountain Workshop on Adaptive and Learning System, SMC/CALS*, July-2006, Utah, USA, pp. 116-121.

National Conferences:

1. **G. Kannan**, S. N. Merchant and U. B. Desai, "Space time block coded MPOE detector for DS-CDMA systems", in *Proc. National conference on communication NCC 2006*, 21-23 Jan 2006, India.

Other Related Publications

Journals:

1. Sarath Gopi, **G. Kannan**, Deepthi Chander and S. N. Merchant and U. B. Desai, “Path unaware layered routing protocol (PULRP) with nonuniform node distribution for underwater sensor networks”, *Wireless Communications and Mobile Computing (Wiley)-2008* to appear.

2. Sarath Gopi, **G Kannan**, U. B. Desai and S. N. Merchant, “E-PULRP: Energy optimized path unaware layered routing protocol for underwater sensor networks”, *ACM Trans. on Sensor Networks* [*under review*].

International Conferences:

1. Sarath Gopi, **G. Kannan**, U. B. Desai and S. N. Merchant, “Energy optimized path unaware layered routing protocol for underwater sensor networks”, *IEEE Global Communications Conference, GLOBECOM 2008*, New Orleans, USA.

2. Sarath Gopi, **G. Kannan**, Dipthi chander, S. N. Merchant and U. B. Desai, “PULRP: Path unaware layered routing protocol for underwater sensor networks”, in *Proc. IEEE International Conference on Communications, ICC 2008*, Beijing, China, pp. 3141-3145.

National Conferences:

1. Dipthi chander, **G. Kannan**, S. N. Merchant and U. B. Desai, “MCPOE- based cooperative communication in an underwater channel”, in *Proc. National Conference on Communications, NCC 2008*, Mumbai, 1-3 Feb.

Bibliography

[1] Rudolf Tanner and Jason Woodard, *WCDMA Requirements and Practical Design*. Jhon Wiley & Sons, Ltd, 2004.

[2] Heikki Kaaranen, Ari Ahtiainen, Lauri Laitinen, Siamak Naghian, and Valtteri Niemi, *UMTS Networks, Architecture, Mobility and Services*. Jhon Wiley & Sons, Ltd, 2001.

[3] William C. Y. Lee, *Wireless & Cellular Telecommunications*, 3rd ed. Mc Graw Hill, 2006.

[4] Ianki Berenguer, Xiaodong Wang, Manuel Donaire, Daryl Reynolds and Anders Host-Madsen, "Linear precoding versus linear multiuser detection in downlink TDD-CDMA systems," *IEEE Trans. Wireless Commun.*, vol. 6, no. 1, pp. 1–7, Jan 2007.

[5] J. Jubin and J. Tornow, "The DARPA packet radio network protocols," *Proceedings of the IEEE*, vol. 75, pp. 21–32, 1987.

[6] 3rd Generation Partnership Project (3GPP) Technical Specification Group (TSG) Radio Access Network:(RAN), "Opportunity Driven Multiple Access (ODMA)," *Tech. rep., TS 25.924 V1.0.0.*, 1998.

[7] G.N. Agglou and R. Tafazolli, "On the relaying capability of nextgeneration GSM cellular networks," in *IEEE Pers. Commun.*, vol. 8, 2001, pp. 40–47.

[8] Hyunjeong Lee and Chung-Chieh Lee, "An integrated multi-hop cellular data network," in *Proc. IEEE 58th Vehicular Technology Conference, VTC 2003-Fall*, vol. 4, Oct. 2003, pp. 2232–2236.

[9] B. R. Vojcic and W. M. Jang, "Transmitter precoding in synchronous multiuser communications," *IEEE Trans. Commun.*, vol. 46, pp. 1346–1355, Oct. 1998.

[10] X. Dong, Z. Ding and S. Dasgupta, "Fractional spaced dual channel estimation based on decimated feedback," in *Proc. IEEE Wireless Communications and Networking Conference, WCNC 2004*, vol. 1, March 2004, pp. 489–494.

[11] H. Xu, S. Dasgupta and Z. Ding, "A novel channel identification method for fast wireless communication system," in *Proc. IEEE International Conference on Communications, ICC 2001*, vol. 8, Jun. 2001, pp. 2443–2448.

[12] Q. Ma and C. Tepedelenlioglu, "Multiuser diversity with outdated channel feedback," in *Proc. IEEE Wireless Communications and Networking Conference, WCNC 2004*, vol. 3, March 2004, pp. 1951–1956.

[13] J. C. Roh and B. D. Rao, "An efficient feedback method for MIMO systems with slowly time-varying channels," in *Proc. IEEE Wireless Communications and Networking Conference, WCNC 2004*, vol. 2, March 2004, pp. 760–764.

[14] S. L. Georgoulis and D. G. M. Cruickshank, "Transmitter based inverse filters for MAI and ISI mitigation in a TDD/CDMA downlink," in *Proc. IEEE 56th Vehicular Technology Conference, VTC 2002-Fall*, vol. 2, Sep. 2002, pp. 681–685.

[15] S. L. Georgoulis, "Transmitter based inverse filters for MAI and ISI mitigation in a TDD/CDMA downlink, Ph.D dissertation, The University of Edinburg," 2003. [Online]. Available: http://www.see.ed.ac.uk/~sasg/Thesis/sg/thesis.pdf

[16] S. L. Georgoulis and D. G. M Cruickshank, "Transmitter-based inverse filters for reducing MAI and ISI in CDMA-TDD downlink," *IEEE Trans. Wireless Commun.*, vol. 3, no. 2, pp. 353–358, March 2004.

[17] T. P. Kurpjuhn, M. Joham and J. A. Nossek, "Optimization criteria for linear precoding in flat fading TDD-MIMO downlink channels with matched filter receivers," in *Proc. IEEE 59th Vehicular Technology Conference, VTC 2004-Spring*, vol. 2, May 2004, pp. 809–813.

[18] Aditya Dua and Uday B. Desai, "MPOE based adaptive space-time multiuser detector for multipath CDMA channels," in *Proc. IEEE International Conference on Acoustics, Speech, and Signal Processing, ICASSP 2002*, vol. 3, May 2002, pp. 2593–2596.

[19] Aditya Dua, Uday B. Desai and Ranjan K. Mallik, "Minimum probability of error based methods for adaptive multiuser detection in multipath DS-CDMA channels," *IEEE Trans. Wireless Commun.*, vol. 3, pp. 939–948, May 2004.

[20] Ritesh Sood and U. B. Desai, "Minimum probability of error demodulation for multipath OFDM-SDMA systems," in *Proc. IEEE Wireless Communications and Networking Conference, WCNC 2004*, vol. 2, March 2004, pp. 948–953.

[21] Mohit Garg, Umesh Nimbhorkar, U. B. Desai and S. N. Merchant, "Efficient minimum probability of error demodulation for DS-CDMA systems," in *Proc. IEEE Wireless Communications and Networking Conference, WCNC 2005*, vol. 1, March 2005, pp. 261–266.

[22] Yuhang Wang, Xian-Da Zhang and He Huang, "Minimum probability of error-based adaptive multiuser decision feedback detection," *IEEE Signal Processing Letters*, vol. 13, no. 5, pp. 257–260, May 2006.

[23] Sheng Chen, Samingan A. K, Mulgrew B and Hanzo L, "Adaptive minimum-BER linear multiuser detection for DS-CDMA signals in multipath channels," *IEEE Trans. Signal Processing*, vol. 49, no. 6, pp. 1240–1247, June 2001.

[24] ——, "Adaptive minimum-BER linear multiuser detection," in *Proc. IEEE International Conference on Acoustics, Speech, and Signal Processing, 2001, ICASSP 2001,* vol. 4, May 2001, pp. 2253–2256.

[25] I. N Psaromiligkos, S. N Batalama and D. A. Pados, "On adaptive minimum probability of error linear filter receivers for DS-CDMA channels," *IEEE Trans. Commun.*, vol. 47, no. 7, pp. 1092–1102, July 1999.

[26] J. M. Luna-Rivera and D. U. Campos-Delgado, "A simple transmitter precoding technique for MAI/ISI rejection in the forward link of a wireless TDD/DS-CDMA system," in *Proc. IEEE 61st Vehicular Technology Conference, VTC 2005-Spring*, vol. 2, May 30-June 1 2005, pp. 826–830.

[27] F. Tufvesson, M. Faulkner and T. Maseng, "Pre-compensation for Rayleigh fading channels in time division duplex OFDM systems," in *Proc. 6th IEEE International Workshop on Intelligent Signal Processing and Communication Systems*, Nov. 5-6 1998, pp. 53–57.

[28] D. Reynolds, Xiaodong Wang and K. N. Modi, “Interference suppression and diversity exploitation for multiantenna CDMA with ultra-low complexity receivers,” *IEEE Trans. Signal Processing*, vol. 53, no. 8, part 2, pp. 3226–3237, Aug. 2005.

[29] Koilpillai R. D, Channakeshu S and Toy R. L, “Low complexity equalizers for US digital cellular system,” in *Proc. IEEE 42nd Vehicular Technology Conference*, vol. 2, 1992, pp. 744 – 747.

[30] E. S. Hons, A. K. Khandani and W. Tong, “An optimized transmitter precoding scheme for synchronous DS-CDMA,” *IEEE Trans. Commun.*, vol. 54, pp. 32–36, Jan-2006.

[31] D. Reynolds, A. Host-Madsen and X. Wang, “Transmitter precoding for CDMA in fading multipath channels: strategy and analysis,” in *Proc. IEEE International Conference on Communications, ICC 2003*, May 2003, pp. 3331–3335.

[32] O. Simeone, U. Spagnolini and Y. Bar-Ness, “Linear and non-linear precoding/decoding for MIMO systems using the fading correlation at the transmitter,” in *Proc. IEEE Workshop on Signal Processing Advances in Wireless Communications*, June 2003, pp. 6–10.

[33] M Brandt-Pearce and A. Dharap, “Transmitter-based multiuser interference rejection for the downlink of a wireless CDMA system in a multipath environment,” *IEEE J. Select. Areas Commun.*, vol. 18, pp. 407–417, March 2000.

[34] J. Tuthill and A. Cantoni, “Optimum precompensation filters for IQ modulation systems,” *IEEE Trans. Commun.*, vol. 47, no. 10, pp. 1466–1468, Oct. 1999.

[35] S. Chen, B. Mulgrew, E. S. Chang and G. J. Gibson, “Space translation properties and the minimum-BER linear-combiner DFE,” *IET Commun.*, vol. 145, pp. 316 – 322, Oct. 1998.

[36] Y. Ding, T. N. Davidson, Z. Q. Luo and K. M. Wong, “Minimum BER block precoders for zero-forcing equalization,” *IEEE Trans. Signal Processing*, vol. 51, no. 9, pp. 2410–2423, Sep. 2003.

[37] D. P. Palomar, M. Bengtsson and B. Ottersten, “Minimum BER linear transceivers for MIMO channels via primal decomposition,” *IEEE Trans. Signal Processing*, vol. 53, no. 8, Part 1, pp. 2866–2882, Aug 2005.

[38] Tero Ojanpera and Ramjee Prasad, *Wideband CDMA for Third Generation Mobile Communications*. Artech House, 1998.

[39] Titus K Y Lo, "Maximum ratio transmission," *IEEE Trans. Commun.*, vol. 47, no. 10, pp. 1458–1461, Oct. 1999.

[40] A. K. Jagannatham, C. R. Murthy and B. D. Rao, "A semi-blind MIMO channel estimation scheme for MRT," in *Proc. IEEE International Conference on Acoustics, Speech, and Signal Processing, ICASSP 2005*, vol. 3, March 2005, pp. 585–588.

[41] T. Salzer, D. Mottier and D. Castelain, "Comparison of antenna array techniques for the downlink of multi-carrier CDMA systems," in *Proc. IEEE 57th Vehicular Technology Conference, VTC 2003-Spring*, vol. 1, April 2003, pp. 316–320.

[42] T. Salzer and D. Mottier, "Design of a multi-carrier CDMA downlink with different transmit antenna array strategies," in *Proc. IEEE 62nd Vehicular Technology Conference, VTC 2005-Fall*, vol. 1, Sep. 2005, pp. 109–113.

[43] Adio Silva and Atilio Gameiro, "Pre-filtering antenna array for downlink TDD MC-CDMA systems," in *Proc. IEEE 57th Vehicular Technology Conference, VTC 2003-Spring*, April 2003, pp. 641–645.

[44] Mohit Garg, "Multiuser signal processing techniques for DS-CDMA communication systems, MTech dissertation, IIT Bombay," June 2005. [Online]. Available: http://www.mohrahit.in/learn/MohitGargDDPThesis.pdf

[45] S. Moshavi, "Multi-user detection for DS-CDMA communications," *IEEE Commun. Mag.*, vol. 34, no. 10, pp. 124–136, 1996.

[46] S. Verdu, *Multiuser Detection*. Cambridge:Cambridge University Press, 1998.

[47] M. K. Simon and M. S. Alouini, *Digital communication over fading channel: A unified approach to performance analysis*. New York: John & Wiley Sons, 2000.

[48] Mohit Garg, G. Kannan, S. N. Merchant and U. B. Desai, "MPOE based prefiltering for DS-CDMA systems," in *Proc. 2006 IEEE Mountain Workshop on Adaptive and Learning Systems SMCals/06*, July 2006, pp. 116–121.

[49] G. Kannan, Mohit. Garg, U. B. Desai and S. N. Merchant, "MPOE based prefiltering and MRT beamforming for DS-CDMA systems," in *Proc. IEEE Asia Pacific Conference on Circuits and Systems, APCCAS 2006*, Dec. 2006, pp. 1188–1191.

[50] H Sampath and A Paulraj, "Linear precoding for space-time coded systems with known fading correlations," *IEEE Commun. Lett.*, vol. 6, no. 6, pp. 239–241, June 2004.

[51] June Chul Roh and Baskar. D. Rao, "Multiple antenna channels with partial channel state information at the transmitter," *IEEE Trans. Wireless Commun.*, vol. 3, no. 2, pp. 677–688, March 2004.

[52] Athanasios P Liavas, "Tomlinson-harashima precoding with partial channel knowledge," *IEEE Trans. Commun.*, vol. 53, no. 1, pp. 5–9, Jan 2005.

[53] C. Windpassinger, R. F. H. Fischer, T. Vencel and J. B. Huber, "Precoding in multi-antenna and multiuser communications," *IEEE Trans. Wireless Commun.*, vol. 3, no. 4, pp. 1305–1316, July 2004.

[54] Aditya Dua, "MPOE based multiuser detection for DS-CDMA communications, Dual degree dissertation (BTech and MTech), IIT Bombay," June 2002. [Online]. Available: http://www.stanford.edu/~dua/pubs/dua_thesis.pdf

[55] Computational complexity of mathematical operations. [Online]. Available: http://en.wikipedia.org/wiki/Computational_complexity_of_mathematical_operations

[56] Y.D. Lin and Y.C. Hsu, "Multi-hop cellular: A new architecture for wireless communications," in *Proc. 19th IEEE Annual Conference on Computer and Communications, INFOCOM 2000*, vol. 3, March 2000, pp. 1273–1282.

[57] K.J. Kumar, B.S. Manoj and C. Siva Ram Murthy, "RT-MuPAC: A new multi-power architecture for voice cellular networks," *Elsevier: Computer Networks*, vol. 47, pp. 105–128, Jan. 2005.

[58] Hongyi Wu, Chunming Qiao, De S and Tonguz O, "Integrated cellular and ad hoc relaying systems: iCAR," *IEEE J. Select. Areas Commun.*, vol. 19, pp. 2105–2115, Oct. 2001.

[59] Anand A. Janefalkar, Kaushik Josiam and Dinesh Rajan, “Cellular ad-hoc relay for emergencies (CARE),” in *Proc. IEEE 60th Vehicular Technology Conference, VTC 2004-Fall*, vol. 4, Sep. 2004, pp. 2873–2877.

[60] Fei Hu and Sunil Kumar, “The integration of ad hoc sensor and cellular networks for multi-class data transmission,” *Elsevier:Ad Hoc Networks*, no. 4, pp. 254–282, 2006.

[61] Ioannis Ioannidis and Bogdan Carbunar, “Scalable routing in hybrid cellular and ad-hoc networks,” in *Proc. IEEE International Conference on Mobile Ad-hoc and Sensor Systems*, vol. Oct. 2004, pp. 522–524.

[62] Sreng. V, Yanikomeroglu. H and Falconer. D, “Coverage enhancement through two-hop relaying in cellular radio systems,” in *Proc. Wireless Communications and Networking Conference, WCNC 2002*, vol. 2, March 2002, pp. 881–885.

[63] Naouel Ben Salem, Levente Buttyan, Jean-Pierre Hubaux and Markus Jajobsson, “Node cooperation in hybrid ad hoc networks,” *IEEE Trans. Comput.*, vol. 5, no. 4, pp. 365–376, April 2006.

[64] ——, “A charging and rewarding scheme for packet forwarding in multi-hop cellular networks,” in *Proc. ACM MobiHoc 2003*, June 2003, pp. 13–24.

[65] Yuan Xue and Baochun Li, “A location-aided power-aware routing protocol in mobile ad hoc networks,” in *Proc. IEEE Global Communications Conference, GLOBECOM 2001*, vol. 5, Nov. 2001, pp. 2837–2841.

[66] Weifa Liang and Yang Yuansheng, “Maximizing battery life routing in wireless ad hoc networks,” in *Proc. 37th Annual Hawaii International Conference on System Sciences, 2004*, Jan. 2003, pp. 460–469.

[67] Jang-Ping Sheu, Chen-Wei Lai and Chih-Min Chao, “Power-aware routing for energy conserving and balance in ad hoc networks,” in *Proc. IEEE International Conference on Networking, Sensing and Control*, vol. 1, Mar. 2004, pp. 468–473.

[68] Francesco Chiti, Romano Fantacci and Irene Innocenti, “Power aware routing protocols for wide area ad hoc networks,” in *Proc. International Workshop on Wireless Ad-Hoc Networks*, 31 May-3 June 2004, pp. 53–57.

[69] Marwan Krunz, Alaa Muqattash and Sung-Ju Lee, “Transmission power control in wireless ad hoc networks: Challenges, solutions, and open issues,” *IEEE Network*, vol. 18, pp. 8–14, Sep-Oct 2004.

[70] Jae-Hwan Chang and Leandros Tassiulas, “Maximum lifetime routing in wireless sensor networks,” *IEEE/ACM Trans. Networking*, vol. 12, no. 4, pp. 609–619, Aug 2004.

[71] Shih-Lin Wu, Sze-Yao Ni, Yu-Chee Tseng and Jang-Ping Sheu, “Route maintenance in a wireless mobile ad hoc network,” in *Proc. 33rd Annual Hawaii International Conference on System Sciences*, vol. 2, Jan 2000, pp. 1–10.

[72] Dongkyun Kim, Jaewoo Park, Toh C.-K., and Yanghee Choi, “Power-aware route maintenance protocol for mobile ad hoc networks,” in *Proc. 10th International Conference on Telecommunications, ICT 2003*, vol. 1, 23 Feb-1 March 2003, pp. 501–506.

[73] Jianxin Wang and Xicheng, “Route recovery based on anycast policy in mobile ad hoc networks,” in *Proc. IEEE International Conference on Communication Technology, ICCT 2003*, vol. 2, April 2003, pp. 1262–1265.

[74] Jaeki Lee, Yongi Kim and Hwang Soo Lee, “Fast route recovery methods for cellular IP access network,” in *Proc. IEEE 61st Vehicular Technology Conference, VTC 2005-Spring*, vol. 4, 30 May-1 June 2005, pp. 2580–2584.

[75] ——, “Route recovery with one-hop broadcast to bypass compromised nodes in wireless sensor networks,” in *Proc. IEEE Wireless Communications and Networking Conference, WCNC 2007*, vol. 4, March 2007, pp. 2495–2500.

[76] A. A. N. Ananda Kusuma, Lachlan L. H. Andrew and Stephen V. Hanly, “On Routing in CDMA Multihop Cellular Networks,” in *Proc. IEEE Global Communications Conference, GLOBECOM 2004*, 29 Nov-3 Dec 2004, pp. 3063–3067.

[77] P. Gupta and P. R. Kumar, “The capacity of wireless networks,” *IEEE Trans. Inform. Theory*, vol. 46, no. 2, pp. 388–404, March 2000.

[78] T. Clausen and P. Jacquet. (2003, Oct) Optimized link state routing protocol. [Online]. Available: http://www.ietf.org/rfc/rfc3626.txt

[79] Feng Xue and P. R. Kumar, “The number of neighbors needed for connectivity of wireless networks,” *Springer:Wireless Networks*, vol. 10, pp. 169–181, Mar 2004.

[80] Michele Zorzi and Silvano Pupolin, “Optimum transmission ranges in multihop packet radio networks in the presence of fading,” *IEEE Trans. Commun.*, vol. 43, no. 7, pp. 2201–2205, Jul 1995.

[81] M. R. Souryal, R. Vojcic and L. Pickholtz, “Adaptive modulation in ad hoc DS/CDMA packet radio networks,” *IEEE Trans. Commun.*, vol. 54, no. 4, pp. 714–725, Apr 2006.

[82] C. S. Patel, G. L. Stuber and T. G. Pratt, “Simulation of Rayleigh-faded mobile-to-mobile communication channels,” *IEEE Trans. Commun.*, vol. 53, no. 11, pp. 1876–1884, Nov 2005.

[83] Martin Haenggi, “On routing in random Rayleigh fading networks,” *IEEE Trans. Wireless Commun.*, vol. 4, no. 4, pp. 1553–1562, Jul 2005.

[84] Athanasios Papoulis and S. Unnikrishna Pillai, *Probability, Random Variables and Stochastic Processes*, 4th ed. Tata McGraw-Hill, 2002.

[85] Prince Samar and Stephen B. Wicker, “Link dynamics and protocol design in a multihop mobile environment,” *IEEE Trans. Mobile Comput.*, vol. 5, no. 9, pp. 1156–1172, 2006.

[86] Greert Heijenk and Fei Liu, “Interference-based routing in multi-hop wireless infrastructures,” *Elesevier: Computer Communications*, vol. 29, pp. 2693–2701, 2006.

[87] Martin Haenggi, “Twelve reasons not to route over many short hops,” in *Proc. IEEE 60th Vehicular Technology Conference, VTC 2004-Fall*, vol. 5, Sep. 2004, pp. 3130–3134.

[88] Jaeweon Cho and Haas Z. J, “Impact of concurrent transmissions on downstream throughput in multihop cellular networks,” in *Proc. IEEE International Conference on Communications, ICC 2004*, vol. 6, June 2004, pp. 3748–3753.

[89] S. Ramanathan and E. L. Lloyd, “Scheduling algorithms for multihop radio networks,” *IEEE/ACM Trans. Networking*, vol. 1, no. 2, pp. 166–177, Apr 1993.

[90] A. A Bertossi and M. A Bonuccelli, “Code assignment for hidden terminal interference avoidance in multihop packet radio networks,” *IEEE/ACM Trans. Networking*, vol. 3, no. 4, pp. 441–449, Aug. 1995.

[91] A. Behzad and I. Rubin, “On the performance of graph-based scheduling algorithms for packet radio networks,” in *Proc. IEEE Global Communications Conference, GLOBECOM 2003*, vol. 6, Dec 2003, pp. 3432–3436.

[92] T. Moscibroda and R. Wattenhofer, “The complexity of connectivity in wireless networks,” in *Proc. 25th IEEE Annual Conference on Computer and Communications, INFOCOM 2006*, April 2006, pp. 1–13.

[93] T. Moscibroda, R. Wattenhofer and A. Zollinger, “Topology control meets SINR: The scheduling complexity of arbitrary topologies,” in *Proc. ACM MobiHoc 2006*, May 2006, pp. 310–321.

[94] Arjunan Rajeswaran, Gyouhwan Kim and Rohit Negi, “A scheduling framework for UWB & cellular networks,” in *Proc. First International Conference on Broadband Networks, BroadNets 2004*, 2004, pp. 386–395.

[95] Tamer ElBatt and Anthony Ephremides, “Joint scheduling and power control for wireless ad-hoc networks,” *IEEE Trans. Wireless Commun.*, vol. 3, no. 1, pp. 74–85, Jan 2004.

[96] Emilio Leonardi, Marco Mellia, Marco Ajmone Marsan and Fabio Neri, “Joint optimal scheduling and routing for maximum network throughput,” in *Proc. 24th IEEE Annual Conference on Computer and Communications, INFOCOM 2005*, vol. 2, March 2005, pp. 310–321.

[97] M. Johansson and Lin Xiao, “Scheduling, routing and power allocation for fairness in wireless networks,” in *Proc. IEEE 59th Vehicular Technology Conference, VTC 2004-Spring*, vol. 3, May 2004, pp. 1355–1360.

[98] Alan A. Bertossi and Maurizio A. Bonuccelli, “Code assignment for hidden terminal interference avoidance in multihop packet radio networks,” *IEEE/ACM Trans. Networking*, vol. 3, no. 4, pp. 441–449, Aug. 1995.

[99] Saurabh Srivastava, Sachee Tripathi, Dheeraj Sanghi and Ajit K. Chaturvedi, “A code allocation protocol for maximizing throughput in CDMA based adhoc networks,” in *Proc. IEEE Global Communications Conference, GLOBECOM 2003*, vol. 2, Mar 2003, pp. 1385–1390.

[100] Ashutosh Deepak Gore, Abhay Karandikar and Srikanth Jagabathula, "On high spatial reuse link scheduling in STDMA wireless ad hoc networks," in *Proc. IEEE Global Communications Conference, GLOBECOM 2007*, Nov. 2007, pp. 736–741.

[101] R. Motwani and P. Raghavan, *Randomized Algorithms*. Cambridge University Press, 1995.

[102] H. N. Gabow and H. H. Westermann, "Forests, frames, and games: Algorithms for Matroid sums and applications," *Algorithmica*, vol. 7, pp. 465–497, 1992.

[103] C. Bettstetter. (June 2003) Topology properties of ad hoc networks with random waypoint mobility. [Online]. Available: http://www.sigmobile.org/mobihoc/2003/posters/p245-bettstetter.pdf

[104] DeFaria M and Sousa E. S, "Effect of intercell interference on the SINR of a multihop cellular network," in *Proc. IEEE 61st Vehicular Technology Conference, VTC 2005-Spring*, vol. 5, 2005, pp. 3107–3111.

[105] Sousa E. S and Silvester J. A, "Optimum transmission ranges in a direct-sequence spread-spectrum multihop packet radio network," *IEEE J. Select. Areas Commun.*, vol. 8, no. 5, pp. 762–771, June 1990.

[106] Gomez J and Campbell A.T, "Variable-range transmission power control in wireless ad hoc networks," *IEEE Trans. Mobile Comput.*, vol. 6, no. 1, pp. 87–99, Jan. 2007.

[107] Bettstetter C, "On the connectivity of wireless multihop networks with homogeneous and inhomogeneous range assignment," in *Proc. IEEE 56th Vehicular Technology Conference, VTC 2002-Fall*, vol. 3, Sep. 2002, pp. 1706–1710.

[108] Cardei Mihaela, Pervaiz O. Mohammad and Cardei Ionut, "Energy-efficient range assignment in heterogeneous wireless sensor networks," in *Proc. International Conference on Wireless and Mobile Communications, ICWMC 2006*, July 2006, pp. 11–17.

[109] Kun-Da Wu and Wanjiun Liao, "On constructing low interference topology in multihop wireless networks," in *Proc. IEEE International Conference on Communications, ICC 2006*, vol. 8, June 2006, pp. 3759–3764.

[110] Chi-Fu Huang, Yu-Chee Tseng, Shih-Lin Wu, and Jang-Ping Sheu, “Increasing the throughput of multihop packet radio networks with power adjustment,” in *Proc. 10th International Conference on Computer Communications and Networks, 2001*, Oct. 2001, pp. 220–225.

[111] Zorzi M and Pupolin S, “Optimum transmission ranges in multihop packet radio networks in the presence of fading,” *IEEE Trans. Commun.*, vol. 43, no. 7, pp. 2201 – 2205, July 1995.

[112] P. Gupta and P. R. Kumar, “Critical power for asymptotic connectivity,” in *Proc. 37th IEEE Conference on Decision and Control*, vol. 1, 1998, pp. 1106–1110.

[113] E. Hyytia and J. Virtamo, “Random Waypoint model in n-dimensional space,” *Elsevier:Operations Research Letters*, no. 33, pp. 567–571, 2005.

[114] T. Ohseki, N. Fuke, O. Maeshima, H. K. Sugiyama and M. Nohara, “Multihop mobile communications system using MC-CDMA in forward links,” in *Proc. IEEE Wireless Communications and Networking Conference, WCNC 2005*, vol. 1, March 2005, pp. 189–194.

[115] Jing Shi, Guanding Yu, Zhaoyang Zhang and Peiliang Qiu, “Resource allocation in OFDM based multihop wireless networks,” in *Proc. IEEE 63rd Vehicular Technology Conference, VTC 2006-Spring*, vol. 1, May 2006, pp. 319–323.

[116] M. Herdin, “A chunk based OFDM amplify-and-forward relaying scheme for 4G mobile radio systems,” in *Proc. IEEE International Conference on Communications, ICC 2006*, vol. 10, June 2006, pp. 4507–4512.

[117] J. Gross, H. Paoluzzi Karl and A. Wolisz, “Throughput study for a dynamic OFDM-FDMA system with inband signaling,” in *Proc. IEEE 59th Vehicular Technology Conference, VTC 2004-Spring*, vol. 3, May 2004, pp. 1787–1791.

[118] Z. Dawy, S. Davidovic and I. Oikonomidis, “Coverage and capacity enhancement of CDMA cellular systems via multihop transmission,” in *Proc. IEEE Global Communications Conference, GLOBECOM 2003*, vol. 2, Dec 2003, pp. 1147–1151.

[119] M. AI-Riyami, A. M. Safwat and H. S. Hassanein, “Channel assignment in multi-hop TDD W-CDMA cellular networks,” in *Proc. IEEE International Conference on Communications, ICC 2005*, vol. 3, May 2005, pp. 1428–1432.

[120] A. N. Zadeh and B. Jabbari, “Analysis and modeling of upstream throughput in multihop packet CDMA cellular networks,” *IEEE Trans. Commun.*, vol. 54, no. 4, pp. 680–692, April 2006.

[121] M. D. Vose, *Simple genetic algorithm : Foundations and Theory*. Cambridge : MIT Press, 1999. [Online]. Available: http://mitpress.mit.edu/catalog/author/default.asp?aid=1682

Acknowledgments

Although my name sits on the front cover, many others have assisted in various forms to bring this research to its conclusion. Here in this small section I attempt to thank all.

First, I would like to thank my supervisor Prof. S. N. Merchant not only for his unfailing encouragement, support and guidance but also for his belief in me. He was available all the time from day one (literally) to hear my problems and give timely solutions.

I wish to thank my faculty mentor Prof. U. B. Desai for providing me with wonderful insights into technical concepts and giving clear and commanding guidance whenever sought. Prof. V. M. Gadre's feedback during progress seminars highly helped me to improve the thesis quality.

I owe thanks to Microsoft Research India for their financial support and the travel grants due to which I could attend international conferences and interact with fellow researchers.

Prof. Saleem Bhatti of University of St. Andrews Scotland and Dr. Yangcheng of Ericsson Research Lab Ireland provided wonderful technical support during my internship at Scotland. Mohit Garg, Sarath Gopi and Ravi Ojha helped me in various stages of this thesis.

All my SPANN lab members particularly Mrs. Nair were extremely cooperative.

Most of all, I would like to thank Sireesha Chilakamarri and my family for their love, endless support and encouragements.

Date: _____ Kannan. G